Fachrichtung der Physiologie

der Medizinischen Fakultät

Universitätsklinik des Saarlandes, Homburg/Saar

Role of the SNARE protein VAMP2 and the SNARE regulatory protein Complexin II in Ca^{2+} triggered exocytosis

Dissertation

zur Erlangung des Grades eines Doktors der Naturwissenschaften

der Medizinschen Fakultät

der UNIVERSITÄT DES SAARLANDES

2021

vorgelegt von: Maria Mantero Martinez, M.Sc (Neurophysiology)

geb. am. 16.03.1993 in Girona, Spain

Doctoral supervisor: Prof. Dr. Dieter Bruns

Homburg, 2021

Tag des Promotionskolloquiums:	05.01.2022
Dekan:	Prof. Dr. M. D. Menger
Berichterstatter:	Prof. D. Bruns
	Prof. A. Cavalié

Dedicated to my parents Rafael Mantero and Mercedes Martinez and to my brother Manel

Summary

Regulated exocytosis of secretory cells is a calcium-dependent process that enables the release of neurotransmitter-storing vesicles. The major proteins involved in exocytosis are the SNAREs (soluble N-ethylmaleimide sensitive factor attachment protein receptor), which provide the essential energy for the actual membrane fusion through their membrane-bridging interactions. Since SNARE proteins assemble spontaneously, regulatory proteins such as Complexin (Cpx) are required to regulate complex formation. In this work, we investigated how transmembrane domains (TMD) of different v-SNARE variants and membrane curvature-mediating lipid molecules affect membrane fusion. In addition, the regulatory roles of the C-terminal domain (CTD) as well as the accessory alpha-helix (AH) domain of Cpx II were investigated.

The first part of this work shows that two different naturally occurring v-SNARE TMD variants (responsible for secretion of different sized vesicles) support initiation and extent of granule exocytosis in the same manner as wild-type (wt) protein, a finding that is distinct from the differential effect of TMD variants on the membrane fusion process itself.

Moreover, the results show that intracellular application of lipid molecules such as oleic acid (OA, negative curvature mediating) or lysophosphatidylcholine (LPC, positive curvature mediating) enhance or decrease secretion, respectively. This observation can be well explained by the existence of a lipid-based fusion intermediate in the exocytosis of chromaffin granules.

The second part of this work addresses the role of the SNARE regulatory protein Cpx II. Previous findings suggested that Cpx II assumes opposing functions in the control of exocytosis, acting as an inhibitor but also as a promoter of exocytosis. Thus, it inhibits premature vesicle exocytosis at submicromolar Ca^{2+}-concentrations, thereby enhancing the assembly of a pool of exocytosis-competent vesicles for synchronous secretion. In the present work, we demonstrated that the last 34 amino acids of the CTD of Cpx II are responsible for preventing premature vesicle secretion. Moreover, electrophysiological experiments show that a Cpx II:SNAP25-SN1 chimera is able to restore Cpx II function, suggesting that Cpx II competes with SNAP-25 for binding to the other SNARE proteins, thus preventing the progressive 'zipping' of partially-assembled SNARE complexes. In addition, we examined several interesting point mutations in the C-terminal domain to better understand the role of this region. Finally, the results show that also, the accessory α-helix of Cpx II partially inhibits premature vesicle exocytosis. Overall, these results demonstrate that both the C-terminus and the accessory α-helix are required for inhibition of premature vesicle exocytosis

Zusammenfassung

Die regulierte Exozytose sekretorischer Zellen ist ein calciumabhängiger Prozess, der die Freisetzung von Neurotransmitter-speichernder Vesikel ermöglicht. Die wichtigsten an der Exozytose beteiligten Proteine sind die SNAREs (soluble N-ethylmaleimide sensitive factor attachment protein receptor), die durch ihre membran-verbindenden Interaktionen die wesentliche Energie für den eigentlichen der Membranverschmelzung liefern. Da SNARE-Proteine spontan assemblieren, werden regulatorische Proteine wie Complexin benötigt, um die Komplexbildung zu regulieren. In dieser Arbeit untersuchten wir, wie Transmembrandomänen (TMD) unterschiedlicher v-SNARE-Varianten und Membrankurvatur-vermittelnde Lipidmoleküle die Membranfusion beeinflussen. Darüber hinaus wurde die regulatorische Rolle der C-terminalen Domäne (CTD) sowie der akzessorischen Alpha-Helix (AH) Domäne von Complexin II (CpxII) untersucht.
Der erste Teil dieser Arbeit zeigt, dass zwei verschiedene natürlich vorkommende v-SNARE TMD-Varianten (die für die Sekretion unterschiedlich großer Vesikel verantwortlich sind) Auslösung und Ausmaß der Granulenexozytose Fusion in gleicher Weise wie das Wildtyp-Protein (wt) unterstützen, ein Befund, der sich von der unterschiedlichen Wirkung der TMD-Varianten auf den eigentlichen Membranfusionsvorgang unterscheidet. Darüber hinaus zeigen die Ergebnisse, dass die intrazelluläre Applikation von Lipidmolekülen wie der Ölsäure (OA, negative Kurvatur vermittelnd) oder des Lysophosphatidylcholins (LPC, positive Kurvatur vermittelnd) die Sekretion verstärken bzw. verringern. Diese Beobachtung lässt sich gut mit der Existenz eines Lipid-basierten Fusionsintermediates in der Exozytose chromaffiner Granulen erklären.
Der zweite Teil dieser Arbeit befasst sich mit der Rolle des SNARE-Regulatorproteins Cpx II. Bisherige Befunde legen nahe, dass CpxII gegensätzliche Funktionen in der Kontrolle der Exozytose übernimmt und zum einen als Inhibitor aber auch als Promotor der Exozytose wirkt. . So hemmt es die vorzeitige Vesikelexozytose bei submikromolaren Ca2+-Konzentrationen und verstärkt somit den Aufbau eines Pools exozytose-kompetenter Vesikel für die synchrone Sekretionsantwort. In der vorliegenden Arbeit konnten wir nachweisen, dass die letzten 34 Aminosäuren der CTD von Cpx II für die Verhinderung der vorzeitigen Vesikelsekretion verantwortlich sind. Darüber hinaus zeigen elektrophysiologische Experimente, dass eine Cpx II: SNAP25-SN1-Chimäre in der Lage ist, die Funktion von Cpx II wiederherzustellen. Diese Beobachtung legt nahe, dass Cpx II mit SNAP-25 um die Bindung an die anderen SNARE-Proteine konkurriert und so die fortschreitende Verbindung partiell-assemblierte SNARE Komplexe verhindert. Darüber hinaus haben wir mehrere interessante Punktmutationen in der CTD untersucht, um die Rolle dieser Region besser zu verstehen. Schließlich zeigen die Resultate, dass

die auch AH von Cpx II die vorzeitige Vesikelexozytose teilweise hemmt. Insgesamt demonstrieren diese Ergebnisse, dass sowohl der C-Terminus als auch die akzessorische - Helix für die Hemmung der vorzeitigen Vesikelexozytose erforderlich sind.

Abbreviations

$[Ca^{2+}]i$: Intracellular free calcium
µl:microliters
Å: angstrom
aa: amino acid
AH: accessory α-helix
ANOVA: one-way analysis of variance
ATP: adenosine triphosphate
BAPTA: 1,2-bis(o-aminophenoxy)ethane-N,N,N′,N′-tetraacetic acid
BoTx: Botulinum Toxin
BSA: Bovine Serum Albumin
Ca^{2+}: calcium
CAPS: Calcium-dependent Activator Protein for Secretions
Ceb: Cellubrevin
Cpx II: complexin II
CsOH: cesium hydroxide
ΔCm: Delta (change) in membrane capacitance
Dko: Double knockout
DMEM: Dulbecco´s Modified Eagles´s Medium
DMSO: Dimethyl sulfoxide
DNA: Deoxyribonucleic acid
DPTA: 1, 3-diaminopropane-N,N,N′,N′-tetraacetic acid
EB: Exocytotic burst
EDTA: Ethylenediaminetetraacetic acid
EGFP: Enhanced green fluorescent protein
EGTA: Ethyleneglycol tetraacetic acid
fF/s: Femtofarad per second
fF: Femtofarad
g: gram
Gm: membrane conductance
Gs: series conductance
GTP: Guanosine triphosphate
h: Hour
H_2O: water
HCl: Hydrochloric acid
HEPES: 2-[4-(2-hydroxyethyl)piperazin-1-yl] ethanesulfonic acid
Hz: Hertz
I-Tasser: Iterative Threading Assembly Refinement
JMD: juxtamembrane domain
KCl: Potasium chloride
ko: knockout

LDCV: large dense-core vesicles
ml: milliliter
mM: mili Molar
ms: mili second
Munc-13: Mammalian-Unc13
Munc-18: Mammalian-Unc18
nM: Nano molar
nm: nanometer
NP-EGTA: Nitrophenyl-EGTA
NSF: N-ethylmaleimide sensitive factor
PBS: Phosphate Buffer Saline
PCR: Polymerase Chain Reaction
PFA: Paraformaldehyde
rpm: revolutions per minute
RRP: Ready Releasable Pool
RT: Room Temperature
SDS: Sodium Dodecyl Sulfate
SFV: Semiliki Forest Virus
SIM:Structured Illumination Microscopy
SM: Sec1/munc18
SNAP: soluble NSF attachment protein
SNAP-25: Synaptosomal-Associated Protein-25
SNARE proteins: soluble N-ethyl-maleimide-sensitive factor attachment protein receptor
SNS: Sympathetic Nervous System
SR: Sustained Release
SRP: Slow Releasable Pool
Syb II ko: Synaptobrevin II knockout
Syt I: Synaptotagmin I
TeTx: tetanus toxin
TMD: transmembrane domain
TMD: transmembrane domain
T-SNARE: target-SNARE
UV: Ultraviolet Illumination
VAMPs: vesicle associated membrane proteins
VGCC: voltage-gated calcium channels
V-SNARE: vesicular-SNARE
Wt: wild type

List of figures and tables

1. Introduction

Neuronal communication is fundamental to all physiological functions, from the most complex, such as learning, to the simplest, such as motor reflexes. Neurons communicate with each other via the release of neurotransmitters at specialized contact sites called synapses. There are two types of synapses in the nervous system: the electrical and the chemical. Electrical synapses are less common and mostly found in lower vertebrates or invertebrates, whereas chemical synapses are found in higher vertebrates and are the most common ones (Kandel et al., 2000). Therefore, since the latter are more common and physiologically very relevant, this thesis will focus on them. Chemical synaptic transmission is triggered in the presynaptic nerve terminal when an action potential mediating membrane depolarization opens voltage-gated Ca^{2+} channels. The consequence of channel opening is an increase in the intracellular calcium concentration leading to vesicle fusion with the cell membrane. This fusion allows the release of the neurotransmitters that rapidly bind to receptors on the post-synaptic neuron. The vesicle fusion with the plasma membrane is the final stage of the so-called Exocytosis process. Exocytosis is necessary for all cells, not only for cellular communication and homeostasis, but also for cellular growth and differentiation. Therefore, understanding the mechanisms that regulate this process is key to understanding natural processes and addressing anomalies that may have severe consequences in the living system.

1.1 Classification of exocytosis

For exocytosis to occur, previous steps are required. First, the endoplasmic reticulum synthesizes proteins or molecules and sorts them into vesicles. Next, these vesicles fuse with the Golgi apparatus, which is responsible for deciding whether the vesicles will be secreted in a constitutive or regulated manner (Viotti, 2016).

-Constitutive exocytosis: this type of secretion is the most abundant in cells and plays a very important role since it allows to maintain and restore the cells by supplying proteins and lipids to the plasma membrane. It is characterized by being independent of any stimulus, (Edwardson and Daniels-Holgate, 1992) this implies that molecules are secreted as soon as they are synthesized and so, the only way to alter the rate of secretion is to change the rate of synthesis (Kelly, 1985) **(Figure 1)**.

-Regulated exocytosis: this form of exocytosis is present in specialized cells, such as neuroendocrine cells and neurons (Kelly, 1985; Masedunskas et al., 2012). In contrast to constitutive exocytosis, it needs a stimulus that causes an increase in intracellular calcium for fusion to occur

(Burgess and Kelly, 1987; Lindau and Gomperts, 1991). This form of exocytosis is very important because is the one used for neurotransmission release and thus allows the nervous system to transmit messages. In this present work, we studied the importance of proteins and lipids in this calcium dependent exocytosis **(Figure 1)**.

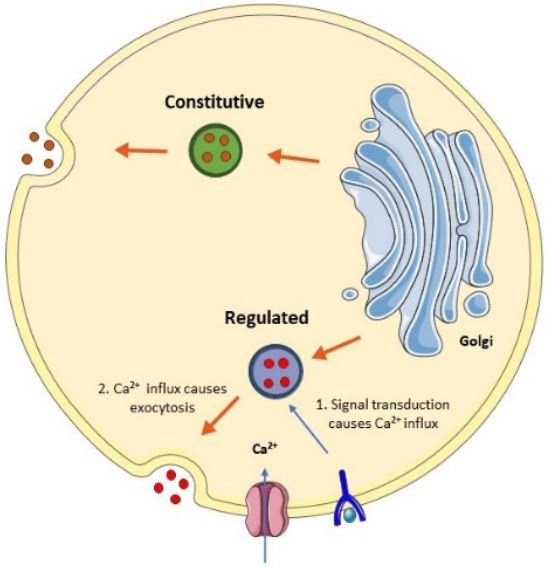

Figure 1. Schematic drawing of constitutive and regulated exocytosis. Constitutive exocytosis is the most common form of exocytosis, vesicles are synthesized and secreted without the need of a stimulus. Regulated exocytosis requires a signal transduction (causing a Ca^{2+} influx) for fusion to take place.

1.1.1 Steps in regulated exocytosis

Regulated exocytosis occurs when intracellular calcium ($[Ca^{2+}]i$) rises (Gustavsson et al., 2012). Prior to that, vesicles are in a pre-fusion state, close to the plasma membrane. From the time the vesicles are near the plasma membrane until the full fusion of the vesicles and their cargo release, 5 steps can be distinguished **(Figure 2)**:

-Docking: It is a morphological define step, a vesicle is consider as docked when it is in close apposition to the plasma membrane. For fusion to take place, the docking step is a prerequisite. Over the years, several studies have been conducted to unravel the molecular processes involved in docking. Despite all the efforts, there are disagreements in the literature about the proteins engaged in this process. These disagreements are due to the fact that it is technically challenging to assess when a vesicle is docked (Imig et al., 2014). Until now, the most commonly used technique to determine docked vesicles is electron microscopy (EM) (Verhage and Sorensen, 2008), the downside of this technique is that the use of ultrathin sections impedes the identification of several dock synaptic vesicles, because not all of them are present in the section. Yet, despite the technical challenge of this fusion step two proteins have been proposed as essential for docking, these proteins are: Mammalian-Unc18 (Munc18) and syntaxin. Munc18 is a member of the SM (Sec1/munc18) protein family and syntaxin is a SNARE (Soluble NSF attachment protein) protein (SNARE proteins

will be addressed in section 1.3). These two proteins interact with each other and the deletion of one of them disrupts docking (Toonen et al., 2006).

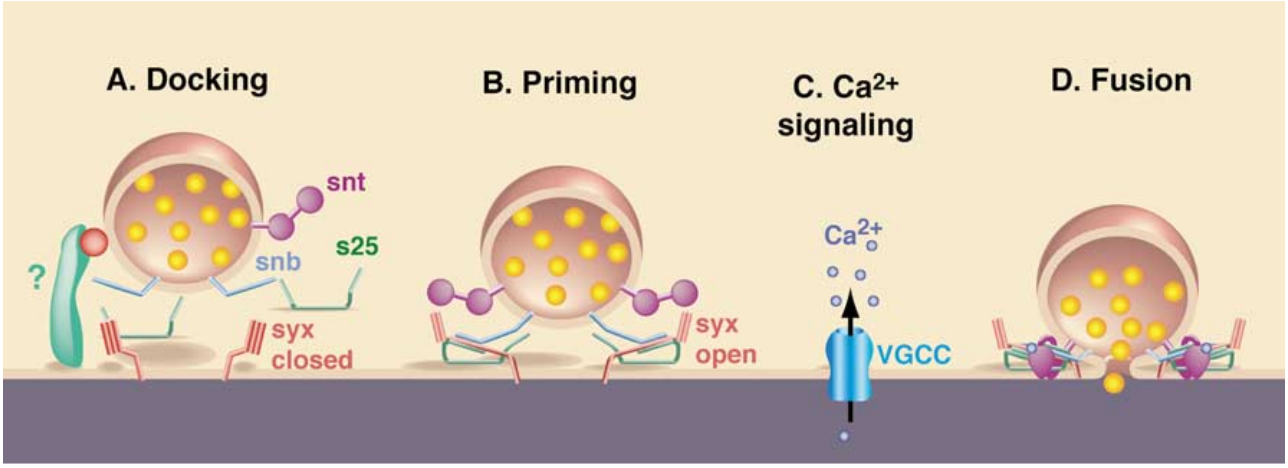

Figure 2. Steps in regulated exocytosis. (A) Docking, the vesicle is in close apposition to the plasma membrane. **(B)** Priming, the vesicle becomes competent for release. **(C)** Calcium triggering, calcium influx through calcium channels enabling fusion of primed vesicles. **(D)** Fusion, the vesicle fuses with the plasma membrane (Weimer and Richmond, 2005).

-Priming: Priming is the subsequent step after docking. Vesicles are considered as primed when they are biochemically maturated into a state that enables them to be released upon a calcium influx (Verhage and Sorensen, 2008). Priming has been characterized by electrophysiological measurements. Indeed, experiments done in neuroendocrine cells have shown the existence of a primed pool, also called ready releasable pool (RRP) (Klenchin and Martin, 2000). This step is facilitated in a calcium-dependent manner, therefore, low levels of Ca^{2+} reduce the prime pool (Voets, 2000). The first molecular players that have been found to be involved in priming were Mammalian-Unc13 (Munc-13), CAPS and two SNARE proteins: Synaptosomal-Associated Protein-25 (SNAP-25) and Synaptobrevin (Verhage and Sorensen, 2008). However, two SNARE regulatory proteins, synaptotagmin and complexin, have also been subsequently identified as essential for priming (Mohrmann et al., 2015). In this thesis, the underlying mechanisms of complexin to ensure efficient priming is addressed.

-Ca^{2+} triggering: primed vesicles fuse upon an increase of $[Ca^{2+}]i$ following an action potential (Sudhof, 1995). Indeed, for fusion to take place the entry of calcium through the calcium channels is needed. The sites where the calcium enters the cytoplasm are called calcium microdomains (Berridge, 2006). Its existence has been demonstrated for the first time in chromaffin cells by fura-2 (fluorescent dye which binds to free intracellular calcium) calcium imaging experiments (O'Sullivan et al., 1989). The localization of the calcium microdomains is cell dependent, while in synapses they are localized near the active zones, in chromaffin cells, there are randomly distributed over the entire cell surface

near voltage gated calcium channels (Garcia et al., 2006). The random distribution of calcium microdomains in chromaffin cells allows fusion to happen over the entire surface of the cell. As for the molecular players that synchronizes calcium-dependent fusion, it has been shown that synaptotagmin (a SNARE regulatory protein) plays a major role (Sudhof, 2012). Indeed, the C2 domains of synaptotagmin, can bind calcium. Therefore, this protein has an important role as Ca^{2+}sensor for fast synchronous release (Fernandez-Chacon et al., 2001). It is thought that when Ca^{2+} binds to synaptotagmin, this provokes full zippering of the complex by the withdraw of complexin (Zhou et al., 2017). The role of synaptotagmin and more specifically the role of complexin in Ca^{2+} triggering exocytosis will be discussed in more detail.

-Fusion with the plasma membrane: following the influx of calcium, vesicles fuse with the plasma membrane due to the synergistic action of the SNARE proteins as well as of other regulatory proteins like synaptotagmin and complexin (Lin and Scheller, 2000). Several steps are needed for the two membranes to fuse **(Figure 3)**. Experiments carried out on viral fusion suggest that the first step of membrane fusion is the formation of a lipid stalk, which is an hourglass-like structure (Earp et al., 2005; Yang and Huang, 2002). The lipid stalk is formed when the proximal lipid layers of the opposing membranes merge into one curved layer, while the distal layers are still intact (Aeffner et al., 2012) **(Figure 3B)**. The expansion of the stalk results in hemifusion. At the time that hemifusion was discovered, it was considered as a dead-end scenario of membrane fusion, (Kemble et al., 1994) but later studies on viral fusion have shown that it is a state that can progress to full fusion (Melikyan et al., 2000). In this state, the inner leaflets are separate while the outer leaflets merge **(Figure 3C)**. Then, rupture of the distal leaflet membrane results in opening of the fusion pore, followed by fusion pore expansion and release of the vesicle cargo (Chen and Scheller, 2001) **(Figure 3D)**.

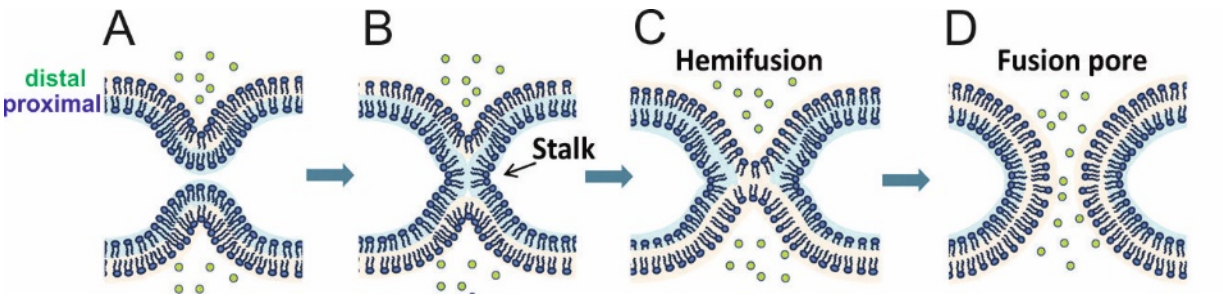

Figure 3. Schematic drawing of the fusion of the vesicle membrane with the plasma membrane. Vesicle fusion starts upon an increase of intracellular calcium. **(A)** Approximation of the vesicle membrane and the plasma membrane, **(B)** the fusion of the two membranes form in the first place the lipid stalk, **(C)** the expansion of the lipid stalk results in hemifusion, **(D)** the lipid bilayer is ruptured resulting in the opening of the fusion pore and its further expansion allowing the released of the vesicle cargo (Melikyan, 2010).

-Fusion pore: the last step of the fusion machinery is the opening of the fusion pore which enables the release of neurotransmitters. Different experimental approaches like freeze-fracture electron microscopy and patch clamp electrophysiology coupled with carbon fiber amperometry have shown the existence of the fusion pore (Breckenridge and Almers, 1987; Chandler and Heuser, 1980). Despite extensive studies on the fusion pore, its nature has been controversially discussed over the years. First, it was thought to be proteinaceous, consisting of a protein that separates the bilayer (Almers and Tse, 1990). Later on, it has been shown that it was more likely form of lipids, with proteins acting as external scaffolds (Monck and Fernandez, 1996). Nowadays, the debate about the nature of the fusion pore being proteinaceous, lipidic or even a mix of both is still open (Dhara et al., 2020; Zhang and Jackson, 2010). However, new technologies may help soon to unravel this open question. Other than its nature, the extent of expansion of the fusion pore has been studied extensively because it determines how the vesicles fuse. So far, two fusion modes have been found. On one hand, there is the full-collapse fusion which consists on releasing all the vesicular content in a rapid manner through a pore that opens and expands, reaching diameters bigger than 15 nm. In this type of fusion, the vesicle is completely merged with the pore (Wu et al., 2014). On the other hand, there is the kiss-and-run mode where the fusion pore opens briefly and then closes (He et al., 2006; Wu et al., 2014). In the "kiss-and-run" mode the vesicle does not fuse completely, therefore it can be recycled and also, the number of neurotransmitters release can be limited (Alabi and Tsien, 2013). The choice of which fusion will take place, between full fusion and "kiss-and-run", depends on how much the fusion pore is opened, but the decision is made before the opening of the fusion pore and it is somehow dependent on the SNARE or the SNARE regulatory proteins (Alabi and Tsien, 2013). However, it is yet not clear the exact mechanism of each fusion (Alabi and Tsien, 2013).

Overall, different steps and proteins are required for Exocytosis to take place. The lack or mutations of some proteins can disrupt one of these 5 essential steps and therefore, disrupt the Exocytosis machinery.

1.2 Endocytosis

Once the exocytosis process ends, endocytosis takes place. Endocytosis is important for the maintenance of exocytosis and of the cell membrane integrity (Wu et al., 2014). Indeed, vesicle recycling through endocytosis allows exocytosis to take place. To trigger endocytosis, an influx of calcium is necessary. Several studies have shown that reducing extracellular calcium diminish endocytosis (Wu et al., 2014). One example of this are the studies perform by Wu and colleagues where they have shown that reducing the extracellular calcium from 5 to 0.25 nM decreases the

endocytosis rate around 50 fold (Wu et al., 2009b). Overall, it can be concluded that endocytosis is a necessary process for exocytosis and that, as well as exocytosis, a calcium influx is crucial for this process to take place.

1.3 Main actors: SNARE proteins

The SNARE proteins (soluble N-ethyl-maleimide-sensitive factor attachment protein receptor) have been first identified around 30 years ago (Block et al., 1988). In fact, around that time, important discoveries were made which led years later to the elaboration of the SNARE hypothesis (Block et al., 1988; Link et al., 1992; Trimble et al., 1988). To unravel the function and the topology of SNARE proteins, crucial studies using neurotoxins and yeasts have been done. One of this studies, revealed that tetanus toxin inhibits neurotransmitter release via the proteolysis of VAMP2 (Link et al., 1992). Subsequent studies have shown specifically which neurotoxin cleaves which SNARE protein. For example, it has been found that VAMP proteins are cleaved by tetanus toxin (TeTx) and different types of botulinum toxin (BoTx) and syntaxin and SNAP-25 are cleaved only by BoTx (Blasi et al., 1993; Humeau et al., 2000) **(Figure 4 B)**. With regard to the topology of the SNARE proteins, studies made in yeast have shown the importance of the SNAREs localization to form a functional complex for fusion (McNew et al., 2000a; Parlati et al., 2000). In summary, many studies have been performed to unravel the mechanisms by which SNARE proteins interact with each other and overcome energetic barriers so that the vesicle fuses with the plasma membrane. Indeed, for fusion to happen vesicular-SNARE proteins (v-SNARE) bind to target-SNAREs (t-SNAREs), allowing the vesicle and the plasma membrane to get in close apposition (Martens and McMahon 2008).

Based on the **localization**, the SNARE proteins can be classified in two groups. The first group are the v-SNARE proteins, which are localized on the vesicle membrane. Only one family of proteins belongs to this group: the VAMPs (vesicle associated membrane proteins). The second group are the t-SNARE proteins, which are localized on the plasma membrane or target membrane. Two family of proteins belong to this group: syntaxin and SNAP-25. It is well known that when the t-SNAREs and v-SNAREs zip together, a very stable SNARE coiled complex is formed. This complex assembly allows to overcome repulsive electrostatic forces for membrane fusion to happen. Moreover, this complex is very stable since it is resistant to heat (the melting temperature is more than 90 °C) and to sodium dodecyl sulfate (SDS) (Fasshauer et al., 1997) **(Figure 4)**. In 1993, Sollner and colleagues have proposed the so-called SNARE hypothesis. This hypothesis affirms that the paring of the v-SNAREs and the t-SNAREs are responsible for dictating the vesicle membrane target (Sollner et al., 1993). In fact, the specificity of this complex has first been show by *in vitro*

experiments where vesicle fusion was asses by measuring lipid mixing. In this study, different SNARE proteins pairs where used to evaluate whether they could mediate fusion. The results have shown that only few of this pairs of proteins could mediate vesicle fusion (Weber et al., 1998). These findings may explain why a vesicle fuses with the plasma membrane instead of another organelle. This hypothesis was also confirmed later on by using liposome reconstitution assays with different yeast SNARE proteins (McNew et al., 2000a). In summary, 3 SNARE proteins are needed for fusion, each of these proteins possess different isoforms. As explain below, each isoform has a specific localization and specific role:

V-SNARE: -Vesicle associated membrane protein (VAMP): up to date, 8 isoforms have been identified, most of them have an active role in vesicle fusion. All the isoforms have similar structures and contain around 120 amino acids. Their structure consists on a N-terminus of around 25-35 amino acids, one or two amphipathic α-helix that have coiled-coil structures (as shown with *in vivo* and *in vitro* studies) (Grote et al., 1995; Regazzi et al., 1996) and a transmembrane domain in the C-terminus (Gerst, 1999). The major v-SNARE protein driving synaptic vesicle exocytosis is VAMP2, this isoform is involved in secretion in different cell types. For example, in neurons with the release of neurotransmitters, in pancreatic β-cells with the insulin release or even in adrenal chromaffin cells with the release of catecholamines (Baumert et al., 1989; Regazzi et al., 1995; Schoch et al., 2001). The closest isoform of VAMP2 is VAMP1, which despite its structure similarities with VAMP2, its expression is limited to few cell types. VAMP1 is mostly expressed in the nervous tissue, for instance it is highly expressed in the spinal cord (Elferink et al., 1989; Gerst, 1999). Another isoform is VAMP3 or cellubrevin, this isoform is expressed ubiquitously but it has not been detected in neurons (McMahon et al., 1993). Cellubrevin is functionally redundant with respect to VAMP2 in chromaffin cells (Borisovska et al., 2005), so in this thesis in which chromaffin cells were used and VAMPs were study, the use of the dko (synaptobrevin/cellubrevin) mice was necessary. Finally, there are two other isoforms, VAMP7 and VAMP8 which are involved in the secretion of mast cells (Sander et al., 2008). In this work, the role of the synaptobrevin TMD was studied. For this purpose, genetically modify proteins expressing the cytosolic domain of VAMP2 and the transmembrane domain of either VAMP8 or VAMP1 was used to assess whether the vesicle secretion was altered.

T-SNARE: -Syntaxin: it was first discovered in 1992 by Bennett and others while they were searching for interacting partners of another protein, the so-called p65 and nowadays called synaptotagmin, a protein that will be addressed later in this thesis. Syntaxin, previously called p35, it is a 35kDa protein which was first identified on the plasma membrane, at the site of

neurotransmitter release (Bennett et al., 1992). Until now, 15 mammalian syntaxin genes have been found; but only four (syntaxin 1-4) appear to play a role in exocytosis and are localized in the plasma membrane (Salaun et al., 2004). This protein contains around 300 amino acids, at least three coiled-coil regions (named H1, H2 an H3) and a transmembrane domain (Bennett et al., 1993). The H3 C-terminus region binds to VAMP and to SNAP-25 (Hayashi et al., 1994). Syntaxins do not only interact with the SNARE proteins but also with other proteins or channels. For example, it has been shown that they interact with voltage-gated calcium channels (VGCC) via their C-terminus, meaning that syntaxin influences fusion by playing a role in the channel conductance (Gerst, 1999). They also bind to synaptotagmin and its N-terminus binds, among others, to munc-13 and munc-18 (Betz et al., 1997; Kee et al., 1995).

-SNAP-25: this 25kDa protein was first discovered in 1989 by Oyler and others. At that time, it was found that this protein was mainly localized in the pre-synapse, meaning that it may play an important role in synaptic function (Oyler et al., 1989). However, now it has also been shown to localize at the post-synapse (Hussain et al., 2019). This protein possesses two alpha-helices, one in the N-terminus (45-90 aa) and another in the C-terminus (157-206 aa), they both contribute to the formation of the SNARE complex. Despite the lack of a TMD in its structure, this protein is anchored in an efficient manner on the plasma membrane thanks to the palmytolation of the cysteine rich domain (Salaun et al., 2004). This cysteine domain is situated in between both helices and its palmytolation is crucial for targeting the protein to the plasma membrane (Veit et al., 1996). Among the members of the SNAP-25 protein family, there are two isoforms, SNAP-25A and SNAP-25B which have high sequence homology and are mostly expressed in neuronal and neuroendocrine cells. Both of these isoforms mediate exocytosis (Bark and Wilson, 1994; Blasi et al., 1993). Moreover, it has been shown that SNAP-25A is expressed at embryonic stages, while SNAP-25B expression is at post-natal stages (Bark et al., 1995). Other members of SNAP-25 protein family have been found, for example SNAP-23; which is involved in regulated exocytosis in non-neuronal cells like mast cells (Rea et al., 1998) and SNAP-29 which is localized in intracellular membranes and does not have a function in SNARE mediated exocytosis (Hohenstein and Roche, 2001). In this thesis, we will study the possible interaction of SNAP-25 with complexin.

Overall, the crystal structure shows that the SNAREs proteins form a four-helical bundle with one coil of syntaxin and of VAMP2 and two coils of SNAP-25 (Sutton et al., 1998). The topology of the fusion complex is a cylinder of 120 Å length. The four components of this complex are organized in parallel, from the N-terminal to the C-terminal domain (Sutton et al., 1998) **(Figure 4 A)**. The formation of this core complex is necessary for bridging the two membranes (Chen et al., 1999). For this to happen, the complex needs to be in a trans-SNARE orientation **(Figure 4 B)**. Then, during the

release of the cargo, the complex orientation changes from trans to cis. The cis orientation is reached when the SNARE complex is present in one membrane. At this point, the SNARE complex is inactive and ready to be recycled (Rizo and Sudhof, 2002).

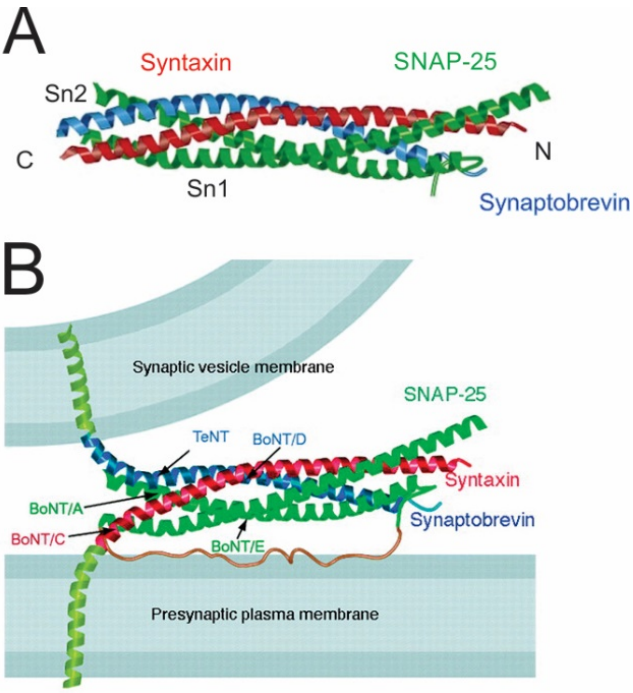

Figure 4. Schematic drawing of the structure of SNARE proteins. **(A)** Drawing of the synaptic fusion complex. The four helical bundle is composed of syntaxin (red), SNAP-25 (green) and synaptobrevin (blue) with the N-terminus at the end and the C-terminus at the membrane anchor. **(B)** Hypothetical model of the SNARE fusion complex and the cleavage sites of clostridia neurotoxins. (Sutton et al., 1998)

The **function** of the SNARE complex has been for long time a source of debate. One of the first hypotheses concerning the role of SNAREs was proposed in 1993 and stated that they were involved in vesicle docking and fusion (Sollner et al., 1993). Nevertheless, the docking hypothesis was refuted in several other studies, one of which showed that docking was unaffected by SNARE-cleaving neurotoxins (Hunt et al., 1994). The rejection of this hypothesis led to other hypotheses, one of them was the zipper model. So far, the zipper model is the most widely accepted, this model states that the SNARE proteins assembly takes place in the last steps of the fusion process and that the SNARE zippering is crucial for membrane fusion because it pulls the vesicle in close apposition to the plasma membrane (Poirier et al., 1998). The fusion process requires lots of energy given the fact that the environment between the fusing membranes is aqueous and that the two fusing membranes are at a distance of 1-2 nm from each other (Risselada et al., 2011). Thus, SNARE proteins provide the energy to overcome electrostatic repulsion and hydration forces to enable fusion (Mostafavi et al., 2017). In addition, it has been shown that in the absence of these proteins, spontaneous fusion hardly occurs, meaning that they are essential for membrane bridging (Risselada et al., 2011). Overall, fusion starts when synaptobrevin assembles with the acceptance complex forming a parallel four-helix bundle. The zippering of the assembled trans-SNARE proteins brings the vesicle closer to the plasma membrane. Then, upon an increase of intracellular calcium, the two membranes merge, the fusion

pore opens and the cargo is released. Once the cargo is released, the SNARE proteins are disassembled. The disassembly of this complex needs two proteins, NSF (N-ethylmaleimide sensitive factor) and alpha-SNAP (soluble NSF attachment protein). However, how these proteins disassemble the complex is still a matter of debate (Ryu et al., 2015; Zhao et al., 2015). In any case, it is known that the dissociation of this complex is driven in an ATP-dependent manner (Yoon and Munson, 2018). Finally, when SNARE proteins are disassembled, they are endocytosed and used again for the next fusion process **(Figure 5)**.

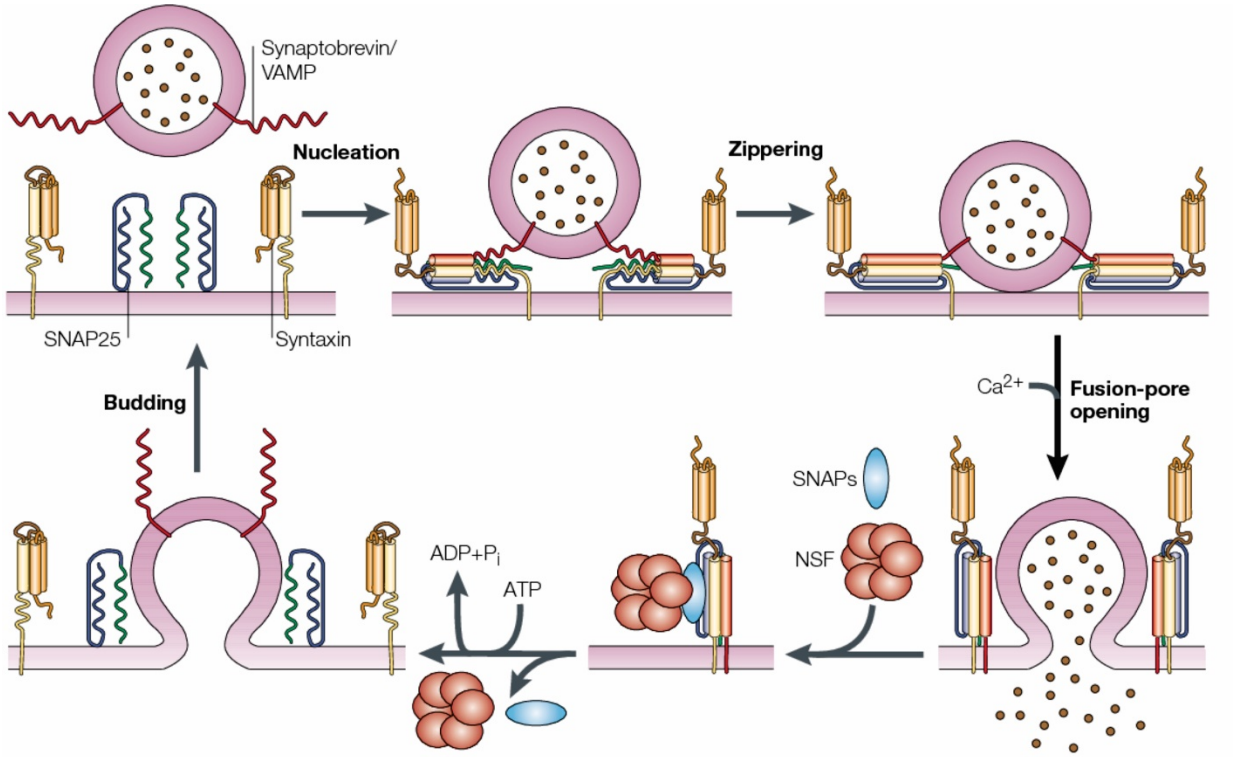

Figure 5. SNARE proteins assembly and disassembly. Synaptobrevin is located in the vesicular membrane, while Syntaxin and SNAP25 are in the plasma membrane. Syntaxin is in a closed conformation. When Syntaxin opens, the SNARE proteins assembles (nucleation). The further zipper of the trans-SNAREs allows the vesicular membrane to come closer to the plasma membrane. Then, in a calcium dependent manner, the fusion pore opens and the cargo is released. Once the cargo is released, the cis-SNAREs are disassembled by NSF and SNAP, this is done in an ATP dependent manner. Finally, the disassembled SNAREs are recycled and will be used again for the next fusion process (Rizo and Sudhof, 2002).

1.3.1 Structure and function of VAMP

As mention before, several VAMP isoforms exist. Among all protein isoforms, this thesis work is focused on VAMP2 (also named synaptobrevin II) and VAMP3 (also named cellubrevin), that is why these isoforms will be described in detail. VAMP2 is the main isoform expressed in the central nervous system, its deletion impairs neurotransmitter release (Deak et al., 2006). VAMP3 is greatly homologous to VAMP2 ,their SNARE motif differs only from one amino acid (Deak et al., 2006).

Interestingly, it has been shown in chromaffin cells that these two isoforms are functionally redundant (Borisovska et al., 2005). For this reason, the experiments performed in this thesis use dko (synaptobrevin and cellubrevin ko) mice for the study of the transmembrane domain of VAMP2. VAMP2 is composed of 116 amino acids, and it is structured in four parts: a rich N-terminal proline comprising residues 1-28, the SNARE motif from residues 28-84, the juxtamembrane region (JMR) from 85-94 and the transmembrane domain (TMD) from 95 to 116. For fusion to take place, the cytosolic part of VAMP2 (the SNARE motif) interacts with the other SNARE proteins (Sudhof and Rothman, 2009). Besides this crucial interaction, it was interesting to study whether other interactions were necessary, that is why the interaction between proteins and lipids was studied **(Figure 6)**. Two different studies performed in chromaffin cells have shown the importance of the juxtamembrane region (JMR) of VAMP2. The first study demonstrated that the introduction of a flexible linker into the JMR (8 amino acids or more) impairs Ca^{2+} triggered exocytosis (Kesavan et al., 2007). In the same line, another study showed that the mutation of two highly conserved tryptophan residues located in the JMD impairs vesicle priming (Borisovska et al., 2012). Overall, these two studies have proven that the JMD mediates protein-lipid interactions and thus helps to bridge the two opposing membranes.

Along the same lines, it was interesting to study the role of the TMD of VAMP2 to know whether it is just a membrane anchor or it has an active role in the fusion of the two membranes. In fact, for many years it was thought that the TMD of VAMP2 served as an anchor that allowed force transduction of SNARE complex formation at the vesicular membrane. For example, a study conducted in the vacuoles of yeast suggested that the TMD was a nonspecific membrane anchor in vacuole fusion (Pieren et al., 2015). In a similar line, another study proposed that the TMD was not required for spontaneous or Ca^{2+} dependent fusion in neurons (Zhou et al., 2013). However, these studies did not verify the steps preceding fusion (like priming, fusion pore expansion…), making it hard to know at which step the TMD plays a role in membrane fusion (Dhara et al., 2016; Fang and Lindau, 2014). There is now sufficient experimental data demonstrating the active role in fusion of the TMD (Dhara et al., 2016; McNew et al., 2000b).

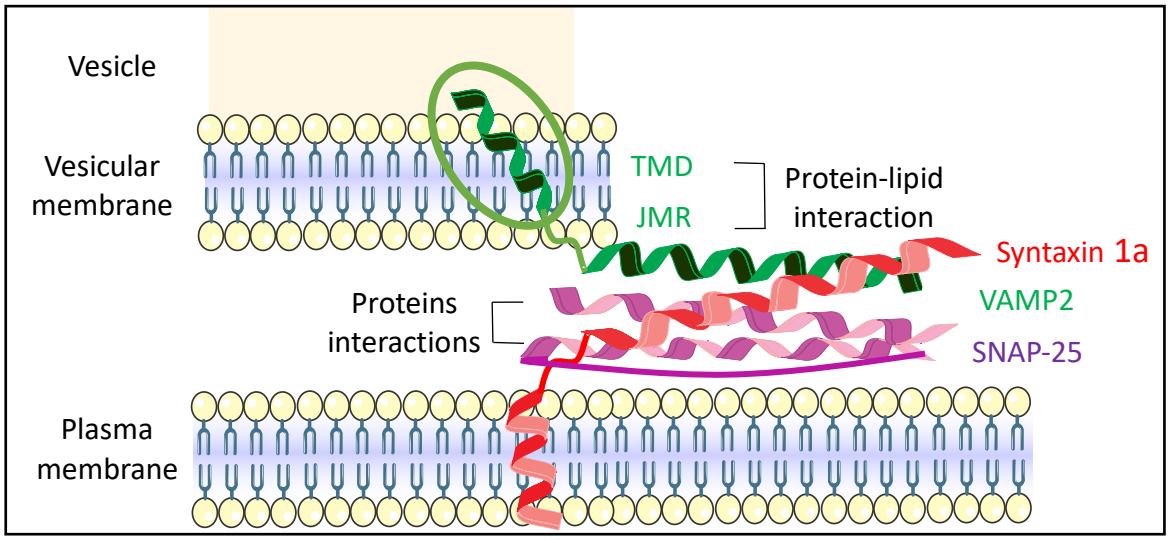

Figure 6: Representation of protein-protein and protein-lipid interaction of SNARE-mediated fusion. Interactions between the cytoplasmic parts of the SNARE proteins as well as protein-lipid interactions (TMD and JMR) are required for fusion to take place. The TMD of VAMP2 (circle in green) promotes vesicle fusion and is crucial for Ca^{2+} triggered exocytosis.

1.3.2. The role of VAMP2 TMD

The TMD of VAMP2 possess a α-helical structure which ends in the JMD (Bowen and Brunger, 2006). Its role in membrane fusion has been studied by using different techniques and models systems (Langosch et al., 2007). For example one study showed that shortening the length of the TMD arrests liposome fusion at the hemifused state (Xu et al., 2005). Two other studies, one in PC12 cells and another in chromaffin cells, demonstrated that changes in the TMD structure affected the pore conductance (Dhara et al., 2016; Han et al., 2004). Additionally, structural analysis studies have shown that the TMD structure contains around 60% of helix destabilizing β-branched amino acids (isoleucine and valine) and only around 25% of helix stabilizing amino acids (leucine) (Langosch et al., 2001). These studies were extended in 2016 by Dhara and colleagues, where they demonstrated by molecular dynamic simulations, that exchanging the TMD sequence for leucines makes the helix much less flexible than the one of the wt protein, while exchanging it for valines or isoleucines increased the helix flexibility in comparison to the wt. Additionally, electrophysiology measurements have proven that when the TMD was exchanged by leucines, secretion was diminished and the time of the fusion pore expansion was prolonged, while when it was exchanged by valines or isoleucines secretion was unchanged and the fusion pore expansion timing was reduced. Overall, these results have shown that the flexibility of the TMD, which is determined by the number of β-branched amino acids, is essential for fusion initiation as well as for fusion pore expansion (Dhara et al., 2016).

Furthermore, a correlation has been found between the number of β-branched amino acids and the size of the cargo release (Dhara et al., 2016). Indeed, v-SNARE isoforms driving fusion of small

vesicles possess less β-branched amino acids in their TMD than the ones driving fusion of large vesicles **(Figure 7B)**. For example, VAMP1 which mediates fusion of small synaptic vesicles (diameter of 40 nm) has a low number of β-branched amino acids in the TMD (22%), whereas VAMP8 which mediates fusion of mast cells and large size zymogens (diameter of around 500-800 nm) has a high number of β-branched amino acids in the TMD (77%) **(Figure 7B)**. In addition to this correlation, other studies have shown that the bending of the membrane is proportional to the size of the fusing vesicle, meaning that the larger the vesicle is the more the membrane bends **(Figure 7A)** (Kawamoto et al., 2015). Indeed, membrane bending represents a resistance to pore expansion (Kawamoto et al., 2015; Zhang and Jackson, 2010). Thus, some mechanisms to facilitate pore expansion are necessary for large vesicles. Therefore, one may hypothesize that v-SNARE variants with a high number of β-branched amino acids in their TMD are a functional crucial adaptation to guarantee the rapid fusion pore expansion and the cargo release. To confirm this hypothesis, the VAMP2 protein was used and the TMD of this protein was exchanged for the one of VAMP8 or VAMP1. In this thesis, the secretion of these chimeric mutants was studied by whole-cell patch camp experiments using photolytic uncaging of intracellular calcium.

(A)

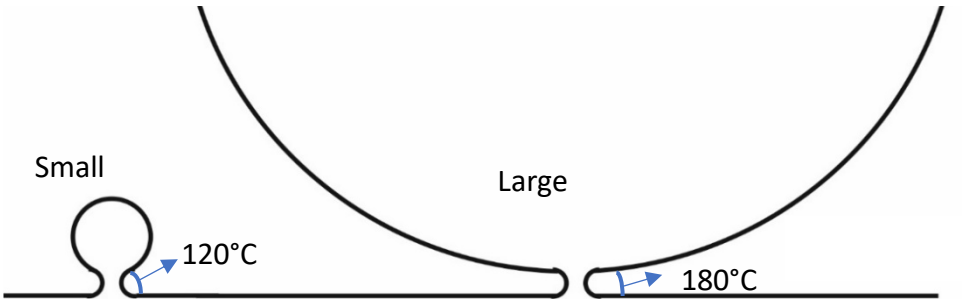

(B)

vesicle size	vesicle type (diameter)	v-SNARE isoform (M. musculus)	Transmembrane domain N term. C term.	no. / % of V or I in the N-terminus
small	small synaptic vesicles (40 nm)	Synapto-brevin 1	^{93}KNCK MM**I**MLGA**I**C AIIVVVIVI YFFT^{118}	**2** / 22
inter-mediate	small synaptic vesicles (40 nm) chromaffin (120 nm), lytic (250 nm) and insulin (240 nm) granules	Cellu-brevin	^{78}KNCK MWA**I**G**I**S**V**L VIIVIIIIV WCVS^{103}	**3** / 33
		Synapto-brevin 2	^{91}KNLK MM**II**LG**VI**C AIILIIIIV YFST^{116}	**4** / 44
large	mast cell and zymogen granules (500-800 nm)	VAMP7	^{185}KNIKLT**IIIIIV**S**IV** FIYIIVSLLCGGFTW^{215}	**8** / 73
		VAMP8	^{72}KNVK M**IVII**C**VIV** LIIVILIIL FATG^{97}	**7** / 77

Figure 7. The number of ß-branched amino acids within the different v-SNARE TMDs appears to be evolutionarily adapted to the vesicle size. (A) Correlation between the vesicle size and the degree of membrane bending, the numbers shown as the degree of membrane bending are exemplary. **(B)** Table with the correlation between the number of β-branched amino acids in the N-terminal of the TMD and the size of the vesicle release by the different isoforms. The amino acids residues of the TMD of the different v-SNARE isoforms are coloured in red, the bold amino acids represent the β-branched amino acids within the N-terminal. The information about the vesicle diameters were taken from different sources; small synaptic vesicles (Takamori et al., 2006) chromaffin granules (Borisovska et al., 2005), cytotoxic T-cell lytic granules (Ming et al., 2015), insulin granules (Fava et al., 2012), mast cell granules (Alvarez de Toledo et al., 1993), zymogen granules (Nadelhaft, 1973). The sequences were obtained from UniProt database. (Figure modified from Dhara et al., 2016).

1.4 The role of lipids in exocytosis

Besides proteins, lipids are also important for fusion (Gasman and Vitale, 2017). Indeed, membrane curvature is influenced by the molecular shape of the lipid molecule. While lipids with an inverted cone-shape promote a positive membrane curvature, those with a cone shape promote a negative one (Brown, 2012) **(Figure 8A)**. The different effects of lipids with opposing curvatures for membrane fusion indicates that exocytosis proceeds through well-defined lipidic intermediates (Amatore et al., 2006; Zhang and Jackson, 2010). For example, the membrane stalk formed by fusion of the proximal leaflets between the vesicle and the plasma membrane adopts a net negative curvature

compared to the unfused bilayer (Langosch et al., 2007) **(Figure 8B)**. Consequently, loss of negative curvature promoting phospholipids in these contacting leaflets should hinder fusion (Churchward et al., 2005). Experiments done in PC12 cells have shown that decreasing the levels of cholesterol in these cells reduces the extent of regulated dopamine secretion (Chamberlain et al., 2001). Other studies extended these findings by showing that reduced dopamine secretion may be due to the loss of negative curvature, which is conferred by the cone-shaped structure of cholesterol (Churchward et al., 2005). Yet, previous studies have also often presented opposing results regarding the impact of membrane-curvature promoting phospholipids on Ca^{2+}-regulated exocytosis. Therefore, experiments presented in this thesis were designed to study how lysophosphatidylcholine (LPC, positive curvature promoting), and oleic acid (OA, negative curvature promoting), affect Ca^{2+} triggered secretion when they are inserted into either the inner or the outer monolayer.

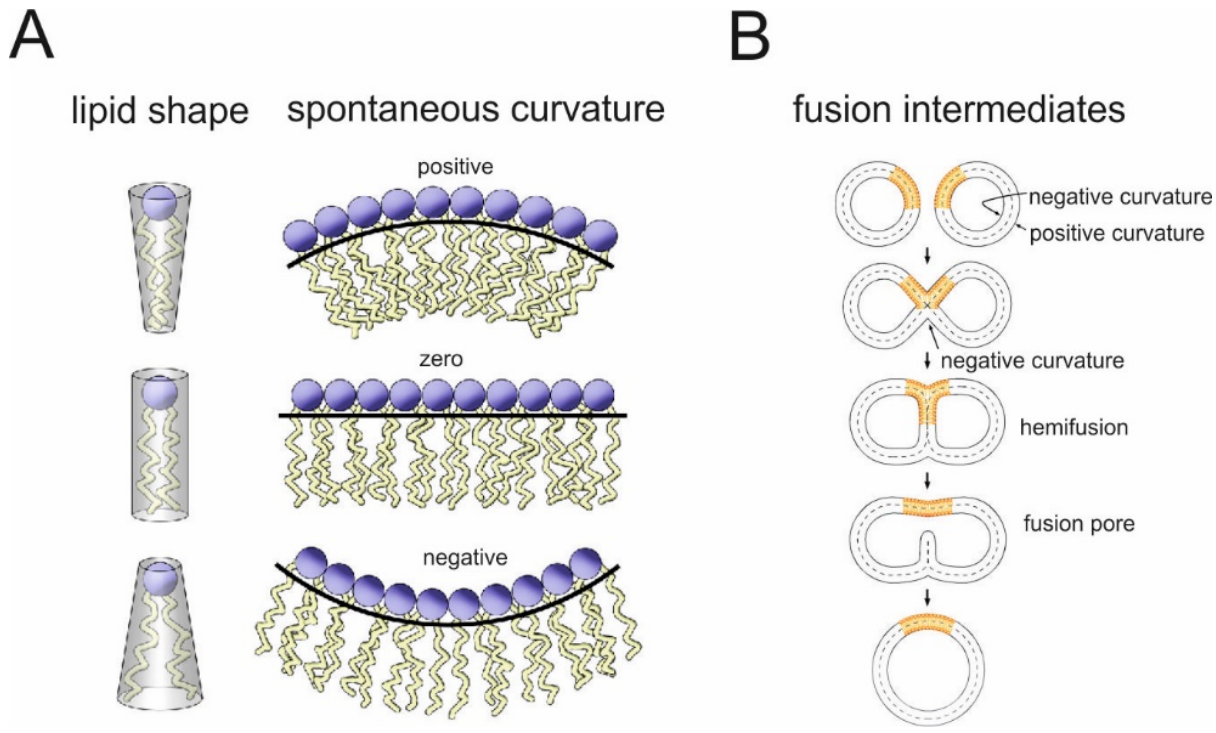

Figure 8. The influence of the lipid molecular shape on spontaneous membrane curvature. (A) Depending on the lipid shape different spontaneous curvatures can be differentiate. An inverted cone-shaped like LPC promotes a positive curvature while a cone-shaped like OA promotes a negative curvature **(B)** Lipid arrangement in the fusion intermediates. A spherical lipid particle (small vesicle or liposome) is form in the outer monolayer of lipids with positive intrinsic curvature like lysophosphatidylcholine (LPC) and in the inner monolayer with negative intrinsic curvature like oleic acid (OA). At the stalk structure or at the hemifusion diaphragm the outer monolayer adopts a negative curvature *(Brown, 2012; Langosch et al., 2007).*

1.5 SNARE regulatory proteins

SNARE proteins assembled spontaneously, therefore regulatory proteins are needed to avoid this spontaneous assembly and so, to avoid uncontrolled fusion. These proteins are called SNARE regulatory proteins and they exert an important role in regulating fusion. Among these proteins synaptotagmin and complexin have a crucial role in preventing full zippering of the SNARE complex (Rizo and Xu, 2015).

1.5.1 Structure and function of complexin II

Complexin, also known as synaphin, is a small cytosolic protein that binds with high affinity to the already assembled SNARE complex and acts as its regulator (Mohrmann et al., 2015). So far, four isoforms of complexin (Cpx) have been identified in vertebrates, CpxI-IV. Complexin I, 18 kDa protein and Complexin II, 19 kDa protein, are highly expressed in neurons and conserved among the animal kingdom (McMahon et al., 1995). Cpx II but not the others isoforms, is expressed on chromaffin cells (Cai et al., 2008). Cpx III (17.6 kDa) and Cpx IV (18.3 kDa) are the only isoforms expressed in retinal ribbon synapses (Reim et al., 2005). Among all these isoforms, Cpx I and Cpx II show higher sequence conservation among the species and higher affinity to bind to the SNAREs than the other two isoforms (Pabst et al., 2002). It has been shown that Cpx II ko mice do not show any phenotypic change while Cpx I ko mice suffers from ataxia, have sporadic seizures, are not able to reproduce and die a few months after birth (2-4 months). Moreover, the double mutant of both isoforms dies few hours after birth (Reim et al., 2001). Altogether, this shows how important this protein is for the organism.

Several studies, *in vivo* and *in vitro*, in many different cell types like neurons, chromaffin cells, mast cell lines and sperm cells among others, have been done over the years to try to unravel the function of complexin in exocytosis (Kaeser-Woo et al., 2012; Makke et al., 2018; Roggero et al., 2007; Tadokoro et al., 2005). Despite all the studies, the function of complexin remains controversial, because depending on the cell type and the approach used, the function differs from inhibitor to facilitator (Brose, 2008). Liposome fusion assays showed that the addition of complexin inhibits SNARE fusion (Schaub et al., 2006). Other studies in mouse and bovine chromaffin cells demonstrated that overexpression of the Cpx II isoform reduces premature exocytosis (Archer et al., 2002; Makke et al., 2018). In the same line of reasoning, the absence of Cpx II in chromaffin cells increases tonic release at high calcium levels (Dhara et al., 2014). A similar phenotype was published in mass cultured cortical neurons where the knockdown of Cpx I/II displayed an increase in the spontaneous release (Yang et al., 2013). Whereas, concerning these experiments it has to be taken

into account that the knockdown of these isoforms increases the expression levels of Cpx III/IV, meaning that the phenotype observed can be, at least in some extent, due to the increase of the expression level of these isoforms (Yang et al., 2013). Overall, most of the studies provide evidences that the central role of complexin is to inhibit premature vesicle exocytosis. However, it should be note that several studies where complexin was not present showed a significant decreased in evoked release, which means that this protein may also have a facilitating role in synchronous neurotransmitter release (Tang et al., 2006; Xue et al., 2008). For example, a study done in chromaffin cells using Cpx II ko cells, exhibited not only a reduction of the synchronous release caused by the premature release, but also a reduction in the rate of the synchronous release and a delay of the response (Dhara et al., 2014). The longer release kinetics and the delay agree with a facilitating role of complexin. Taking into account all the studies, it can be concluded that complexin has a dual role, a facilitating and an inhibitory role (Mohrmann et al., 2015). In order to understand the mechanism behind this dual function, studies on the different regions of Cpx were performed **(Figure 9)**. It has been shown that the N-terminal domain facilitates neurotransmitter release in mouse neurons (Xue et al., 2010) and accelerates fusion of primed vesicles in chromaffin cells (Dhara et al., 2014), meaning that this domain promotes fusion. The central helix is the main binding site of Cpx with the SNARE proteins, therefore it is essential for fusion (Xue et al., 2007). Finally, the two other domains of complexin, the accessory-α-helix (AH) and the C-terminal domain (CTD) have an inhibitory role (Mohrmann et al., 2015). Although it is well known that AH has an inhibitory function, the mechanisms underlying this function are the subject of debate. Different studies have shown that depending on the model use and the experimental approach, different outcomes concerning the mechanism of inhibition of the AH were described (Cho et al., 2014; Giraudo et al., 2009). Some studies proposed that it binds directly to the SNAREs (Bykhovskaia et al., 2013; Cho et al., 2014; Giraudo et al., 2009; Kummel et al., 2011; Yang et al., 2010) or that the AH has electrostatic interactions with membranes (Trimbuch et al., 2014), or even that it stabilizes the central Cpx helix and its SNARE binding through secondary structure interactions (Chen et al., 2002). The same problem is observed with the C-terminal region of Cpx, it is known to inhibit fusion but the mechanism by which this inhibition takes place are not clear (Mohrmann et al., 2015).

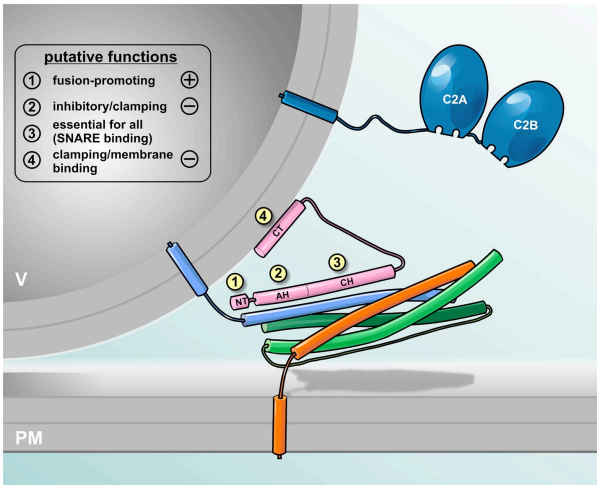

Figure 9. Schematic drawing of Complexin II binding to the SNARE complex. Complexin (pink) binds to the SNARE complex (synaptobrevin: blue, syntaxin: orange, SNAP-25: green). Synaptotagmin with the two binding calcium domains (C2A and C2B) is shown in dark blue. The N-terminal of complexin enhances fusion, the AH and the C-terminal clamps fusion and the CH binds to the SNARE complex. (Mohrmann et al., 2015)

Overall, Complexin is crucial for regulating calcium triggered exocytosis. In spite of knowing the role of the different regions of Complexin, the molecular mechanism of the clamp function of both, the C-terminus and the AH are under debate. That is why, in the second part of this thesis, the underlying mechanism behind the role of these two regions was studied taking advantage of the chromaffin cell model, which express only one Complexin isoform, Complexin II. Complexin II is a 134 aa protein containing four defined regions: The N-terminal (1-27 aa), the accessory α-helix (28-47 aa), the central helix (48-72 aa) and the C-terminal (73-134 aa) **(Figure 10)**. To perform these studies, state-of-the-art electrophysiology and imaging tools were used.

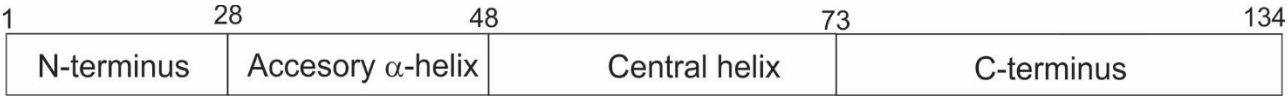

Figure 10. Cartoon showing Cpx II regions. The Cpx II protein contains 134 aa which are divided in four regions, the N-terminal (1-27 aa), the accessory alpha helix (28-47 aa), the central helix (48-72 aa) and the C-terminal (73-134 aa).

1.5.2 Synaptotagmin

Synaptotagmins are 65 kDa proteins, so far 17 isoforms of Synaptotagmin have been identified (Dean et al., 2012). Their main role is the regulation of calcium dependent fusion by acting as calcium sensors (Wolfes and Dean, 2020). The structure of Synaptotagmins consists of a luminal tail, a transmembrane domain and two cytoplasmic C2, calcium sensors domains: C2A and C2B (Perin et al., 1991). Among all the isoforms, Synaptotagmin I (Syt I) has been studied in detail because of its function on mediating ultrafast exocytosis in neurons and neuroendocrine cells (Wolfes and Dean, 2020). Despite all the studies done on Syt I, the mechanisms underlying its function are still arguable (Park and Ryu, 2018). Electrophysiological experiments done on hippocampal neurons have shown that the absence of Syt I diminishes fast synchronous exocytosis, pointing out that this protein is a

Ca^{2+} sensor for synchronous release (Geppert et al., 1994). One of the possible mechanisms by which Syt I may mediate fusion is by removing Complexin from its binding to the partially zippered SNARE complex (Zhou et al., 2017). Indeed, high resolution crystal structures studies have shown that a tripartite interface (SNARE- Complexin- Syt I) keeps the SNARE complex partially zippered until the binding of Ca^{2+} to Syt I. Then, once there is a Ca^{2+} binding, this provokes full zippering of the complex by the withdraw of Complexin (Zhou et al., 2017). However, this model is being debated because of the lack of direct evidences (Park and Ryu, 2018). Another model to explain the facilitation function of Syt I is the one proposing that this protein may cause membrane curvature by the insertion of calcium to the C2AB domain (Chernomordik and Kozlov, 2003). This model has been shown by theoretical simulation predictions, but experimental data has not yet proved it. It is also thought that the C2A and C2B domains causes membrane bridging (Arac et al., 2006) and therefore may decrease the energy barrier by dehydrating the lipid bilayer (Park and Ryu, 2018). Altogether, it is yet not clear how calcium triggers Syt I to initiate fusion, whether it is through its binding to the SNARE complex or to the membrane. Also, the interaction of Complexin with Synaptotagmin to control SNARE clamping still needs to be elucidated.

1.6 Chromaffin cells, a model for studying Ca^{2+}-triggered exocytosis

Chromaffin cells are neuroendocrine cells located in the medulla of the adrenal glands (located on top of both kidneys). They derived embryonically from the same precursor as the sympathetic neurons, the neural crest (Morgan and Burgoyne, 1997). The function of these cells is to secrete into the blood stream in a calcium dependent manner, mainly adrenaline and noradrenaline but also dopamine and two peptides, neuropeptide Y and [Met]enkephalin. The adrenal glands participate in the fight-or-flight response by releasing adrenaline and noradrenaline, this response is orchestrated by the sympathetic nervous system (SNS). Indeed, in a dangerous situation, the SNS is activated. This activation leads to acetylcholine released by the sympathetic splanchnic nerves, which in turn activates neuronal-type nicotinic acetylcholine receptors on the membrane of the chromaffin cells (Sala et al., 2008). This activation is in charge of the liberation of catecholamines into the bloodstream. The catecholamines that will be liberated, are previously kept in large dense-core vesicles (LDCV), which have a diameter of about 120 nm (Stevens et al., 2011; Wu et al., 2009a). The exocytotic machinery of chromaffin cells shares many common characteristics with the one of the central nervous system. They both use the same proteins for exocytosis (Morgan and Burgoyne, 1997), they are both calcium dependent and have two steps of maturation before the fusion, docking and priming (Stevens et al., 2011). These common characteristics makes chromaffin cells a suitable

model to study exocytosis. Nevertheless, there are some differences between chromaffin cells and neurons. For example, while neurons release their neurotransmitters in the active zone, chromaffin cells do not have a specific site of release and so they can release their cargo all over the cell surface (Stevens et al., 2011). Besides the common characteristic, several features of chromaffin cells makes them suitable to study exocytosis. For example, their round shape allows controlling membrane voltage and thereby to measure capacitance increase. Also, single vesicle exocytosis can be easily measured by placing the carbon fiber amperometry anywhere in the cell surface (Bruns, 2004). Furthermore, the control of the intracellular solution facilitates the study of the different releasable pools (Heinemann et al., 1994). Taking all together, the common features of the chromaffin cells with neurons and the advantages of these cells, it can be concluded that this model system is very suitable to study Ca^{2+} triggered exocytosis. Therefore, we used this model for our experiments.

1.6 Aim of the study

The SNAREs and their regulatory proteins are critical for membrane fusion (Rizo and Sudhof, 2002). However, despite extensive studies conducted over the last decades, the underlying mechanistic actions of these proteins remain uncertain. Overall, this thesis aims to address two main points to shed light on the molecular mechanism of these proteins in membrane fusion:

1 In the first aim, we studied the role of different v-SNARE TMD variants and membrane curvature modifying phospholipids in facilitating membrane fusion. We were specifically interested in determining how different TMD variants, which release different size cargo molecules, affect fusion. For this purpose, we generated two chimeric mutants by exchanging the TMD of VAMP2 for the TMD of VAMP1 or VAMP8. In addition, we studied two membrane curvature modifying phospholipids: Oleic acid (cone shaped) and Lysophophatidyl choline (inverted cone shape). To study the impact of the chimeric mutants and the phospholipids, we used whole cell capacitance measurements combined with photolytic uncaging of intracellular calcium.

2 In the second aim, we studied the role of the inhibitory regions of Complexin (Dhara et al., 2014). Previous studies proposed that the C-terminal domain and the accessory α-helix exert an inhibitory role, however, the mechanisms are uncertain (Mohrmann et al., 2015). The starting point of this project was the observation that Cpx II C-terminus and SNAP25-SN1 show a strong degree of structure similarity, suggesting a possible competition between both domains for binding to the SNARE proteins. To study this further, we generated chimeric mutants where the C-terminal domain of Cpx II was exchanged with that of SNAP25-SN1. Furthermore, to better understand the inhibitory action of the accessory α-helix of Complexin we studied the possible competition between this region and VAMP2 (Giraudo et al., 2009). For this purpose, we generated two Complexin mutants, one which resembles and one which differs from VAMP2. We used whole cell capacitance measurements combined with photolytic uncaging of intracellular calcium to study how these mutants affect fusion and therefore better understand the inhibitory mechanisms of both the C-terminus domain and the accessory α-helix of Complexin.

Overall, the two main axes studied in this thesis provides further insights underlying the molecular mechanisms involved in the exocytosis process.

2. Materials and Methods

2.1 Transgenic mice

Experiments were performed using chromaffin cells from various mouse genotypes: wild type, Complexin II knockout, v-SNARE double knockout (Synaptobrevin II and Cellubrevin) and v-SNARE Synabtobrevin II knockout.

2.1.1 v-SNARE double knockout mice

v-SNARE double knockout (dko) and Synaptobrevin II knockout (Syb II ko) mice die at birth (Borisovska et al., 2005), so pregnant mice were sacrificed by CO_2 asphyxiation followed by cesarean section at gestation stage E17.5- E18.5 to collect their embryos. The knockout embryos were identified by phenotypical features such as a tucked posture and absence of spontaneous movements and sensorimotor reflexes and they were sacrificed by decapitation. (Borisovska et al., 2005; Schoch et al., 2001) **(Figure 11)**. Polymerase chain reaction (PCR) was performed on the tails of embryonic mice biopsies to ensure that the embryos used for the experiment carried the desired mutation. The breading, the maintenance and the killing of the animals was done according to the German Animal Health Care Regulations. Syb II and Ceb heterozygous mouse strains were provided by Thomas Sudhof (Howard Hughes Medical Institute, The University of Texas Southwestern Medical Center, Dallas, USA) and by Jeffery E.Pessin (University of Iowa, Iowas, USA) respectively.

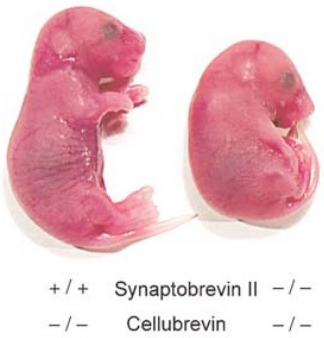

Figure 11. Phenotype of the double v-SNARE ko (Syb II/Ceb) at E18.5. On the right the v-SNARE dko phenotype presents a tucked postured, on the left the littermate (Syb wt, Ceb ko) showing no phenotypical deficiencies (adapted from (Borisovska et al., 2005).

2.1.2 Complexin II ko mice

Complexin II knockout (Cpx II ko) mice were provided by Dr. N. Brose (MPI, Göttingen, Germany). These mice do not show any visible phenotype (Reim et al., 2001) and were obtained by crossing heterozygous Cpx II mice. In this case, the mice were used on day 0 to day 2 postnatal, they were killed by decapitation.

2.2 Genotyping

The genotyping was done on tails biopsies.

2.2.1 Complexin II genotyping

- Extraction of genomic DNA

The extraction of the deoxyribonucleic acid (DNA) was done with the help of an Extracta™ DNA Prep kit (Quanta Bio). Extraction Reagent (100 microliters (µl)) was placed in the tails. The tails were incubated (30 minutes at 95 °C) and the Stabilization Reagent (100 µl) was added. The mixture was then centrifuged in a table-top centrifuge (2 minutes at 13.000 revolutions per minute (rpm)), the DNA mixture (1 µL) was added to the PCR master mix.

- Primers and master mix for the PCR

The primers were all purchased in Eurofins Genomics (Germany)

-CpxII wildtype reaction primers:

✓ Forward primer: 5′-CGG CAG CAG ATC CGA GAC AAG-3′

✓ Reverse primer: 5′-GAG AGG GGC ATG AAG TCA AGT CAG-3′

-CpxII mutant reaction primers:

✓ Forward primer: 5′-CGC GGC GGA GTT GTT GAC CTC G -3′

✓ Reverse primer: 5′-CAG GCA CAC TAC ATC CCA CAA ACA -3′

Mix for 1 PCR reaction

Ingredients	Quantity (µl)
Double Distilled Water (sigma)	12.5
$MgCl_2$ (Thermo Scientific)	0.5
Fw primer (wt/mutant)	1
Rev primer (wt/mutant)	1
HS Red mix	10
DNA	1

-Cpx II wildtype

Temperature (°C)	Time	
94	5 min	
94	**30 s**	41
64	**45 s**	
72	**1 min**	
72	7 min	
4	Pause	

Expected band size: 600 base pairs

- Cpx II mutant

Temperature (°C)	Time	
94	5 min	
94	**45 s**	41
59.1	**30 s**	
72	**1 min**	
72	7 min	
4	Pause	

Expected band size: 350 base pairs

2.2.2 Genotyping for v-SNARE dko

- Extraction of genomic DNA

The extraction of the DNA was done within 2 days using the ethanol/isopropanol extraction method:
-**Day 1**: addition of 400 µl of SNET-Bufer (in milimolar (mM): 20 Tris-HCl, 5 EDTA and 100 NaCl; 1% SDS) and 8µl of Proteinase K (Qiagen) to each tail. The incubation of this mixture was done overnight (56 °C and 550 rpm)

-**Day2**: Eppendorfs were centrifuged (13.000 rpm for 5 minutes) and the supernatant was transferred into a fresh Eppendorf. DNA was precipitated with 100% isopropanol (Merck)) (400 µl) and centrifuge (13.000 rpm for 10 min). The supernatant was discarded and 100% ethanol (Merck) was added to the pellet (400 µl.) Another centrifugation was done (13.000 rpm for 5 minutes), the ethanol was discarded and the Eppendorfs containing DNA were kept in the shaker (37 °C and 550 rpm until all the remaining ethanol was evaporated). Sigma H_2O (200 µl) was added to the precipitated DNA and incubated for 1 hour (37 °C and 550 rpm).

- Primers and master mix for the PCR:

-Syb II wild type reaction primers:

✓ Forward primer: 5´-GCC CAC GCC GCA GTA CCC GGA TG-3`

✓ Reverse primer: 5´-GCG AGA AGG CCA CCC GAT GGG AG -3`

-Syb II mutant reaction primers:

✓ Forward primer: 5´- CAC CCT CAT GAT GTC CAC CAC -3`

✓ Reverse primer: 5´- CAG CAG ACC CAG GCC CAG CG-3`

-Ceb wildtype reaction primers:

- ✓ Forward primer: 5´- CAG ACT CAC TGA ACC TAT GAC AG-3`
- ✓ Reverse primer: 5´- CTC ACC TGA TAC ATG CAG CAC-3`

-Ceb mutant reaction primers:

- ✓ Forward primer: the primer used is the same as the one of the Ceb wild type
- ✓ Reverse primer: 5´- CAG CGC ATC GCC TTC TAT CGC-3`

Mix for one PCR reaction of Syb II

-SybII wildtype

Ingredients	**Quantity (µl)**
Double Distilled Water	13.75
$MgCl_2$	0.25
Fw primer (wt)	1
Rev primer (wt)	1
Kapa (sigma)	8
DNA	2

-SybII mutant

Ingredients	**Quantity (µl)**
Double Distilled Water	14
-	-
Fw primer (mutant)	1
Rev primer (mutant)	1
Kapa	8
DNA	4

Mix for 1 PCR reaction of Ceb

- Ceb wildtype

Ingredients	**Quantity (µl)**
Double Distilled Water	12.5
$MgCl_2$	0.5
Fw primer (wt)	1
Rev primer (wt)	1
Quanta (quanta bio)	10
DNA	1

- Ceb mutant

Ingredients	**Quantity (µl)**
Double Distilled Water	12.5
$MgCl_2$	0.5
Fw primer (wt/mutant)	1
Rev primer (wt/mutant)	1
Quanta (quanta bio)	10
DNA	1

-PCR for SybII wt

Temperature (°C)	Time	
95	4 min	
95	**30s**	35
60	**30s**	
72	**2 min**	
72	10 min	
4	Pause	

Expected band size: 500 base pairs

-PCR for SybII ko, Ceb wt and Ceb ko

Temperature (°C)	Time	
95	5 min	
95	**50 s**	40
55	**45 s**	
65	**1 min 30 s**	
65	10 min	
4	Pause	

Expected band size sybII ko: 550 base pairs

Expected band size ceb wt: 520 base pairs

Expected band size ceb wt: 320 base pairs

2.2.3 Agarose gel electrophoresis

The PCR samples were loaded onto an agarose gel electrophoresis to separate the amplified DNA by length. The 1.8% TAE agarose gel was done by dissolving 1.8 g of agarose in 100 ml 1X TAE buffer (40mM Tris-acetate and 1mM EDTA). This mix was heated in the microwave until the agarose was completely dissolved and poured into a chamber containing 4 µl of ethidium bromide. Ethidium bromide intercalates into the DNA, allowing its visualization upon ultraviolet illumination (UV). When the gel was solidified it was allocated in an electrophoresis chamber (Bio-Rad) loaded with 1x TAE. The PCR samples and a DNA size marker were loaded on the gel wells and electrophoresis was executed for 20 min at a voltage of 120 V. When the migration of the samples was completed, the gel was placed under UV light to visualize the DNA bands.

2.3 Chromaffin cells preparation and culture

-Culture solutions

Locke´s solution

Ingredients	Quantity (mM)
NaCl	154
KCl	5.6
$NaHCO_3$	3.6
Glucose	5.6
Hepes	5.0
pH: 7.3, Osm:320 mosm/kg, filter the solution and store at 4°C	

Culture medium

Ingredients	Quantity (ml)
DMEM (Gibco)	100
Penicillin-Streptomycin (gibco)	0.4
Insulin-Transferrin-Selenium-X (Gibco)	1
Filter the solution and equilibrate it in the CO_2 incubator	

Enzyme solution

Ingredients	Quantity
DMEM	250 ml
l-cysteine	250 mg
$CaCl_2$	2.5 ml (100mM)
Na_2EDTA	2.5 ml (50mM)
pH:7.3, Osm:340 mosm/kg, filter the solution and store at -20°C	

Inactivation solution

Ingredients	Quantity
DMEM	225 ml
Fetal Calf Serum	25 ml
Trypsin Inhibitor	625 mg
Albumin	625 mg
Filter the solution and store at -20°C	

-

-Dissection of the adrenal glands and chromaffin cells culture

As described above, the experiments were performed on mice chromaffin cells prepared from embryonic or newborn mice. Before the dissection of the adrenal glands, 25 units of papain were added to a pH equilibrated 2 ml enzyme solution tube. The enzyme solution was kept at 37 °C during the time of the gland's dissection (~15 minutes). Adrenal glands were prepared using forceps and intermittently stored in a small drop of cold Locke's solution. Glands were cleaned using fine forceps (to avoid contamination with erythrocytes or fibroblasts) and incubated with 200 µl of enzyme solution (37 °C for 18 minutes). Glands were washed multiple time with 1 ml culture medium, before adding the inactivation solution, which served to inactivate papain (200 µl inactivation solution, 37 °C for 18 minutes). Glands were triturated mechanically by pipetting them up and down using a yellow pipette tip. Precautions have been taken to avoid the formation of air bubbles which could compromise the quality of the cells. Once the glands were triturated, 400 µl of culture medium was

added and the cell suspension was distributed into a 6 well plate (two glands were used for each 6 well plate) and kept in the incubator (30 min at 37 °C and 11% CO_2) to allow the cells to settle. Culture medium was added to the 6 well plate (3 ml per well) and the cells were used after 2-3 days for electrophysiological or immunohistochemical experiments.

2.4 Semiliki Forest Virus (SFV) transfection in chromaffin cells

- Solutions

Chymotrypsin (2mg/ml)

▪ **Ingredients**	**Quantity**
Chymotrypsin	20 mg
OptiMEM (Gibco)	10 ml
Filter and store at -20 °C	

Activation Solution

Aprotinin (6mg/ml)

Ingredients	**Quantity**
Aprotinin	60 mg
OptiMEM (Gibco)	10 ml
Filter and store at -20 °C	

BSA (6.5mg/ml)

Ingredients	**Quantity**
Bovine serum albumine	65 mg
OptiMEM (Gibco)	10 ml
Filter and store at -20 °C.	

Inactivation Solutions

- Procedure

SFV viral particles of 200 µl were activated by adding 175 µl of Optimem, followed by 55 µl of chymotrypsin. Then, after 45 minutes at room temperature (RT) they were inactivated with 55 µl of aprotinin and 55 µl of BSA (bovine serum albumin). Then, the aliquots containing the SFV were kept in the fridge for the next day or used immediately. For the cell transfection, 60 µl of SFV were added to each coverslip. Transfected cells were used after 5.5 hours for electrophysiological experiments and after 3.5 or 5.5 hours for immunocytochemistry.

2.5. Constructs expressed in SFV

2.5.1 Complexin II

Construct	Mutation
Cpx II wt	Wt protein
Cpx II 41-134	Truncation of the protein, lacking the N-terminal and the Accessory alpha helix (AH)
Cpx II poor clamp (K26A A30K L41A)	Replacement of three amino acids (essential for the insertion of the AH in the SNARE complex)
Cpx II super clamp (D27L E34F R37A)	Replacement of three amino acids (mutations that increase the insertions of the AH into the SNARE complex)
Cpx II 1-100	Truncation of the protein, lacking the last 34 amino acids
Cpx II 1-100 helix	The last 34 amino acids of Cpx II are replaced with an artificial alpha helical domain
Cpx II 1-100 Long Chimera	The last 34 amino acids of Cpx II are replaced with the residues 44 to 77 of SNAP25-SN1
Cpx II 1-115	Truncation of the protein, lacking the last 19 amino acids
Cpx II 1-115 helix	The last 19 amino acids of Cpx II are replaced with an artificial alpha helical domain
Cpx II 1-115 Short Chimera	The last 19 amino acids of Cpx II are replaced with the residues 59 to 77 of SNAP25-SN1
Cpx II P89,97,102A	Replacement of three prolines by alanine
Cpx II K98/99A	Replacement of two lysines by alanine
Cpx II K98/99E	Replacement of two lysines by glutamic acid

2.5.2 SNAP-25

Construct	Mutation
SNAP25b	Wt protein
SNAP25b D16A/E170A	Replacement of aspartic acid and glutamic acid by alanine

2.5.3 Synaptobrevin II

Construct	Mutation
VAMP2 wt	Wt protein
VAMP2-VAMP1TMD	Replacement of the VAMP2 TMD for the VAMP1 TMD
VAMP2-VAMP8TMD	Replacement of the VAMP2 TMD by the VAMP8 TMD

2.6 Electrophysiology

2.6.1 Patch clamp setup

To perform electrophysiological measurements, mechanical stability is crucial since movements of the pipette can cause unstable recordings. Experiments were done on a stage of a microscope mounted on a vibration isolation table (MKS instruments) to reduce the external vibrations. The microscope was protected from electrical noise with a Faraday cage.

2.6.2 Patch clamp technique and its different configurations

The Patch clamp technique was invented by Erwin Neher and Bert Sakmann around 1981. This technique allows the study of electrical properties of biological membranes. Indeed, with this technique, small currents that pass through single ion channels can be recorded. Therefore, as greatest benefit, ion channels and their functionality can be directly monitored (Sakmann and Neher, 1984). Depending on the goal of the study, different patch clamp configurations can be used. The precursor to all variants is the so-called 'cell attached' configuration, which is used to record single-channel currents with little interference from the intracellular environment. To achieve this configuration, a tight seal between the electrode and the plasma membrane is formed, also called 'gigaseal' **(Figure 12B)**, which is a prerequisite for low noise recordings of single channel activity. The so-called 'whole-cell' configuration can be reached when the membrane patch at the pipette opening is ruptured by applying a short-lasting suction pulse **(Figure 12C)**. In the 'whole-cell' mode, the intracellular milieu is readily replaced by the patch pipette solution, facilitating the isolation of specific ion conductances. Two other patch clamp modes exist which permit to study single channel activity. One of these configurations is the 'Inside out' mode, which is obtained by slowly withdrawing the pipette in the 'cell attached' mode from the cell. As a result, the membrane patch under the patch pipette is separated from the rest of the membrane and the inner membrane side is

directly accessible for bath applied agents. The 'Outside out' configuration, instead, is obtained by withdrawing the electrode in the 'whole cell' mode. In this mode, single channel activity can be studied without changing the original orientation of the membranes with respect to the patch pipette. (Okada, 2012). In this thesis, the 'whole-cell' patch clamp configuration was used and the cells were infused with solutions containing defined calcium concentrations as explained below.

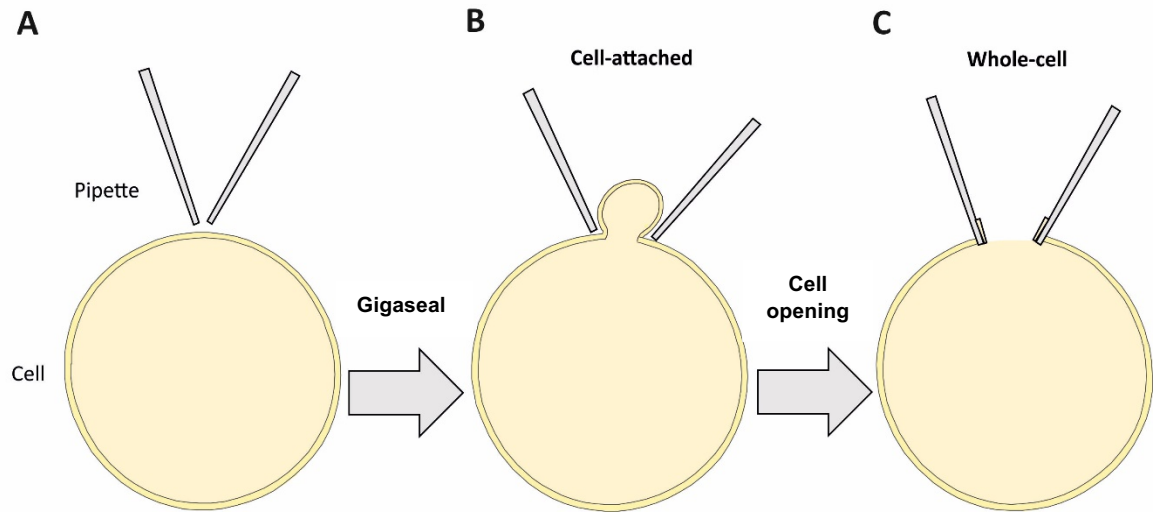

Figure 12. Experimental strategy to establish the 'whole-cell' configuration. From left to right. The electrode is close to the cell. Upon direct contact with the cell membrane, a 'gigaseal' is formed ('cell-attached' configuration). By breaking the membrane patch through the application of a short-lasting suction pulse, the 'whole-cell' configuration is achieved.

2.6.3 Capacitance recordings using 'whole-cell' patch clamp configuration

The lipid bilayer of a cell acts like an electrical capacitor (C), since it separates positive and negative charges. The differential ion distribution on both sides of the membrane, which is the consequence of different transport processes, is a general prerequisite for the excitability of all cells (Hille, 1992). The ion channels within the lipid bilayer establish selective permeabilities (or conductances, G = 1/R) for specific ions. The alternating activation of different ion conductances allows the membrane potential to depolarize or to hyperpolarize. Thus, the lipid bilayer can be electrically defined as a RC-circuit composed of a capacitor (Cm), which corresponds to the bilayer, and a resistor (Rm), which are the ion channels that allow the charges to flow. In the 'whole-cell' configuration, the pipette tip creates an additional resistance, which is also called access resistance. The access resistance (Rs) is in series with the membrane capacitance (Cm) and the membrane resistance (Rm), the latter two being connected in parallel **(Figure 13)**.

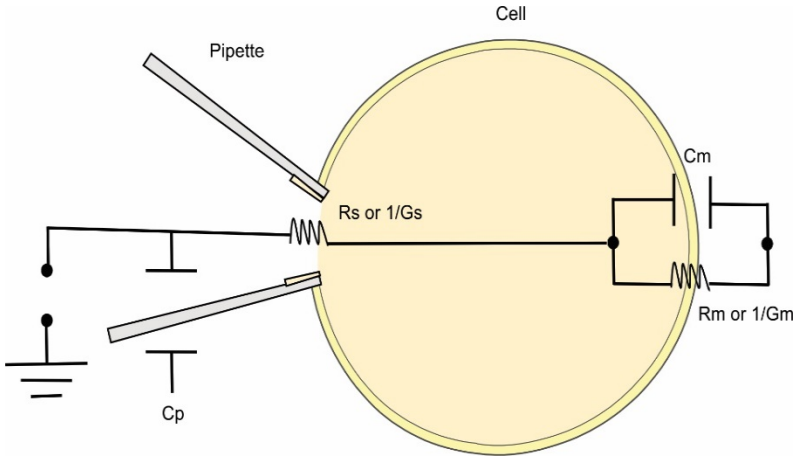

Figure 13. Electrical circuit for the whole-cell configuration. The membrane of the cell is electrically defined as the Cm connected in parallel with the Rm (~1GOhm). The patch pipette is tightly attached to the membrane by Rs (~10MOhm). The Cp is the pipette capacitance (Modified from Gillis 1995).

The membrane capacitance of cells is proportional to the surface area of the cell with a specific membrane capacitance of about 1µF/cm^2 (Cole, 1968). Therefore, the capacitance of a given cell, can either increase or decrease by processes like exocytosis and endocytosis, respectively. Step-like changes in the voltage of an RC element (ΔV) results in a current signal, which is composed of two distinct components. The initial current transient current reflects the charging current of the membrane capacitance (I_0, capacitive current). Its exponential decay (t) is largely determined by the product of Rs x Cm, since Rs<<Rm. The steady-state current (resistive current, I_{ss}) is the inversely related to the membrane resistance (Rm) according to Ohm's law. The overall time course of the current signal can be approximated by: $i(t) = (I_0 - Iss)\ exp(-t/\tau) + I_{ss}$, where τ is the time constant of the capacitive current decay **(Figure 14)**. Thanks to this equation, the parameters described in Figure 13 can be estimated by the following equations:

$Rs = \Delta V / I_0$

$Rm = \Delta V / I_{SS}$

$Cm = \tau \times (1 / Rs + 1 / Rm)$

This approach, which is also called the 'time-domain technique', has several downsides that limits its application. One of them is that current and voltage signals should not be filtered in order to obtain an accurate estimate of the maximum current amplitude (I_0). The accuracy of determining I_0 is compromised by the recording noise and thereby can lead to false estimates of Rs and Cm. The accuracy of the Cm estimate can be judged by comparison with another estimate of Cm given that the integral of the capacitive current transient (Q) divided by the voltage (U) reveals the membrane capacitance, as $Q / V\Delta = Cm$.

Another inconvenience, is that the temporal resolution of the Cm measurement is determined by the duration of the voltage steps.

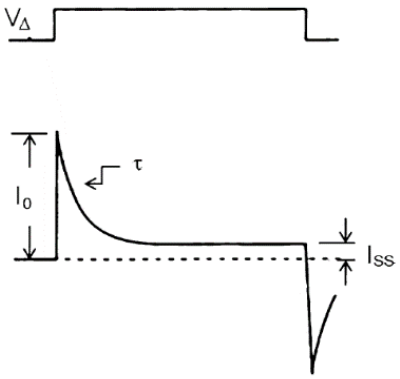

Figure 14. **Drawing showing the step voltage and the derived capacitance currents**. On the top panel the step voltage, on the lower panel the capacitance currents derived from the voltage, where *(I_0)* is the initial transient current *(I_{ss})* is the steady-state current and τ is the time constant of the decay. (Figure taken from the book patch clamp techniques, from beginning to advance protocols, Springer 2012)

One of the most used protocols for high time resolution capacitance measurements it is the so-called sinusoidal excitation. The current i(t) flows either to the resistor (1/Gm) or to the capacitor (Cm). The current flowing across a resistor can again be calculated using Ohm´s law: $I_R(t)= V(t)/R$. When a sinusoidal voltage is applied ($V(t)= Vo \cos\omega t$, where ω is the frequency) across a resistor (R) the resulting Ohm´s law is obtained: $I_R(t)= (Vo/R) \cos\omega t$. In contrast, when it is applied across a capacitor a 90° phase shift is observed between the voltage applied and the current that follows: $I_C(t)= - \omega CV\sin\omega t$. The downside of this protocol is that a sine wave can only measure two independent parameters, magnitude and phase. Therefore, for measuring a third parameter, the resistive current, the "sine wave + DC" method is used (Lindau and Neher, 1988). For this, the DC (direct current) component and two outputs of the amplifier are required.

To measure capacitance, we used the Lindau-Neher technique, which consists of applying a sinusoidal voltage or sine wave stimulus. The sine wave was of 1000 Hz, the peak-to-peak amplitude was 35 mv and the potential was held at -70 mv.

2.6.4 `Whole-cell´ measurements combined with photolytic uncaging of Ca^{2+}

Extracellular Solution (Ringer)

Ingredients	Quantity (mM)
NaCl	130
KCl	4
$CaCl_2$	2
$MgCl_2$	1
HEPES	10
Glucose	30
pH: 7.3 adjusted with NaOH, Osm:320 mosm/kg	

Intracellular Solution

Ingredients	Quantity (mM)
$CaCl_2$	3,5
Cs glutamte	110
ATP/GTP	2/0.3
Fura/Furaptra	0.2/0.3
NP-EGTA	5
pH: 7.4, Osm:300 mosm/kg	

Calcium imaging in chromaffin cells was performed with 2 synthetic calcium indicators to cover a wide range of Ca2+-concentrations (Voets, 2000). While Fura-2 (high affinity dye, Kd of 224 nM) is suitable to measure calcium below 1 µM (to estimate calcium concentrations before the UV flash) (Grynkiewicz et al., 1985), Furaptra (Kd of 25 µM a low affinity dye) provides an estimate of calcium in the micromolar range (calcium concentrations after the UV flash). Nitrophenyl-EGTA (NP-EGTA) is a photolabile calcium caging compound with a high affinity to bind calcium (Kd=80nM). Upon UV illumination, its Kd value increases to about 1 mM allowing the liberation of the caged calcium (Ellis-Davies and Kaplan, 1994).

- Technique

To study exocytosis in adrenal chromaffin cells, photolytic Ca^{2+} uncaging experiments were used. Cells were perfused during 2 minutes with the intracellular solution described above (the 'free' calcium concentration was between 500-800 nM) to build up a pool of primed vesicles. The capacitance increase recorded during this time reflects asynchronous exocytosis of chromaffin granules (in wt cells is around 150 femtofarad (fF)) **(Figure 15A, B)**. The application of a short intense UV light flash, liberated the caged calcium, generating a step like increase of intracellular calcium (calcium concentration was around 20µM) **(Figure 15C)**. As a result of that, a rapid increase (in the millisecond time range) in membrane capacitance occurred, which is also referred to as exocytotic burst (EB). The EB comprises a rapid increase reflecting exocytosis from the ready releasable pool (RRP), which is followed by a slower increase called slow releasable pool (SRP). The subsequent sustained capacitance increase (SR) most likely reflects continuous exocytosis of newly primed vesicles as long as $[Ca^{2+}]_I$ remains high (**Figure 15D)**.

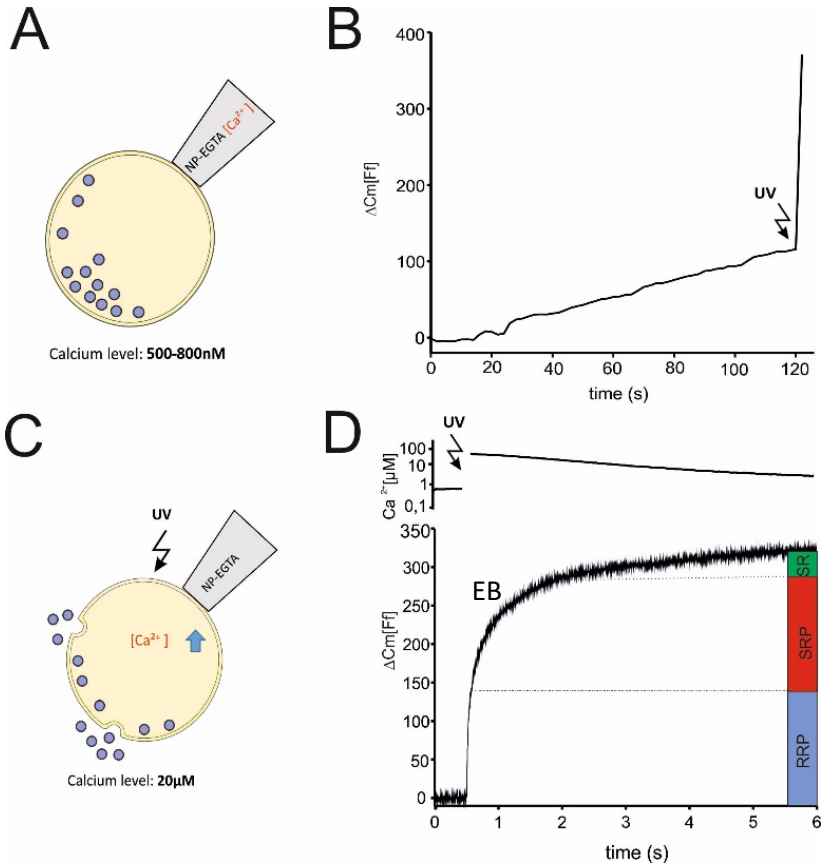

Figure 15. Drawing showing electrophysiological recordings using photolytic intracellular calcium uncaging. (A) The cell is infused with solutions containing 500-800 nM calcium to allow vesicle priming. **(B)** During the two minutes of calcium infusion a sustained increase in Cm is detected, most likely reflecting asynchronous exocytosis. **(C)** UV illumination photolyses NP-EGTA (the arrow indicates the UV flash) generating a step-like increase of the intracellular Ca^{2+} concentration **(D)** In response to the UV flash, a biphasic capacitance increase can be recorded, reflecting the initial exocytotic burst (EB = RRP + SRP) and the subsequent sustained phase of secretion (SR).

The calcium concentration before the flash should not be higher than 800 nM, because high Ca^{2+} concentrations lead to extensive premature exocytosis, thereby, diminishing the pool of primed vesicles and the magnitudes of the RRP and SRP (Voets, 2000). While the pre-flash calcium concentration is important for the magnitude of the synchronous response, the post-flash calcium concentration is important for the kinetics. A decrease in the calcium concentration in the post-flash slows down the kinetics of the RRP and SRP (Voets, 2000).

Before the development of photolytic Ca^{2+} uncaging experiments, other methods were used to study Ca^{2+} dependent exocytosis in chromaffin cells. One of this methods was the study of secretion using permeabilized cells (Bittner and Holz, 1992). With this procedure Bittner and Holz demonstrated the role of calcium in priming. However, the disadvantage of this approach is that it does not allow to resolve the fast components of exocytosis because the time resolution time is around 5 seconds. Another approach used train depolarizations in order to find evidence for different vesicle pools (Neher and Zucker, 1993). However, straight forward conclusions were hampered because the depolarization evoked Ca^{2+}-rise is spatially not uniform but rather produces sharp intracellular gradients (Gillis and Chow, 1997).

.

2.6.5 Calibration curve for fura2-furaptra mix

To provide an accurate estimate of the calcium concentration in our flash experiments, we performed a comprehensive intracellular calibration, by patching cells with solutions containing strongly buffered Ca^{2+}-concentrations (1-11). The solutions were buffered using either the calcium chelator BAPTA (low range calcium) or DPTA (high range calcium) **(Table 1)**. Patch pipette solutions were prepared as follows: 64 µl stock solution (Table 1) was mixed with 8 µl of ATP/GTP and 8 µl of the Fura2/Furaptra mix. The cellular ratio of the 340/380 nm illumination was determined after about 60 s infusion time. The inverse of the 340/380 ration as function of different $[Ca^{2+}]_I$ can be approximated by the following equation **(Figure 16,** (Voets, 2000)):

$R= R_{min}$ - R1. $[Ca^{2+}]i/([Ca^{2+}]i + K_{fura})$ - R2. $[Ca^{2+}]i/([Ca^{2+}]i + K_{furaptra})$

R_{min}: ratio at $[Ca^{2+}]i= 0$ M

R_{min} - R1 - R2: ratio when cells were perfused with the solution containing 10 mM $CaCl_2$

The fitted parameters for the calibration curve were: R_{min}: 5.34, R1: 3.65, R2: 1.44, K_{fura} : 76.8 nM, $K_{furaptra}$: 36µM

-Solutions containing BAPTA:

Solutions	Ca^{2+} mM	$CaCl_2$, µL 100 mM	BAPTA,µL 100 mM	4X Cs-Glu, µL (440Mm+NaCl+HEPES)	H_2O µL
1	0	0	328	267	405
2	13,7	137	328	252	283
3	19,2	192	328	231	249
4	23	230	328	224	218
5	25	250	328	220	202

-Solutions containing DPTA:

Solutions	Ca^{2+} mM	Mg^{2+} mM	$CaCl_2$, µL 100 mM	$MgCl_2$, µL 100 mM	DPTA µL 100 mM	4X Cs-Glu, µL (440Mm+NaCl+HEPES)	H_2O µL
6	2,8	6,5	28	65	400	205	302
7	5,3	6	53	60	400	201	286
8	9	5,5	90	55	400	195	260
9	20	3,5	200	35	400	182	183
10	25	2,5	250	25	400	175	150
11	35	0,5	350	5	400	163	82

Table 1: Preparation of the calibration solutions containing BAPTA and DPTA. For each solution the pH was adjusted with CsOH to 7, 3 and the osmolality was around 370-375mOsm/kg.

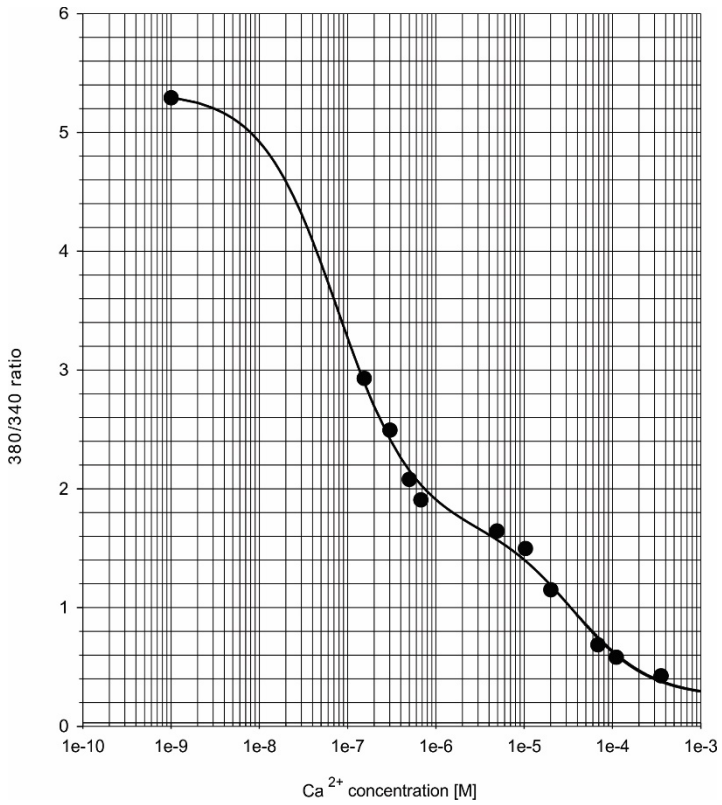

Figure 16. Cellular calibration curve for a Fura2/Furaptra mix. Ratios of the fluorescent signals measured in chromaffin cells during illumination at 380nm and 340nm, 11 different solutions containing different calcium concentrations are used. Each point represents the average of 3 different cells. The ratio is taken when the cell is sufficiently perfused.

2.6.6 Recording and analysis

For the whole cell patch clamp recording, pipettes from 4.5 to 6 MΩ were used. They were pulled using a Sutter instrument puller and then polished with a heating wire. To acquire the data, the PULSE software which was connected to an EPC10 amplifier (HEKA Elektronik, Lambrecht, Germany) was used. A monochromator (Polychrome IV, TILL Photonics, Planegg, Germany) and a flash lamp (Rapp OptoElectronics, Hamburg, Germany) were also essential during the measurement. The flash lamp enabled rapid uncaging of the calcium. The monochromator allows subsequently for limited photolysis in order to compensate for Ca^{2+}-extrusion, thereby, triming up the Ca^{2+}-stimulus in a step like fashion **(Figure 15D, upper panel).** Furthermore, the monchromator was used to identify positive transfectants expressing the enhanced green fluorescence proteins (EGFP) as marker protein. To observe the capacitance before and after the flash, we used the X-Chart plug-in module of the Pulse software. Analysis of the pre-flash and post-flash data were done using IgorPro, with customized Igor routines.

2.7 Immunocytochemistry

- Solutions

1x PBS

▪ Ingredients	Quantity
10 x PBS	100 ml
DDW	900 ml
pH: 7.2-7.4 osm:290-300mosm/kg	

4% PFA

Ingredients	Quantity
PFA	2 g
1x PBS	50 ml
Warm the mix until it is dissolved and once it is dissolved and at RT adjust pH:7,4	

Blocking buffer

Ingredients	Quantity
BSA	3.75 g
Triton x 100	0,185 g
1x PBS	125 ml

Quenching buffer

Ingredients	Quantity
NH_4Cl	0.1 g
1x PBS	125 ml

- Procedure

Immunocytochemistry was used to determine the expression levels of the different mutant constructs, as well as their subcellular localization. For both studies, the same procedure was utilized. Chromaffin cells were infected with SFV during 3.5 h for localization experiments and 5.5 h for expression level analysis. Cells were gently washed with 1x Phosphate Buffer Saline (PBS) and immediately fixed using 4% Paraformaldehyde (PFA) for 30 minutes. The cells were washed 3 times with 1x PBS, quenching buffer was added (10 minutes) and then blocking buffer (1 hour). The primary antibody diluted in blocking buffer was incorporated and let overnight at 4 °C. Blocking buffer was used (3 times, 5 minutes each wash) to wash out the primary-antibody and the secondary-antibody was introduced (1.5 hours in dark conditions). To wash out the secondary-antibody 1x PBS was used (4 times, 15 minutes each). The coverslips were mounted in the slices by using glycerol and sealed.

Primary antibodies:

-Synaptobrevin II 69.1; mouse monoclonal (R.Jahn) (1:1000)

-Complexin II 1-100; rabbit-polyclonal (1:5000)

-Cellubrevin TG-21; rabbit-polyclonal (Synaptic Systems)

-Complexin II; rabbit-polyclonal (1:1000) (Synaptic Systems)

Secondary antibodies: (1:1000)

-Alexa Fluor 555 Goat anti-rabbit (Invitrogen)

- Alexa Fluor 555 Goat anti-mouse (Invitrogen)

-Alexa Fluor 488 Goat anti-rabbit (Invitrogen)

2.7.1 Epifluorescence microscopy

Epifluorescence microscopy was used to determine the expression levels of the different mutant constructs of VAMP2 and Cpx II. The microscope used for this goal was a Zeiss Axio Vert 200. Epifluorescence images (8 bit encoded) were taken with an AxioCam MRm-CCD camera (Carl Zeiss) and analyzed with Image J. For the analysis, the nucleus area was subtracted from the cell area and the exposure time was taken into account to determine the expression levels of the different groups.

2.7.2 Structured Illumination Microscopy (SIM)

This technique was used to assess the localization of the different VAMP2 mutants. The imaging of the cells was done by using a Zeiss Axio Observer microscope with excitation light of 488 and 561 nm wavelengths and a 63x Plan-Apochromat (NA, 1.4) oil-immersion objective. For the acquisition and the processing of the SIM images the ELYRA PS.1 system and ZEN software 2011 (Zeiss) were used. Image J was needed to analyse the z-stack puncta. The Mander's weighted colocalization coefficients were determined after threshold subtraction by summing the VAMP2 pixels that colocalizes with Ceb pixels and dividing them by the total VAMP2 pixels (Bolte and Cordelieres, 2006; Manders et al., 1993)

2.8. Statistical analysis

All the data was tested for statistical significance by using Sigma Plot 12. Depending on the number of groups tested, either Student's t-test (two groups) or one-way analysis of variance (ANOVA) followed by Tukey-Kramer post-test (several groups) were used. The significance levels are the followings: (*) $p<0.05$, (**) $p<0.01$ and (***) $p<0.001$:

3. Results

3.1 Effectors that promote membrane fusion

Membrane fusion is a high energy demanding process. For fusion to take place the vesicle membrane and the plasma membrane need to overcome hydration and electrostatic repulsive forces among others (Zimmerberg et al., 1993). In this part of the thesis we will address different mechanisms that allow membranes to surpass energy barriers to make fusion possible. We will study how different naturally occurring v-SNARE transmembrane domain (TMD) variants drives size dependent vesicle fusion and how differentially shaped lipid molecules affect fusion in a leaflet specific manner.

3.2 Naturally occurring v-SNARE TMD variants support fusion

Previous studies have shown that artificially replacing the N-terminus of the VAMP2 TMD for helix-stabilizing leucine amino acids (poly-L), strongly reduces the exocytosis extent and slows down the expansion of the pore, while changing it for helix-destabilizing valines (poly-V, β-branched amino acids) favors fusion like the wt protein and speeds ups the expansion of the pore (Dhara et al., 2016). Based on these findings, the starting point of our project was to examine the different physiological v-SNARE TMD variants which differ in their content of β-branched amino acids.

For that purpose, two chimeric mutants were generated. They contained the cytoplasmic domain of VAMP2 and the TMD of VAMP1 or VAMP8 **(Figure 17)**. These chimeras were expressed (by using the SFV approach) in dko mouse chromaffin cells. It has previously been shown that secretion is abolished in dko cells, but that this phenotype is rescued by VAMP2 overexpression (Borisovska et al., 2005). To study the two chimeric mutants, we used whole-cell capacitance measurements combined with photolytic uncaging of intracellular calcium. We showed that the expression of VAMP2-VAMP1TMD and VAMP2-VAMP8TMD rescued the synchronous secretion like the wt protein **(Figure 17 A, C)**. Both components of the exocytotic burst (EB): the ready releasable pool (RRP) and the slow releasable pool (SRP) were fully restored with the chimeras, the same rescued phenotype was observed in the sustained release (SR) **(Figure 17 B, D left panel)**. The kinetics of release and the delay were also fully restored **(Figure 17 B, D right panel)**. In the same line, further analyses done by my colleague Dr. Madhurima Dhara using 19μM free calcium infusion and carbon fiber amperometry revealed a similar membrane capacitance phenotype as the one explained above (Dhara et al., 2020). Moreover, amperometric spike analysis showed higher amplitude and faster kinetics of the main spike in VAMP2-VAMP8TMD and the opposite, lower amplitude and slower

kinetics in VAMP2-VAMP1TMD. These findings suggest that increased flexibility of the TMD accelerates the expansion of the fusion pore. (Dhara et al., 2020). Taken together, the experimental data shows that secretion is not impaired when the TMD domain of VAMP2 is exchanged for VAMP1 or VAMP8. Indeed, it demonstrates that few β-branched amino acids are sufficient to drive fusion, as proven with VAMP1, and that increasing the number of β-branched amino acids, as proven with VAMP8, does not increase the number of fused vesicles.

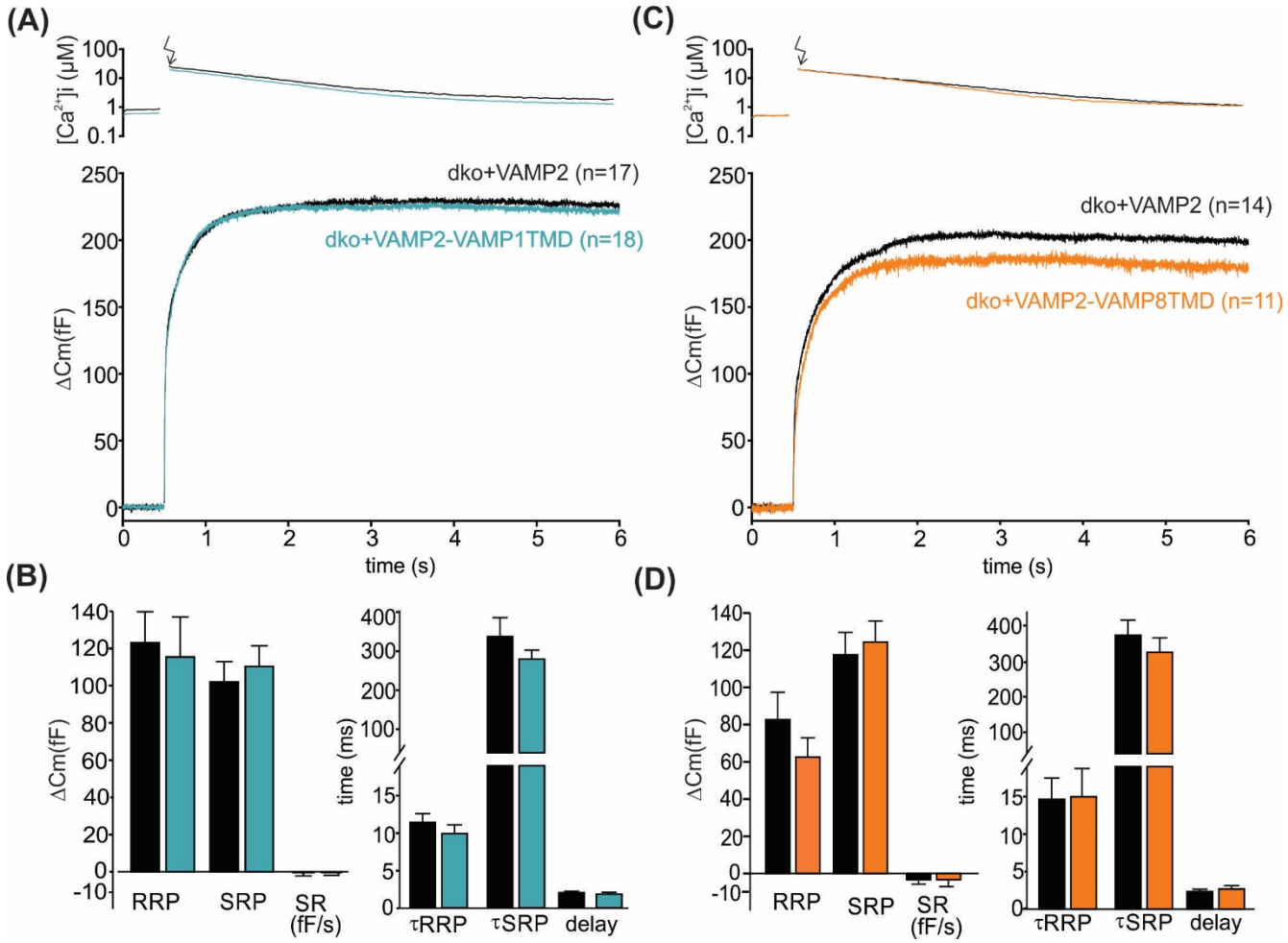

Figure 17. The synchronous secretion is not affected in the naturally occurring v-SNARE TMD variants. (A) The VAMP2-VAMP1TMD mutant does not show any secretion deficit when compare to VAMP2. Averaged trace of flash-induced [Ca^{2+}] i (top), with an arrow indicating the UV-flash, and corresponding capacitance responses (bottom). **(B)** Data quantification of the capacitance measurement. The mutant VAMP2-VAMP1TMD completely restores RRP, SRP and sustained rate (left) as well as the delay and the release kinetics with similar τRRP and τSRP (right) **(C)** The VAMP2-VAMP8TMD mutant does not show any secretion deficit when compare to VAMP2. Averaged trace of flash-induced [Ca^{2+}] i (top) and corresponding capacitance responses (bottom). **(D)** Data quantification of the capacitance measurement. The mutant VAMP2-VAMP8TMD completely restores RRP, SRP and sustained rate (left) as well as the delay and the release kinetics with similar τRRP and τSRP (right). Cell numbers are indicated in brackets.

In parallel, immunocytochemistry analysis showed no differences in protein expression between the VAMP2 wt protein and the two mutants used in the experiment, as shown in the exemplary images **(Figure 18 A)** and in the corresponding quantification **(Figure 18 B).**

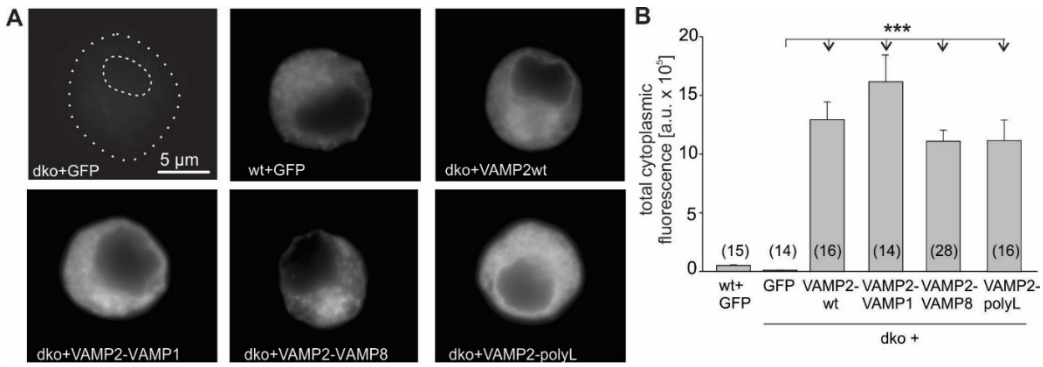

Figure 18. VAMP2-TMD mutants express with similar efficiency as VAMP2-wt protein. (A) Exemplary images of wt cells expressing GFP and dko cells expressing either GFP or the TMD mutants (VAMP2-wt, VAMP2-VAMP1, VAMP2-VAMP8, VAMP2-polyL). Cells were immunostained with a primary antibody against VAMP2 (affinity purify mouse monoclonal antibody, clone 69.1, antigen epitope a.a position 1-14) and a secondary antibody Alexa Fluor 555 goat anti-mouse. The signals of the dko expressing the TMD mutants were stronger than the wt+GFP, different exposure times were used (e.g. wt+GFP: 1.18s and dko+VAMP2: 0.076s) **(B)** Mean total cytoplasmic fluorescence intensity for the different groups mention in A after 5.5 hours after transfection with SFV. Data appears as mean ± SEM, ***, $p<0.001$. Statistical analyses were done using one-way analysis of variance followed by Tukey-Kramer post-test.

In collaboration with my colleague Dr. Yvonne Schwarz we used Structured Illumination microscopy (SIM), to study the subcellular localization of the mutant proteins. This technique provides an enhanced spatial resolution and is based on the use of specific light patterns like the Moiré patterns (Rego and Shao, 2015). The SIM pictures as well as the line scans showed a clear colocalization with VAMP3 (marker protein for secretory granules) suggesting that the mutant proteins are sorted to vesicles like the wt protein. **(Figure 19 A)**. The Mander´s colocalization coefficients also indicated similar colocalization among the groups **(Figure 19 B)**. Notably, the fluorescence intensity of the puncta was around four times less intense in the wt condition compared to the cells expressing either VAMP2 or its mutant proteins, consistent with our experience that semiliki forest virus (SFV) transfection leads to protein overexpression. **(Figure 19 C)**.

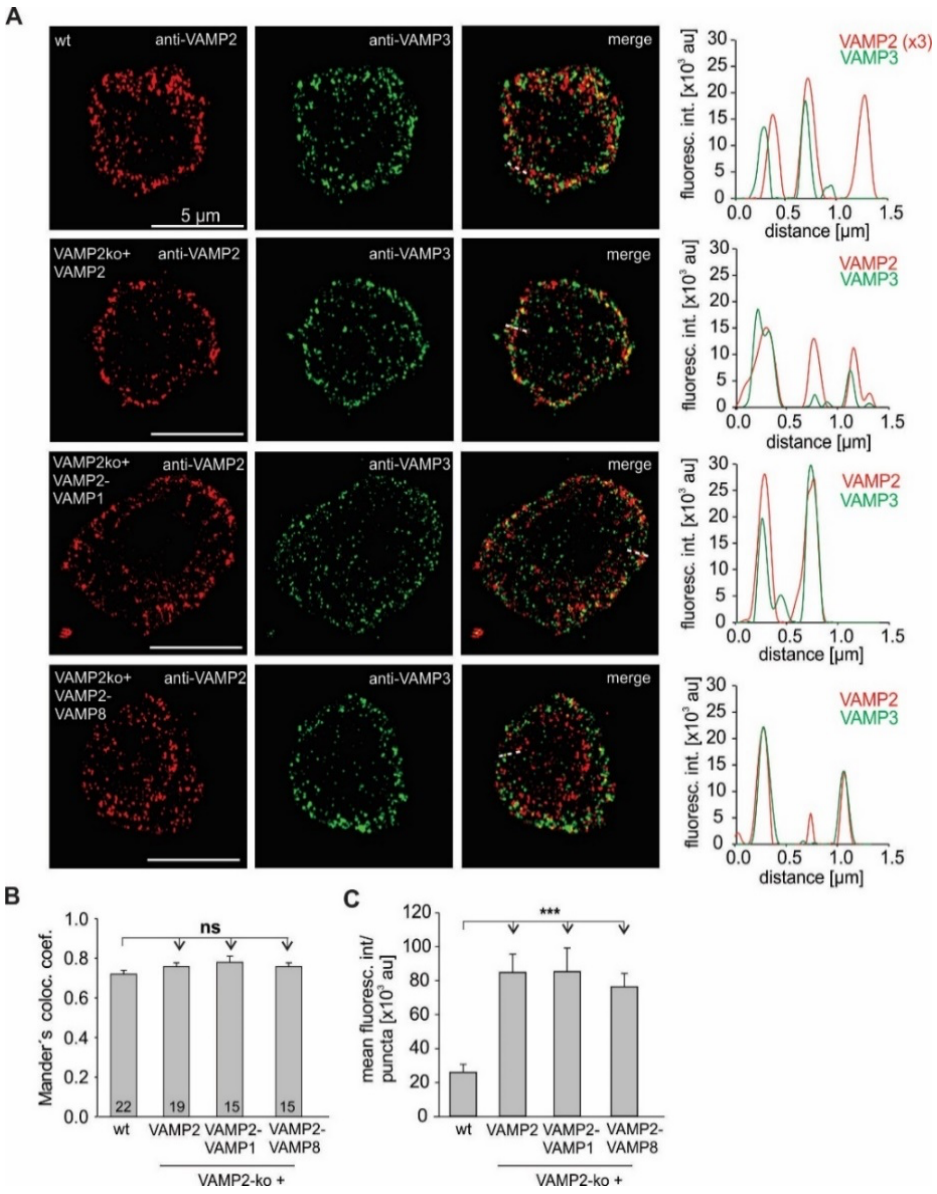

Figure 19. VAMP2-TMD mutants are sorted to granules as the wt protein. (A) Representative images using SIM shows a colocalization between VAMP3 and VAMP2 or the mutant variants. VAMP2 is shown in red and VAMP3 is shown in green, the merge image and the line scans (right panels) shows the colocalization in wt cells as well as in VAMP2-ko chromaffin cells expressing either VAMP2 wt protein or VAMP2-TMD mutants (determined 3.5 hours after transfection). For wt cells, the laser power of VAMP2 was threefold higher than in the cells transfected with SFV. **(B)** Mander´s weighted colocalization shows that VAMP2 and its TMD mutants have similar colocalization coefficient to endogenous VAMP3, the number of cells analyzed are indicated in the bar graph. **(C)** The fluorescence intensity of the puncta is similar for VAMP2 and its TMD mutants, but the wt littermate shows a reduction of the fluorescence intensity (approximately four times less). Images were thresholded to values 6 x SD of the background fluorescence to isolate discrete regions of interest for analysis. Data appears as mean ± SEM, ***, $p<0.001$. Statistical analyses were done using one-way analysis of variance followed by Tukey-Kramer post-hoc test. *(In collaboration with Dr. Y Schwarz)*

Overall, these experiments demonstrate that two naturally occurring v-SNARE TMD variants fully supports secretion, as the membrane capacitance and the release kinetics are unchanged compared to the wt protein **(Figure 17)**. Nevertheless, further experiments done by my colleague Dr.

Dhara provided evidence that TMD flexibility speeds up fusion pore dynamics for TMDs with an overrepresentation of ß-branched amino acids. (Dhara et al., 2020). This observation is not trivial, as it ensures that small and large vesicles (employing either VAMP1 or VAMP8, respectively) on the one hand fuse with the membrane with similar efficiency, but on the other hand support *bona fide* cargo release, which is particularly important for the unloading of large cargo molecules from giant vesicles such as zymogen granules.

3.3 Intracellular methanol application increases synchronous secretion

Given the hypothesis that proteins and membrane cooperate in overcoming the energy barrier for fusion, one might ask to what extent direct perturbation of the membrane bilayer interferes with the vesicle's fusogenicity. It has been previously reported that short-chain alcohols, like methanol, accelerate fusion of liposomes and viral membranes (Chanturiya et al., 1999). One possible explanation could be that short-chain alcohols induce local membrane defects and thereby lower the energy barriers required for fusion (Paxman et al., 2017). In this present work, the goal was to test whether and if so to what extent the addition of methanol affects Ca^{2+} triggered vesicle fusion (Shaaban et al., 2019). In order to study how methanol affects fusion, 2% of methanol was applied in the intracellular solution and changes in membrane capacitance were measured in response to photolytic uncaging of intracellular calcium. Two consecutive flashes with a time interval of 120 seconds were applied to study whether potential changes in secretion were robust. The results showed that independently of the presence of methanol, the second flash evoked more secretion than the first, with an increased RRP size **(Figure 20)**. This observation is the expected consequence if Ca^{2+}-dependent priming of secretory vesicles is enhanced by the first uncaging response (Voets, 2000). In any case, intracellular application of methanol had a profound impact (nearly two-fold increase) on the secretory response **(Figure 20)**. Both, the first and the second flash response were significantly enhanced. In particular, the RRP size was strongly altered, indicating the methanol application preferentially affects the fusogenicity of 'well'-primed vesicles. The RRP kinetics (τRRP) were slower in the second flash compared to the first one for both conditions, with or without methanol, but no changes were observed for the SRP kinetics (τSRP) or the secretory delay **(Figure 20 B).** These alterations in RRP kinetics could be due to unavoidable inaccuracies in the mathematical approximation (routine fitting) or reflect inhomogeneity in the biochemical maturation of newly primed vesicles.

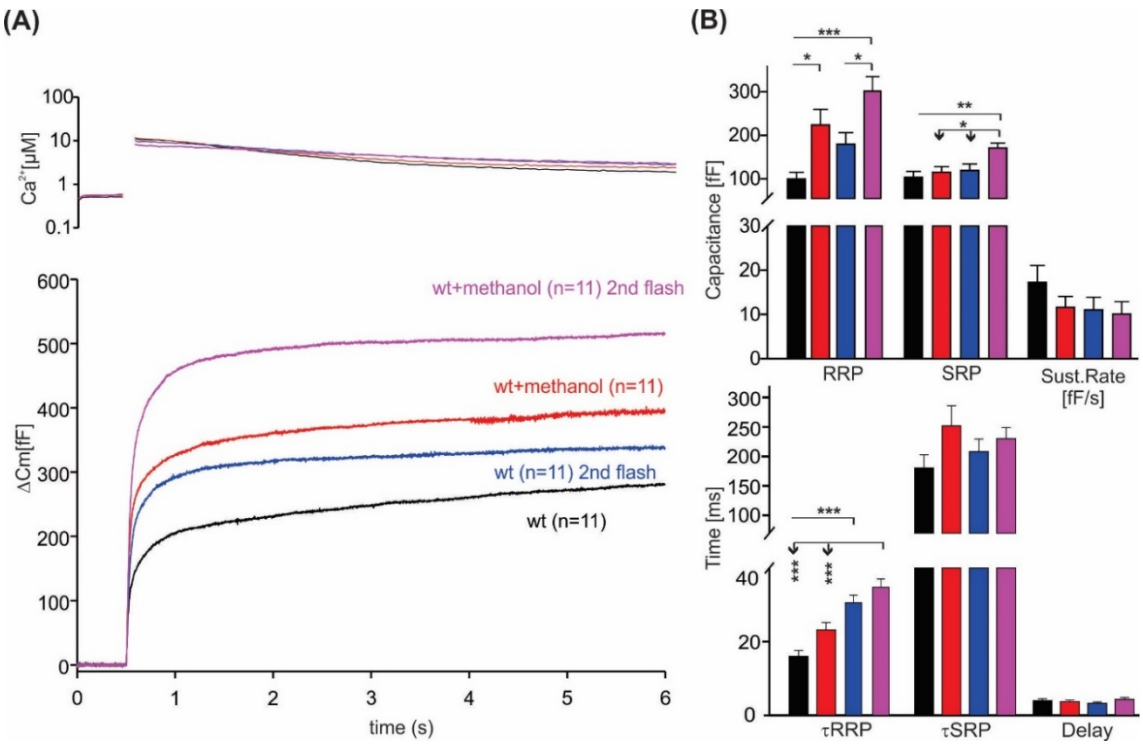

Figure 20. Intracellular application of methanol increases synchronous secretion in wt cells. (**A)** Averaged traces of the levels of $[Ca^{2+}]i$ for the four different conditions (top panel) and the corresponding release response of wt cells (bottom panel) with and without intracellular methanol (2%) application. (**B)** Intracellular methanol application increases the RRP. Quantification of the release kinetics and the delay for each condition, the τRRP is slower in the second flash compared to the first in both conditions. Data represent mean ± SEM, *, $p<0.05$, **, $p<0.01$, ***, $p<0.001$, one-way analysis of variance followed by Tukey-Kramer post –hoc test.

An attractive explanation for the strong methanol effect on the extent of fusion could be that methanol facilitates the dehydration of the membranes and thereby lowers the strong energy barrier that opposes membrane approximation. In this context it stands to reason, that previous experiments within our lab have shown that extracellular application of methanol (2%) had no effect on fusion, which is consistent with the idea that methanol specifically affects approximation of opposing membranes (Borisovska, unpublished observation).

Taken together, this results were encouraging to further study the lipid role in exocytosis. Indeed, if methanol acts on the lipid bilayer and by that enhances fusion, it is interesting to study how the changes in the lipid composition of the membrane bilayer affect fusion.

3.4 Membrane curvature modifying lipids affect fusion in a leaflet specific manner

Lipids that confer spontaneous curvature, like oleic acid (OA) or lysophosphatidyl choline (LPC) have been shown to regulate membrane fusion **(Figure 21)**, most likely because they change the energy barrier of highly-curved membrane intermediates (Brown, 2012; Chernomordik and Kozlov,

2008). Previous studies done in protein-free liposome fusion, have demonstrated that application of cone-shaped lipids like LPC to the *cis* compartment of the fusing membranes (equivalent to the intracellular compartment) inhibits fusion, whereas OA facilitates it (Chanturiya et al., 1999; Chernomordik and Kozlov, 2008). These experiments were instrumental in proposing that fusion may proceed through a highly bent membrane fusion intermediate (hemifused state, see **Figure 3**), which exhibits a net-negative curvature. Thus, depending on the lipid shape and on the curvature-preference of the membrane leaflet, fusion can be either facilitated or impeded. Yet, subsequent studies in secretory cells revealed contradictory results with curvature modifying phospholipids, thereby questioning the existence of a lipidic fusion intermediate (Amatore et al., 2006; Zhang and Jackson, 2010). Here, we have measured in a more physiological manner (using chromaffin cells) how lipids affected membrane fusion. We have comparatively analyzed how the application of OA and LPC affected Ca^{2+} triggered vesicle fusion.

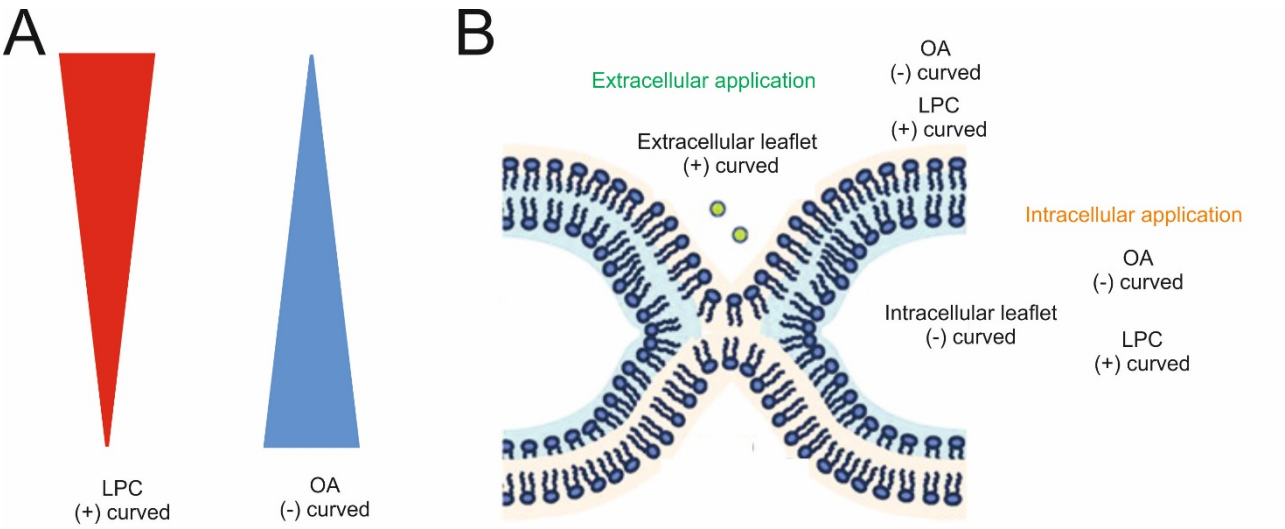

Figure 21. LPC and OA applied to the extracellular and intracellular leaflet. (A) LPC has an inverted cone shaped structure (big head and small tail) which confers a positive curvature while OA has a cone shaped structure (small head and a big tail) which confers a negative curvature. **(B)** LPC better fits in the extracellular leaflet because is positively curved while OA better fits in the intracellular leaflet because it is negatively curved *(*Figure modified from *Melikyan, 2010).*

3.4.1 Lipid molecules applied from the intracellular side impacts synchronous secretion in a leaflet-specific manner

In the first set of experiments, wt cells were infused with the intracellular solution used for the flash experiments containing 5µM of either LPC or OA (dissolved in 0.5% dimethyl sulfoxide (DMSO). The results show that the application of OA intracellularly increased the synchronous secretion whereas the application of LPC decreased it. Indeed, the RRP size of cells infused with OA

was significantly higher than those recorded in the presence of LPC **(Figure 22 A and B, higher panel)**. Furthermore, the kinetics of release and the delay were unchanged, suggesting that curvature modifying phospholipids alter the number of fusion-competent (primed) vesicles but do not interfere with fusion triggering (**Figure 22 B, lower panel)**.

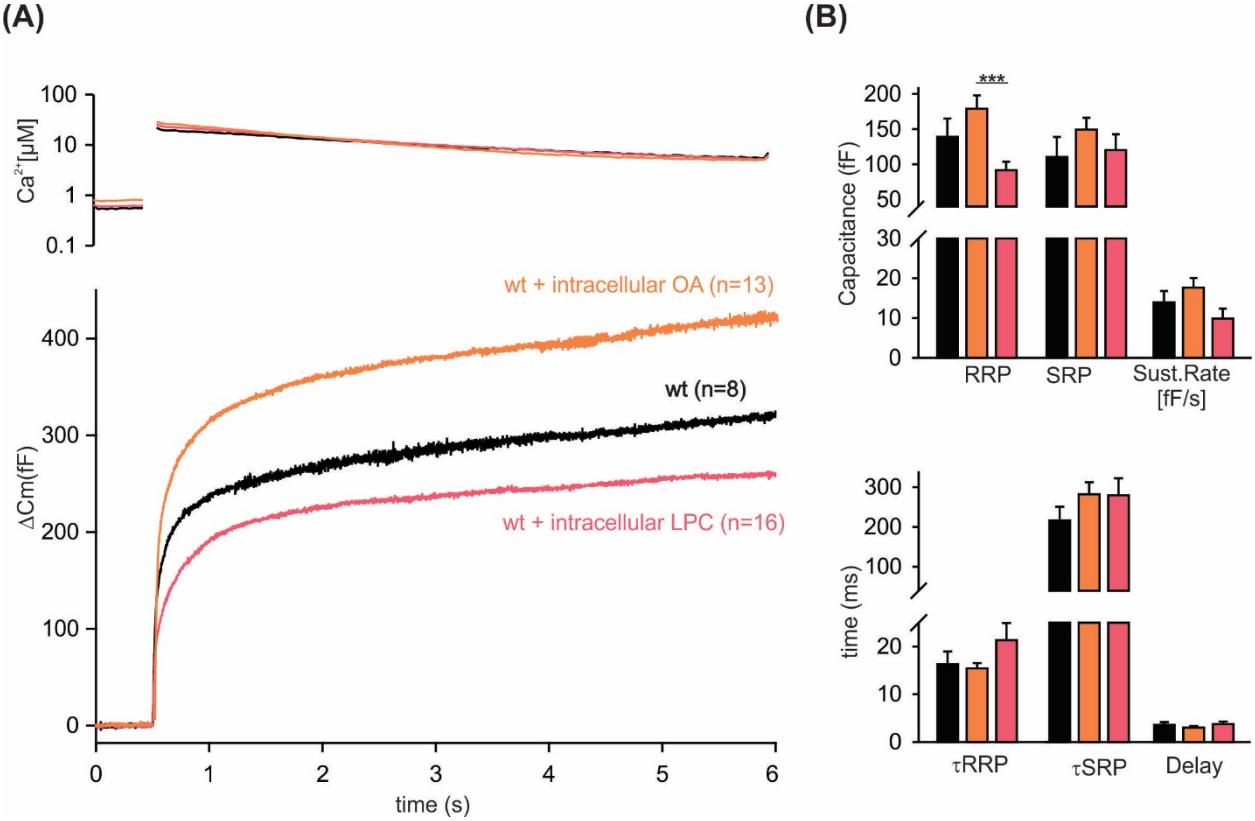

Figure 22. Application of lipid molecules such as LPC or OA intracellularly has an effect on synchronous secretion. (**A)** Average trace of the levels of [Ca^{2+}] i (top) and synchronous secretion (bottom) of wt cells and wt cells infused with the lipid molecules LPC or OA (5µM). Infusion via the patch pipette of LPC and OA has opposite effects in secretion. On the one hand LPC reduce the secretion while on the other hand OA increases it. (**B)** Quantification analysis of capacitance show a significant increase in RRP in wt cells infused with OA compared with LPC infused cells. The other parameters such as SRP and sustained rate remain very similar among the groups (top). The release kinetics (τRRP and τSRP) as well as the delay were unchanged among the groups (bottom). Data appears as mean ± SEM, ***, $p<0.001$. One-way analysis of variance followed by Tukey-Kramer post-hoc test. (In collaboration with M. Makke)

The observed differential effects of LPC and OA are consistent with the notion that exocytosis of chromaffin granules occurs via a lipid fusion intermediate. Indeed, OA confers a negative spontaneous curvature which probably stimulates the transition to the intermembrane stalk (which is net negatively curved) (Chernomordik and Kozlov, 2008). Alternatively, molecular dynamic simulations have suggested that OA as a cone-shaped phospholipid may lower the hydration repulsive energy between the two membranes and therefore enhances fusion (Chernomordik and Kozlov, 2008; Smirnova et al., 2019).

3.4.2 Lipid molecules applied from the extracellular side do not alter synchronous secretion

To study the effects on fusion of OA and LPC in the extracellular leaflet, wt cells were incubated for 3 minutes in Ringer's solution containing either OA or LPC, 2µM concentration, and 0.5% DMSO. After that, the cells were transferred to the Ringer solution (without DMSO and lipids) to facilitate seal formation with the patch pipette. The results showed that neither the application of LPC nor extracellular OA altered Ca^{2+} triggered exocytosis **(Figure 23 A, B, top panel)**. Neither the overall secretion nor the kinetic and the delay were modified. Only a slight, but significant increase in the sustained rate of secretion with LPC could be detected. (p=0.04) **(Figure 23 A, B, lower panel)**.

Altogether, these experiments (the intracellular and extracellular lipid application) indicate that for membrane merge, the hemifusion intermediate is a necessary step. This conclusion is in accordance with previous studies where fusion was study using protein-free liposomes or viral membrane fusion (Chernomordik and Kozlov, 2003; Melia et al., 2006)

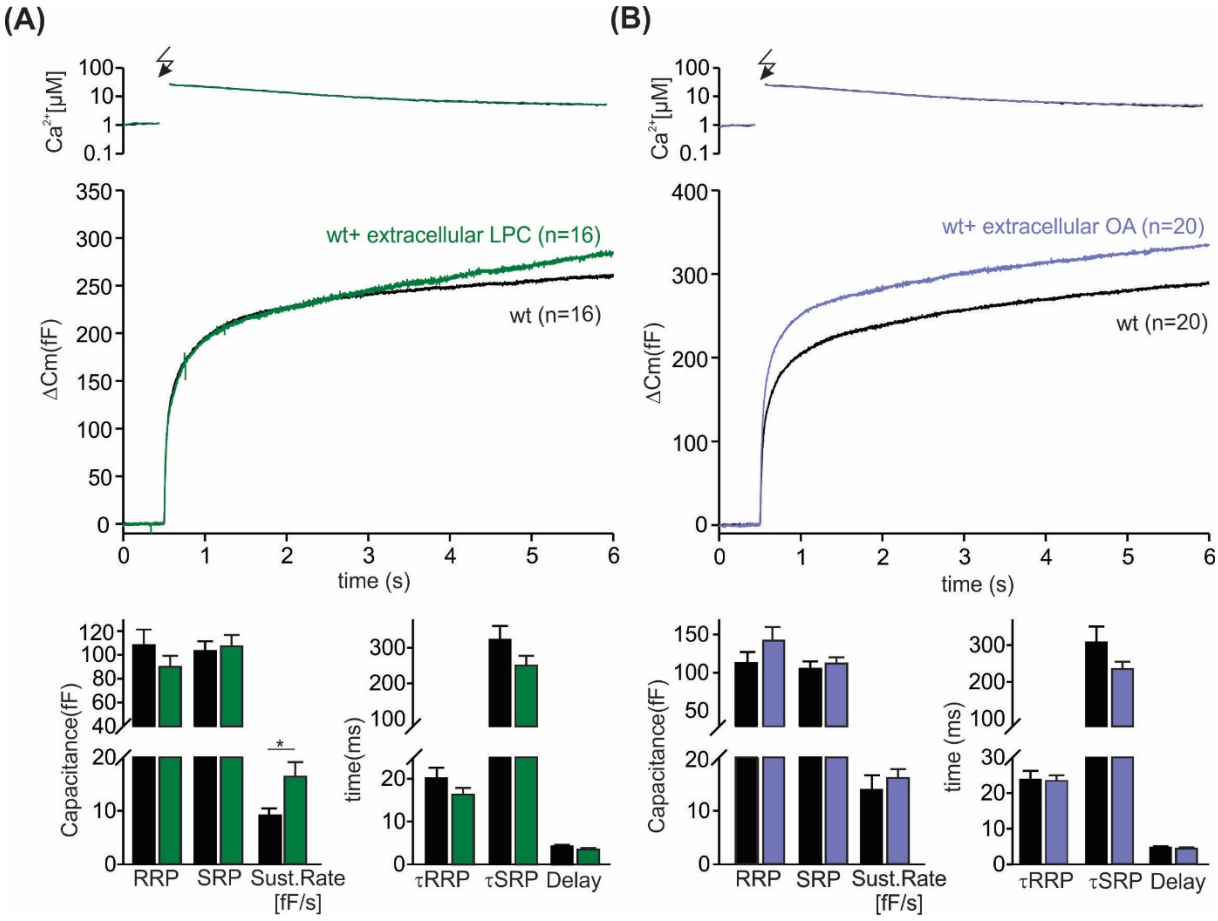

Figure 23. Extracellular application of curvature-modifying lipid molecules does not affect synchronous secretion. (**A**) Average trace of $[Ca^{2+}]i$ (top) and capacitance response after the flash for wt cells as well as for wt cells with application of LPC on the extracellular side (middle). Quantification analysis of the overall capacitance response shows no major effects in membrane capacitance when LPC is applied, only a slight increase in the sustained rate upon application of LPC is observed (bottom left). The kinetics of the response are also unchanged (bottom right). **(B)** Average trace of $[Ca^{2+}]$ (top) and capacitance response after the flash for wt cells as well as for wt cells with application of OA on the extracellular side (middle). Quantification analysis of the overall capacitance response shows no significant effects in the release when OA is applied (bottom left). The kinetics of the response are also unchanged (bottom right). Data represent mean ± SEM, *, $p<0.05$. Statistical analyses were done using t-test. The concentration of LPC and OA was of 2µM.

3.5 Function of the SNARE regulatory protein Complexin II

Cpx II is a small cytosolic protein of 134 amino acids essential for calcium trigger exocytosis (Mohrmann et al., 2015). The role of this protein is dual, it has a facilitatory and an inhibitory function (Dhara et al., 2014; McMahon et al., 1995). Indeed, each protein region exerts a different role, while the N-terminus facilitates fusion, the AH and the C-terminus inhibit fusion. In the present work, we studied the inhibitory role of the C-terminus and the AH of Complexin by measuring membrane capacitance with photolytic uncaging of intracellular calcium. For this study, we expressed in Cpx II ko cells, using SFV, Cpx II and its corresponding mutants **(Figure 24 A)**. To enable the calcium dependent priming of the chromaffin granules, capacitance measurements were

recorded before the flash during 120s (free calcium = 600nM). This pre-flash or asynchronous release showed a significant increase in capacitance in Cpx II ko cells and a great reduction of capacitance in Cpx II wt cells **(Figure 24 E, F)**. Indicating a role of Cpx II in the regulation of tonic secretion. Following this measurement, a UV flash was applied which permitted to uncage the calcium and therefore increase the free calcium to 20µM. This increase in calcium resulted in a strong reduction of the EB for Cpx II ko cells while for the cells expressing Cpx II a strong increase in the EB was observed **(Figure 24 B-C)**. On top of that, the release kinetics were slower in the absence of Cpx II showing significant differences in the τRRP and the secretory delay **(Figure 24 D)**. This data indicates that Cpx II controls the magnitude of the synchronous secretion and that its loss slows down the release kinetics and the delay of the response.

Overall, we show that Cpx II is required to prevent premature vesicle fusion at submicromolar levels of calcium. This prevention of premature vesicle loss thus translates into an increase in the magnitude of synchronous exocytosis (Dhara et al., 2014).

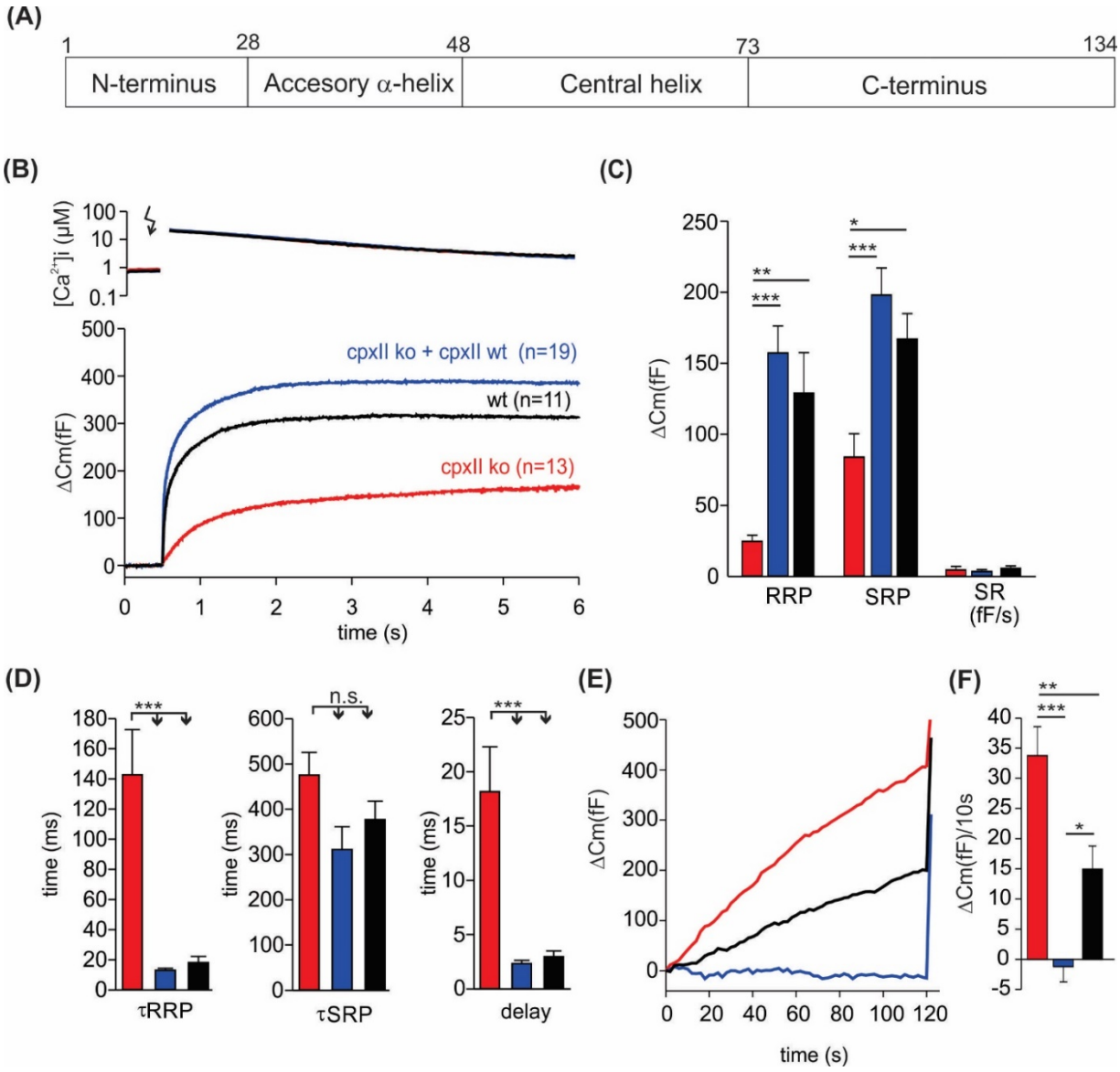

Figure 24. Loss of Complexin II (Cpx II) unclamps asynchronous release and diminishes synchronous secretion. (**A)** Schematic drawing of the structure of Cpx II, a cytosolic protein of 134 aa. **(B)** Average calcium trace with arrow indicating the UV flash (top), average capacitance trace of the synchronous secretion (bottom). Overexpression of Cpx II increases synchronous secretion compared to Cpx II ko cells. **(C)** Quantification of capacitance measurement. The loss of Cpx II strongly reduces the magnitude of the RRP and the SRP compare to the endogenous protein and to Cpx II overexpression The SR was unchanged in the three conditions. **(D)** Quantification of the secretion kinetics. Overexpression of Cpx II as well as the wt protein displays faster τRRP and delay compare to Cpx II ko **(E)** Average of asynchronous secretion or pre-release measurement. Overexpression of Cpx II clamps the pre-release while the absence of Cpx II unclamps the pre-release. **(F)** Quantification of the asynchronous secretion shows that the loss of Cpx II strongly increases the capacitance per 10s compare to the endogenous protein. Statistical analyses were done using one-way ANOVA followed by Tukey-Kramer post-hoc test. $p<0.05$, **, $p<0.01$, ***, $p<0.001$. Error bars indicate mean ± SEM.

3.6 The role of the C-terminal domain of Complexin II

3.6.1 The far C-terminal domain of Complexin II (the last 34 amino acids) is essential to arrest premature fusion.

Previous work of our laboratory has shown the importance of the C-terminal domain (73-134 aa, CTD) in the inhibitory function of Cpx II (Dhara et al., 2014), but the precise molecular mechanism how the C-terminus arrests fusion was still unclear. In the first set of experiments we tried to narrow down the protein region responsible for the inhibition. For this, a truncated variant of Cpx II lacking only the last 34 amino acids (Cpx II $^{1-100}$) was generated (Makke et al., 2018). The truncated region of the protein is characterized by a glutamate cluster which may be an interaction site for Synaptotagmin I (Tokumaru et al., 2008) and by an amphipathic helix which has been implicated in lipid binding (Snead et al., 2014). Our previous experiments showed that the Cpx II $^{1-100}$ mutant "unclamps" premature secretion and largely fails to restore synchronous secretion, showing a similar phenotype as Cpx II ko cells (Makke et al., 2018). In contrast, the kinetics rates and the delay of the synchronous secretion were restored, with similar properties as those observed in wt cells (Makke et al., 2018). Overall, this data indicates that the last 34 amino acids of the C-terminal domain contains key structures that are responsible for the inhibition of premature fusion, which in turn allows for the buildup of a pool of primed vesicles (Makke et al., 2018).

3.6.2 Tethering Cpx II (Cpx II $^{1-100}$) by an alternative membrane anchor does not support fusion

Previous studies in our and other laboratories have shown that Cpx II $^{1-100}$ does not accumulate on vesicles like the Cpx II protein (Gong et al., 2016; Makke et al., 2018). Furthermore, experiments done in worm and with mammalian Cpx (Gong et al., 2016; Snead et al., 2014) have provided evidence that the localization of Cpx II by the CTD to the vesicle membrane is a necessary feature for the regulation of spontaneous fusion. Thus, it has been speculated that binding of the CTD to vesicular membranes allows Cpx to inhibit fusion in a proximity-accelerated fashion by concentrating other inhibitory domains, like the accessory alpha helix (AH) at the site of fusion (Gong et al., 2016; Snead et al., 2014; Wragg et al., 2013). These considerations raise the question whether simply mislocalization of this truncated protein is the reason for the disinhibition phenotype seen in the electrophysiology experiments. To test this possibility, the cysteine rich region of CSP-α was added to the truncated protein Cpx II $^{1-100}$. CSP-α is a vesicular membrane anchor which is expected to tether Cpx II $^{1-100}$ at the vesicle membrane (Gong et al 2016). Indeed, immunofluorescence analyses

have shown that Cpx II $^{1-100}$ CSP-α concentrated on LDCV, but failed to support fusion like the wt protein (Makke et al., 2018).

To test whether the mutant Cpx II $^{1-100}$ CSP-α was functional, electrophysiological recordings of membrane capacitance were performed in a wt background **(Figure 25 A)**. The result of this experiment showed a strong reduction of the Exocytotic Burst (EB) **(Figure 25 B, C)** and a longer delay compared to controls **(Figure 25 D)**. Furthermore, this mutant was not able to clamp asynchronous release **(Figure 25 E, F)**.

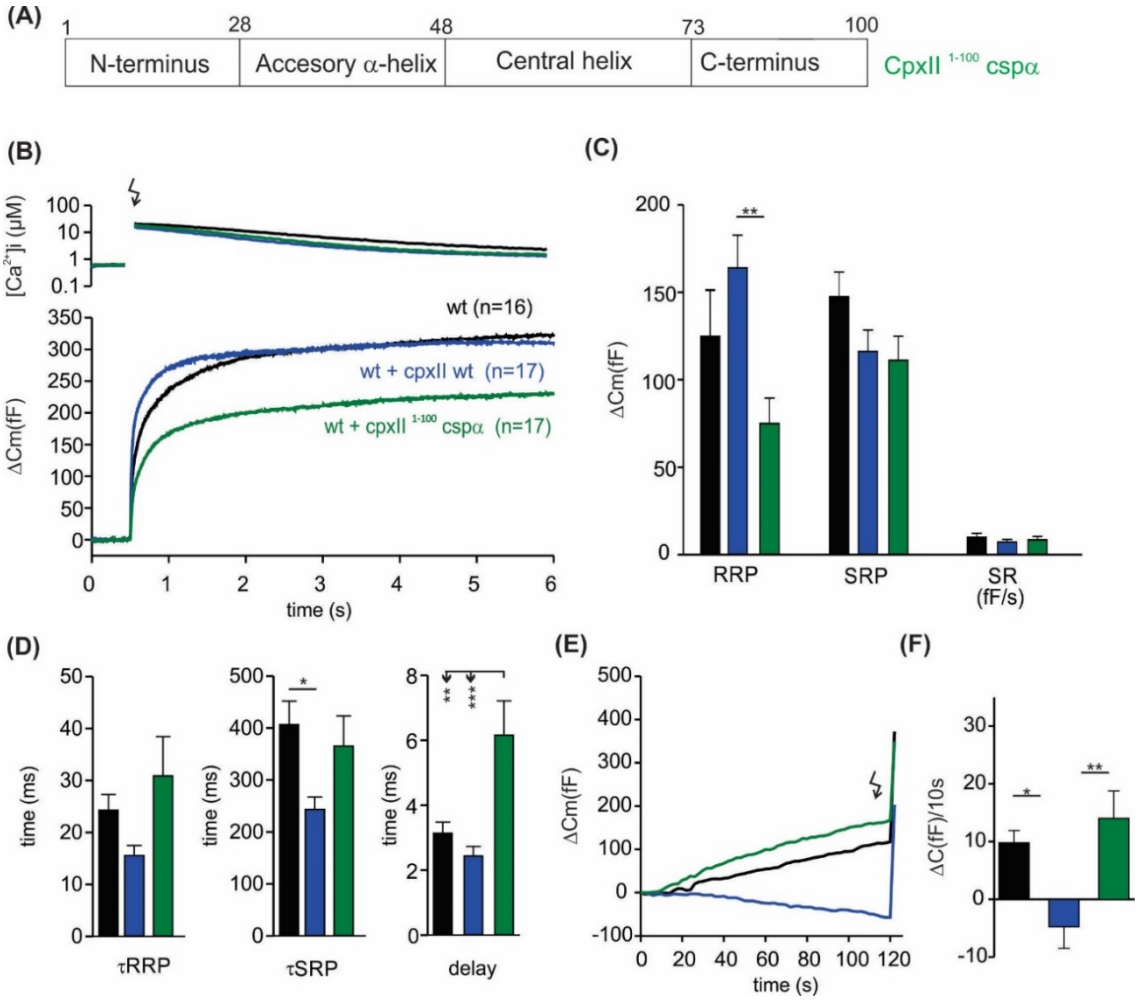

Figure 25. Tethering Cpx II $^{1-100}$ by an alternative membrane anchor fails to support secretion as the Cpx II wt protein. (A) Scheme showing the cpxII $^{1-100}$ cspα mutant. **(B)** Calcium (top) and capacitance response after flash (bottom) **(C, D)** CpxII $^{1-100}$ cspα diminish the RRP size, τRRP and τSRP are unchanged whereas there is an increase in the delay compared to the Cpx II wt. **(E, F)** Cpx II $^{1-100}$ cspα shows an unclamping phenotype compared to Cpx II wt. One-way ANOVA followed by Tukey-Kramer post test were used for statistical analyses $p<0.05$, **, $p<0.01$, ***, $p<0.001$. Error bars indicate mean ± SEM.

Overall, these results demonstrated that Cpx II $^{1-100}$ CSP -α is a functional protein because of its ability to compete with the endogenous protein. They also showed, that this mutated protein is not able to rescued secretion like the wt protein. Therefore, it can be concluded that the inhibitory

phenotype of the Cpx II CTD is not due to the tethering of Cpx II domains by the Cpx II CTD. Instead, the CTD may interact with other proteins to mediate its inhibitory action.

3.6.3 The Cpx II CTD shows strong similarities with the SNARE motif SNAP25a SN1

As the inhibitory action of the CTD does not depend on the presence of Synaptotagmin 1 (Dhara et al., 2014), one might speculate whether CTD may directly interfere with the assembly of SNAREs and thereby inhibits secretion. To follow up on this, we have compared the sequences of the membrane-proximal layers of the SNARE motif with that of the Cpx II CTD. Sequence alignments between the Cpx II CTD and the membrane-proximal layers of SNAREs showed a particularly strong similarity with the SNARE motif of SNAP25-SN1 (hydrophobic layers +2 to +7, 50% similarity) in comparison with other attempted alignments like with SNAP25a-SN2, Syx 1A, or Syb II (27.8%, 38.9%, and 16.7% similarity, respectively). Indeed, the CTD exhibits a similar periodicity of hydrophobic residues **(Figure 26, underlined residues)** and contains similar if not identical amino acids at certain positions within its helix **(Figure 26, orange labelled residues)**. Moreover, Cpx II CTD and SNAP25-SN1 have a nearly identical hydrophobic momentum (μH Cpx II C-terminal: 0.506, μH SNAP25-SN1: 0.509) (Makke et al., 2018), which is a measure of amphiphilicity for a helix . Taken together, these structural similarities point to the possibility that the CTD of Cpx may indeed compete with SNAP25-SN1 for binding to its SNARE partners and thereby hinder progressive SNARE assembly and premature secretion. To further explore this hypothesis, we replaced the CTD with the corresponding protein region from SNAP25. Two chimeric mutants were generated, the short chimera (SC) and the long chimera (LC). For the SC, the last 19 amino acids of Cpx II were replaced by residues 59 to 77 of SNAP25-SN1 (referred as Cpx II 1-115SC) and for the long chimera, the last 34 amino acids of Cpx II were replaced by residues 44 to 77 of SNAP25-SN1 (referred as Cpx II 1-100 LC).

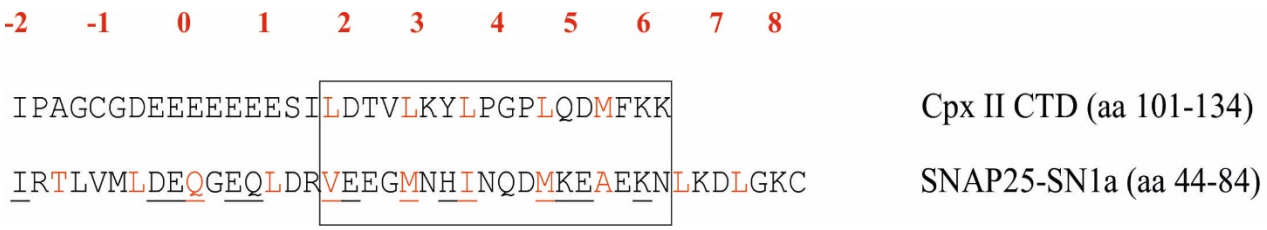

Figure 26. Sequence alignment between Cpx II CTD and the SNARE motif of SNAP25-SN1. In red, the hydrophobic layer regions -2 to +8 are shown. Cpx II CTD shows a high degree of similarity to SNAP25-SN1 (underlined residues). The degree of similarity is 50%, this was calculated from the underlined residues on the box (layers + 2 to +7) using the BLOSUM62 matrix.

3.6.4 A SNAP25-SN1 short chimera restores the function of Cpx II

The experimental data showed that Cpx II $^{1\text{-}115}$SC **(Figure 27 A)** fully restored the kinetics and the magnitude of the synchronous secretion **(Figure 27 B-D)** and also clamped the asynchronous secretion like the wt protein **(Figure 27 E).** In contrast, the truncated mutant Cpx II $^{1\text{-}115}$ **(Figure 27 F**) displayed a similar phenotype as the one observed with Cpx II $^{1\text{-}100}$. It failed to restore the synchronous secretion and to clamp asynchronous secretion, but restored the kinetics and the delay of the response **(Figure 27 G-J)**. Taken together, these results support our hypothesis that the CTD of Cpx II acts as a 'molecular clamp' by competing with the SNARE motif of SNAP25-SN1 for binding to other SNARE partners.

In view of these results, the question arises whether specific properties, such as helicity or certain key residues, could be responsible for the interchangeability of the two protein domains. To further investigate this question, we tested another mutant in which the CTD was replaced by the sequence of an unrelated length-matched alpha helix (Cpx II $^{1\text{-}115}$ A$(EAAK)_4$A). Indeed, this mutant entirely failed to restore synchronous secretion **(Figure 27 G-J).** It neither increased the EB component **(Figure 26 G-I),** nor was it able to hinder premature secretion **(Figure 27 J)**. These results suggest that other structural similarities between the two protein domains, other than their helical structure, are responsible for the inhibitory function of the CTD of Complexin II.

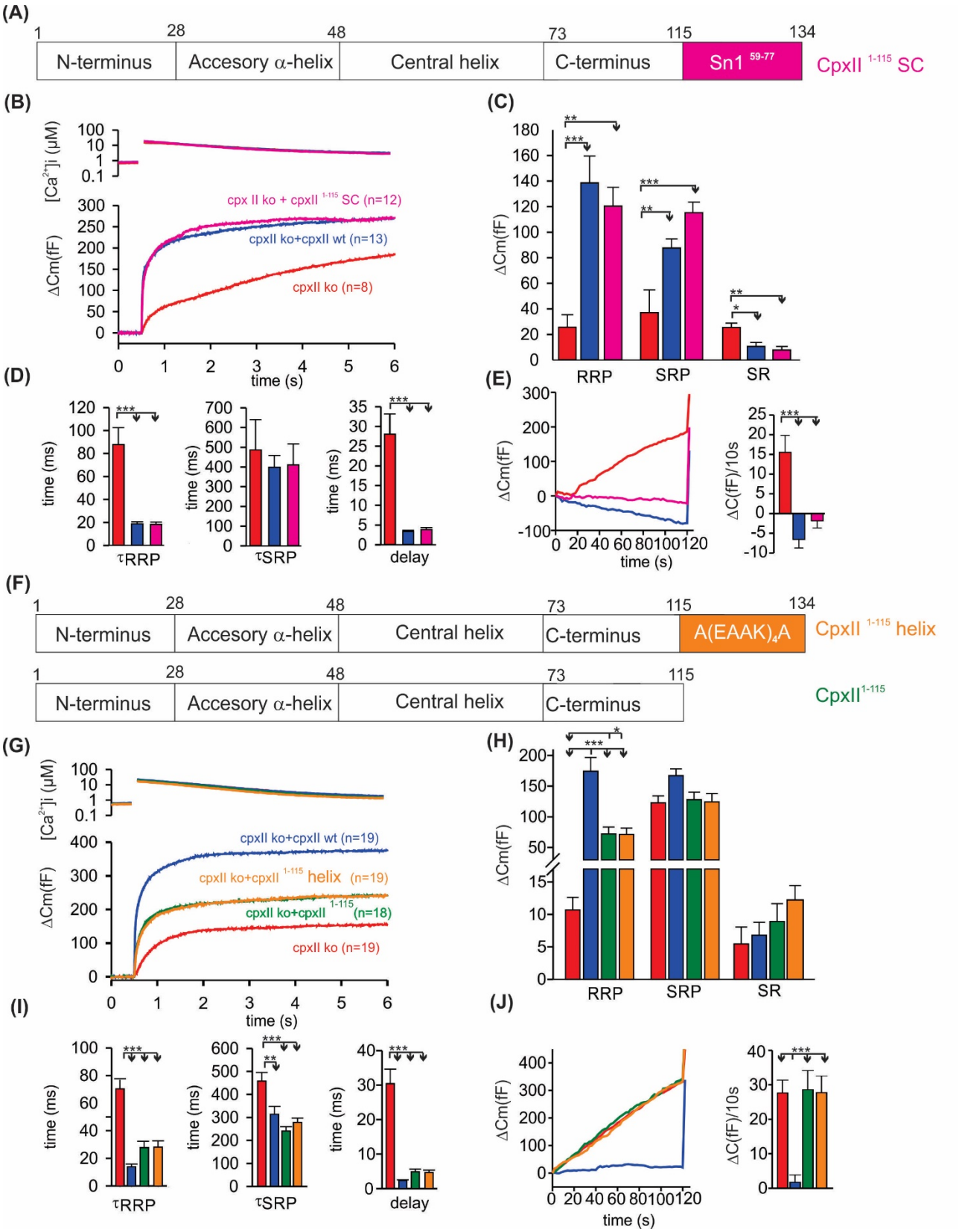

Figure 27. The Short Chimera mutant restores synchronous secretion. (A) Schematic drawing showing the Cpx II $^{1-115}$ SC mutant. **(B)** Expression of Cpx II $^{1-115}$ SC restores the synchronous secretion at the level of Cpx II wt protein: Mean calcium trace (top) and corresponding CM signals (bottom). **(C)** Cpx II $^{1-115}$ SC restores the RRP, SRP and SR at similar levels to Cpx II wt protein **(D)** The time constant (τRRP and τSRP) and the delay are also similar to Cpx II wt. **(E)** The Cpx II $^{1-100}$ SC clamps tonic secretion. **(F)** Schematic drawing showing the two Cpx II mutants tested. **(G)** Expression of

Cpx II $^{1\text{-}115}$ helix and Cpx II $^{1\text{-}115}$ do not restore secretion, showing similar levels to the Cpx II ko. Mean calcium trace (top) and corresponding CM signals (bottom). **(H)** Cpx II $^{1\text{-}115}$ helix and Cpx II $^{1\text{-}115}$ does not restore the RRP **(I)** The time constant (τRRP and τSRP) and the delay are similar to the Cpx II wt. **(J)** Cpx II $^{1\text{-}115}$ helix and Cpx II $^{1\text{-}115}$ unclamps asynchronous secretion like the Cpx II ko protein. One-way ANOVA followed by Tukey-Kramer post test were used for statistical analyses $p<0.05$, **, $p<0.01$, ***, $p<0.001$. Error bars indicate mean ± SEM.

3.6.5 A SNAP25-SN1 long chimera restores the function of Cpx II

To further explore the limits of interchangeability of Cpx II CTD with the SNAP25 SNARE motif, we studied the functional properties of an even longer chimeric mutant. This mutant consists of exchanging the last 34 amino acids of Cpx II for the residues 44 to 77 of SNAP25-SN1 (this mutant is called Cpx II $^{1\text{-}100}$LC) **(Figure 28 A)**. The results showed a similar phenotype as the one observed in the previous experiment. Indeed, Cpx II $^{1\text{-}100}$LC restored functionality of Cpx II, while an unrelated alpha-helix (Cpx II $^{1\text{-}100}$helix) resulted in unclamping of the asynchronous secretion and failed to restore synchronous secretion **(Figure 28 B, J)**.

Taken together, the replacement of the CTD of Cpx II (exchanging either the last 19 or 34 aa) with a length-matched region of SNAP25-SN1 (long or short stretched) completely restores Cpx II function. The extent and goodness in the restoration of exocytosis by the chimeric mutant are remarkable, as there are many ways to cripple a protein but few to restore it to function. Overall, the results strongly support the hypothesis that Cpx II CTD impedes the binding of SNAP25 to its SNARE partners and thus arrests the formation of the SNARE complex. The observed reduction in premature secretion consequently allows for the buildup of a pool of primed vesicles and for elevated synchronized secretion (Makke et al., 2018).

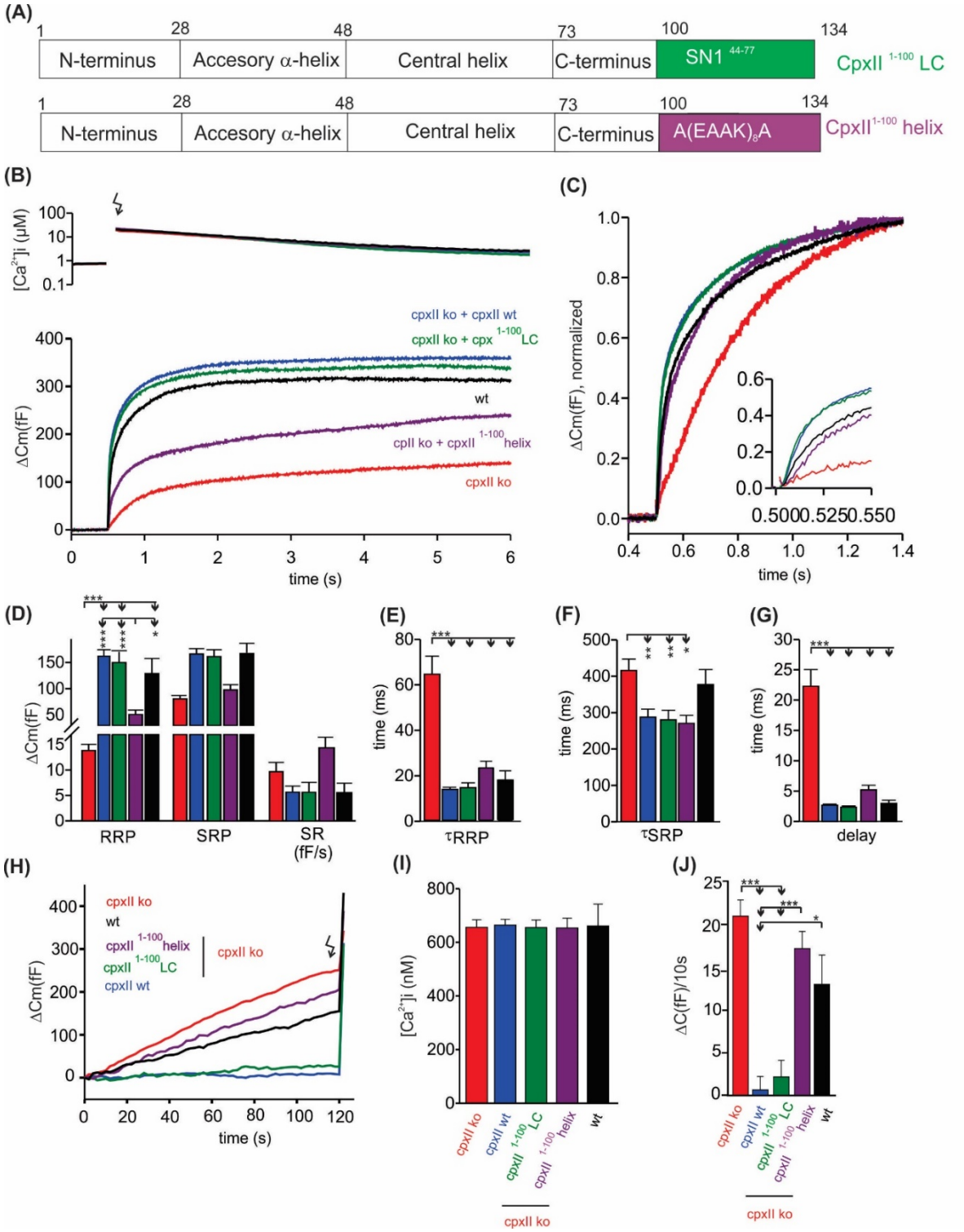

Figure 28. The Long Chimera mutant restores the function of Cpx II while Cpx II $^{1-100}$ helix fails. (A) Schematic drawing showing the two Cpx II mutants tested. **(B)** Expression of Cpx II $^{1-100}$ LC restores the synchronous secretion at the level of Cpx II wt protein while Cpx II $^{1-100}$ helix fails to do it, showing similar levels as the Cpx II $^{1-100}$ (Makke et al., 2018). Mean calcium trace (top) and corresponding CM signals (bottom) of wt cells (n=11), Cpx II ko cells (n=40), Cpx II ko cells expressing Cpx II wt (n=49), Cpx II $^{1-100}$ LC (n=24) and Cpx II $^{1-100}$ helix (n=18). **(C)** Normalized CM of figure B**. (D)** Cpx II $^{1-100}$ LC restores the RRP while Cpx II $^{1-100}$ helix does not restore it. **(E, F, G)** The time constant (τRRP and τSRP) and the delay are similar for both mutants and Cpx II wt. **(H, J)** The Cpx II $^{1-100}$ LC clamps tonic secretion while Cpx II $^{1-100}$ helix does not, showing similar levels as the Cpx II ko protein. **(I)** The asynchronous secretion for the different groups was measured at similar $[Ca^{2+}]$ i levels. One-way ANOVA followed by Tukey-Kramer post test were used for statistical analyses $p<0.05$, **, $p<0.01$, ***, $p<0.001$. Error bars indicate mean ± SEM.

3.6.6 Perturbation of a potential Cpx's binding site within SNAP25 may be essential for Cpx II clamping function

Previous studies using liposome fusion have shown that specific mutations within SNAP25-SN2 (D166A and E170A) compromises the clamping function of Cpx II (Schupp et al., 2016). Interestingly, those residues reside on the opposite side of the CPX-CH-SNARE interface (Chen et al., 2002), which may point to an independent interaction site. In fact, those mutations were already studied by Mohrmann and colleagues (Mohrmann et al., 2013) by using chromaffin cells and performing an experiment in which the capacitance increase was measured in response to photolytic Ca^{2+} uncaging. Mohrmann reported that SNAP25 D116A/E170A only partially rescues synchronous secretion and slows down RRP release kinetics (Mohrmann et al., 2013), an observation which has been interpreted in the context of a perturbed interaction with Synaptotagmin. This result, in combination with others, suggested that these amino acids contribute to the interaction between Synaptotagmin-1 and SNAP25 (Mohrmann et al., 2013). Yet, more recent studies point out to a possible function of these amino acids in Complexin clamping function (Dhara et al., 2014; Schupp et al., 2016). For this reason, in our study, we focused on how these mutations affect the clamping function of Cpx II. For this purpose, we used SNAP25 ko mice expressing the wt protein or the mutation under study (D116A/E170A) and we monitored, besides the synchronous secretion, the increase in capacitance previous to the flash- evoked response (the asynchronous secretion).

Our data showed similar results in response to photolytic Ca^{2+} uncaging to those observed in 2013 by Morhrmann. Indeed, the mutant protein exhibited a decrease in the synchronous release compared to the wt protein **(Figure 29 A, B)** as well as slower τRRP **(Figure 29 C)**. Regarding the capacitance increase previous to the flash-evoked response, the mutant protein D116A/E170A showed a significant increase in the secretion compared to the ko and a tendency of increase compared to the wt **(Figure 29 D, E)**. In addition, to rule out the possibility that the phenotype observed was not a consequence of differences in protein expression, immunochemistry analyses were done to compare the expression levels of the wt protein with the mutant. These analyses show that both constructs used in these experiments (SNAP-25 wt as well as SNAP25 D166A/E170A) were expressed with similar efficiency **(Figure 30 A, B)**.

Overall, the increase in the asynchronous secretion observed with the mutant protein may suggest that Cpx II interacts with two amino acids of SNAP25- SN2 (D166 and E170) and that this interaction is important for Cpx II clamping function. To study the possible amino acids of Cpx II that interact with D166 and E170, a sequence alignment was done **(Figure 31)**. The alignment shows that two lysine residues K98/K99, which are known for being conserved among the animal kingdom, may

present electrostatic interactions with E170 **(Figure 31)**. To test if these two lysines are functionally relevant they were mutated and tested by using photolytic uncaging of intracellular calcium experiments.

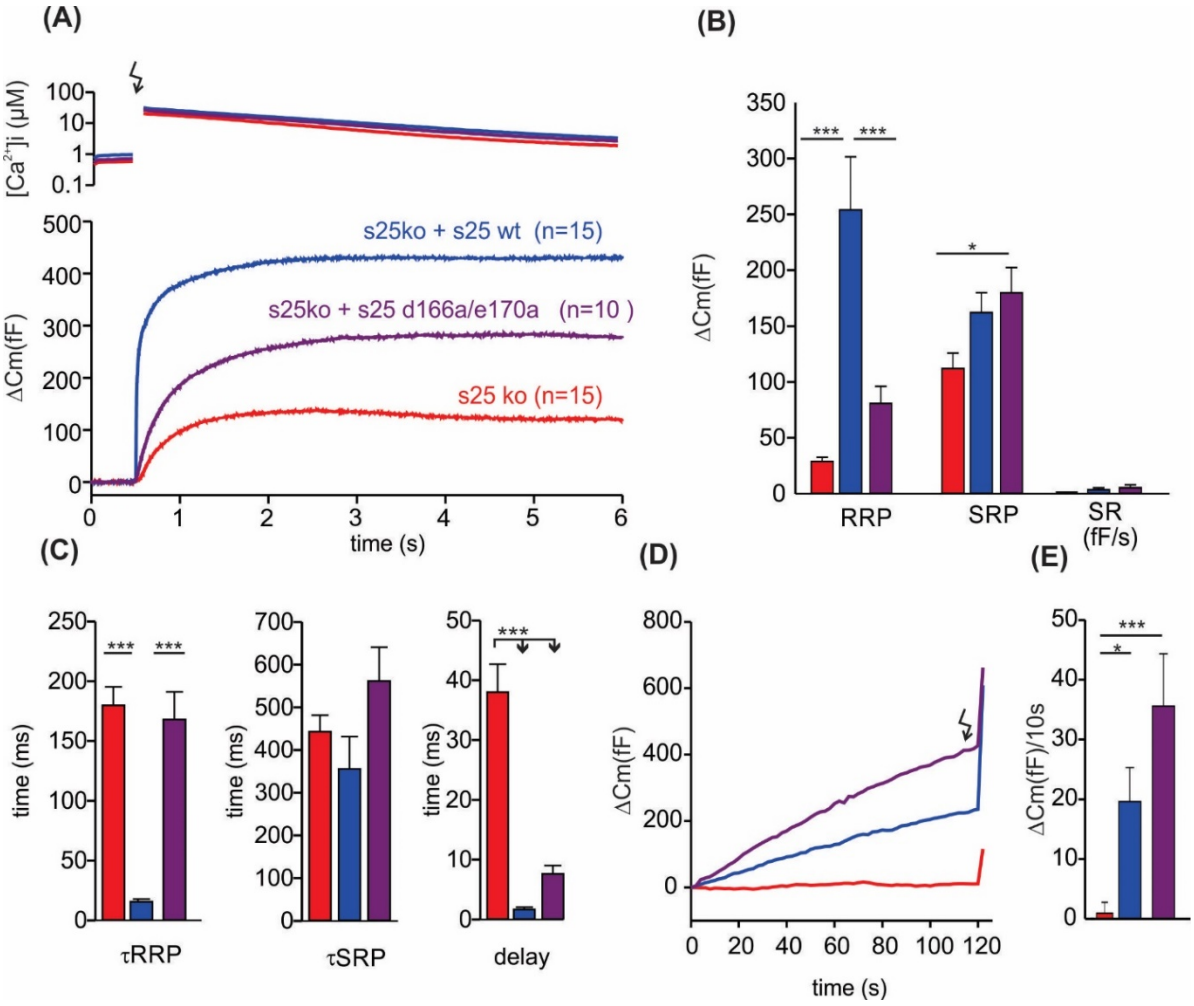

Figure 29.Mutation of two amino acids in the SNAP25-SN2 region (D166A and E170A) increases asynchronous secretion and impairs synchronous secretion. **(A)** Calcium levels after UV-flash (top) capacitance traces after UV-flash (bottom). **(B)** Average analysis of the capacitance traces show a strong decrease in the RRP in the mutant variant compared to the wt protein **(C)** The τRRP of the mutant variant is at the same level as Cpx II ko cells. **(D)** Capacitance traces of the asynchronous release. **(E)** Average of the rate of tonic secretion, the mutant variant shows a significant increase compared to the ko as well as an increase, even though is not significant compared to the wt. Statistical analyses were done using one-way ANOVA followed by Tukey-Kramer post test. $p<0.05$, **, $p<0.01$, ***, $p<0.001$. Error bars indicate mean ± SEM,

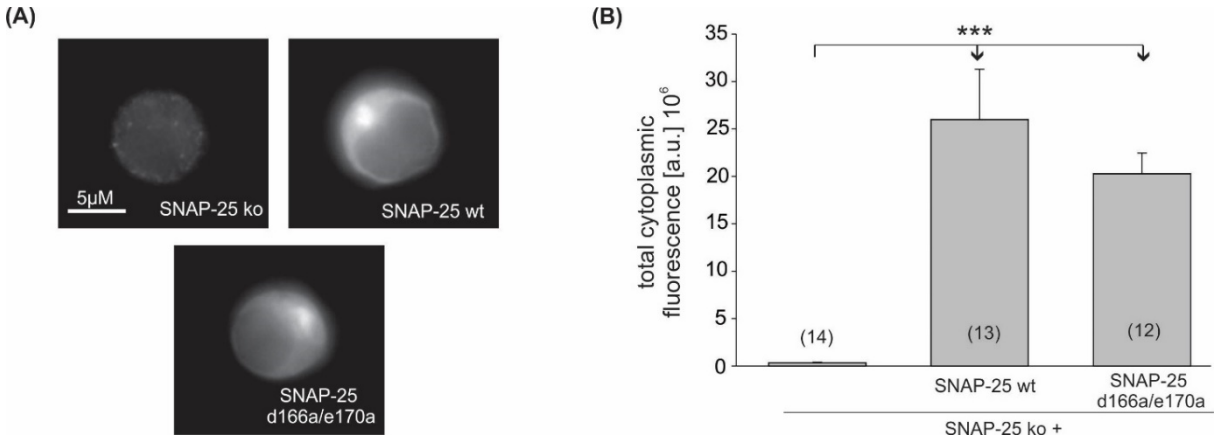

Figure 30. SNAP25 D166A/E170A mutant express with similar efficiency as SNAP25 wt. (A) Exemplary images of SNAP25 wt, SNAP25 ko and SNAP25 d166a/e170a. Cells were immunostained with a primary antibody against SNAP25 (mouse anti-SNAP25 71.1 at 1:500, Synaptic Systems) and a secondary antibody (Alexa Fluor 555-conjugated goat anti-mouse antibody; dilution 1:400, Invitrogen). The signals of SNAP25 expressing the wt protein or the mutant one were stronger than the SNAP25 ko, different exposure times were used (e.g. SNAP25 wt: 0.080s and SNAP25 ko: 1.5s). **(B)** Mean total cytoplasmic fluorescence intensity for the different groups mention in A, 5.5 hours after transfection with SFV. Data appears as mean ± SEM, ***, $p<0.001$. Statistical analyses were done using one-way analysis of variance followed by Tukey-Kramer post-test.

Figure 31. Sequence alignment between Cpx II CTD and the SNARE motif of SNAP25-SN2. In red, the hydrophobic layer regions -6 to +8 are shown. The amino acids K98 and K99 from Cpx II CTD may interact with E170 of SNAP25-SN2.

3.6.7 Mutation of two conserved lysine amino acids (K98/K99) of the Cpx II CTD does not alter Cpx II function.

To study whether K98/K99 are functionally relevant and interact with E170 of SNAP25-SN2, in a first set of experiments, both amino acids were exchanged by alanines **(Figure 32 A).** The results indicated that the expression of the mutant protein clamps the pre-release and rescues secretion like the wt protein **(Figure 32 B-F)**. Both, the extent of secretion (synchronous and asynchronous secretion) and also its kinetics as well as the secretory delay were unchanged compared to the Cpx II wt protein **(Figure 32 B-F)**. To maximize the perturbation, we also replaced the positively charged lysine residues with negatively charged glutamate residues to deliberately create a charge reversal **(Figure 33 A)**. Yet, the charge reversal exchange did not show any phenotypic changes **(Figure 33 B-F)**, displaying similar results to those described in the previous figure **(Figure 32 B-F)**. Indeed,

nor the synchronous secretion or the asynchronous secretion were perturbed. On top of that, the kinetics of release (τRRP and τSRP) showed a similar result to that of the Cpx II wt protein **(Figure 33 D)**. Furthermore, immunofluorescences analyses showed that the different mutants used in this experiment expressed with similar efficiency as the Cpx II wt protein **(Figure 40 A-B)**.

These functional observations suggest that the two conserved lysines of the Cpx II CTD (K98, K99) do not appear to be essential for fusion. They also suggest that they may not provide electrostatic interactions with E170 in SNAP25-SN2.

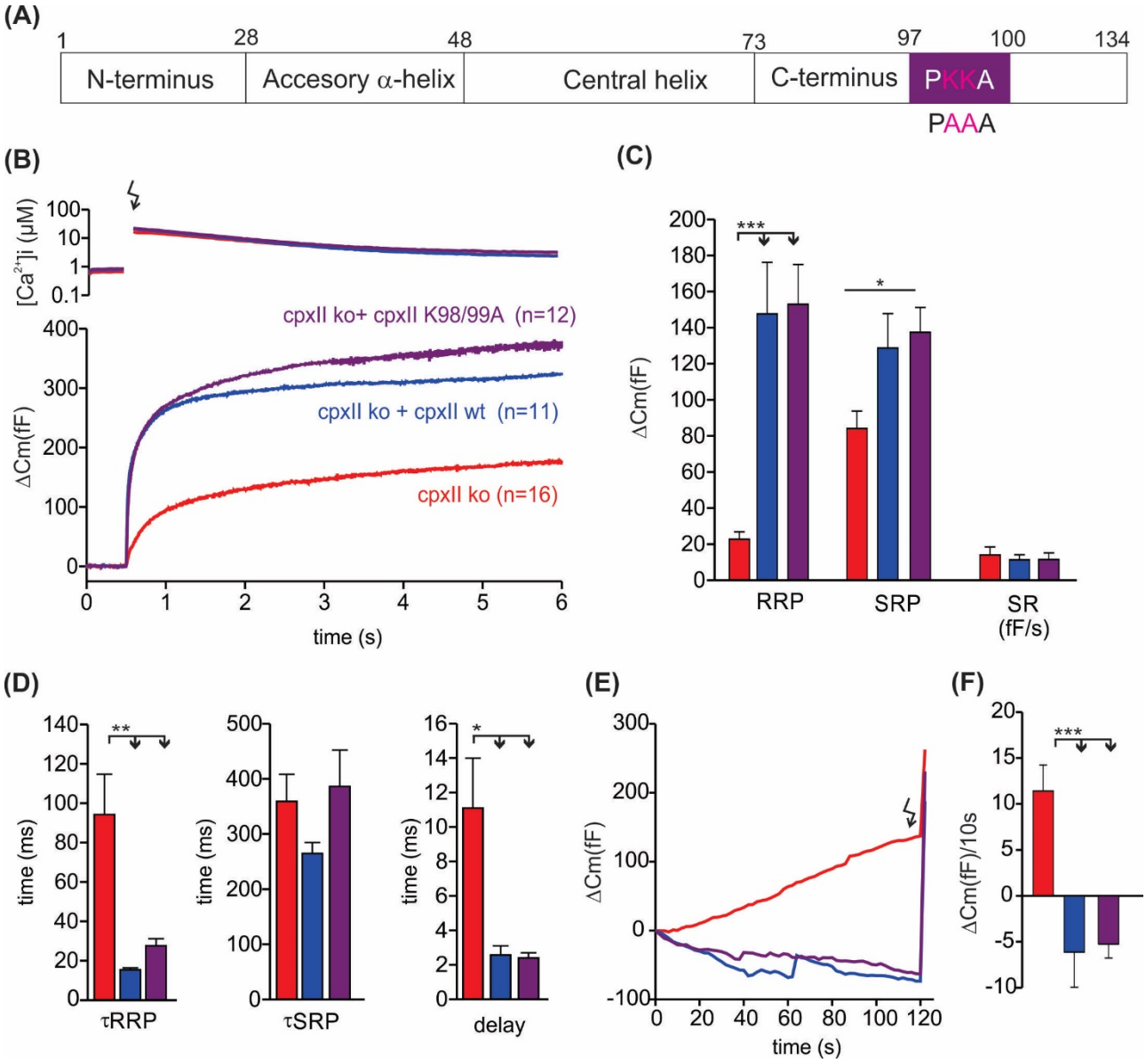

Figure 32. Replacing two conserve amino acids (K98, K99) of Cpx II CTD by alanines completely restores exocytosis. **(A)** Drawing representing the different Cpx II domains as well as the mutation tested. **(B)** Calcium levels after UV-flash (top) capacitance traces after UV-flash (bottom). **(C)** Average analyses of the capacitance trace. **(D)** Release kinetics (τRRP, τSRP) and delay **(E)** Capacitance traces of the asynchronous release. **(F)** Average of the rate of

tonic secretion, the ko cells have significantly higher release in this phase. Statistical analyses were done using one-way ANOVA followed by Tukey-Kramer post test. p<0.05, **, p<0.01, ***, p<0.001. Error bars indicate mean ± SEM,

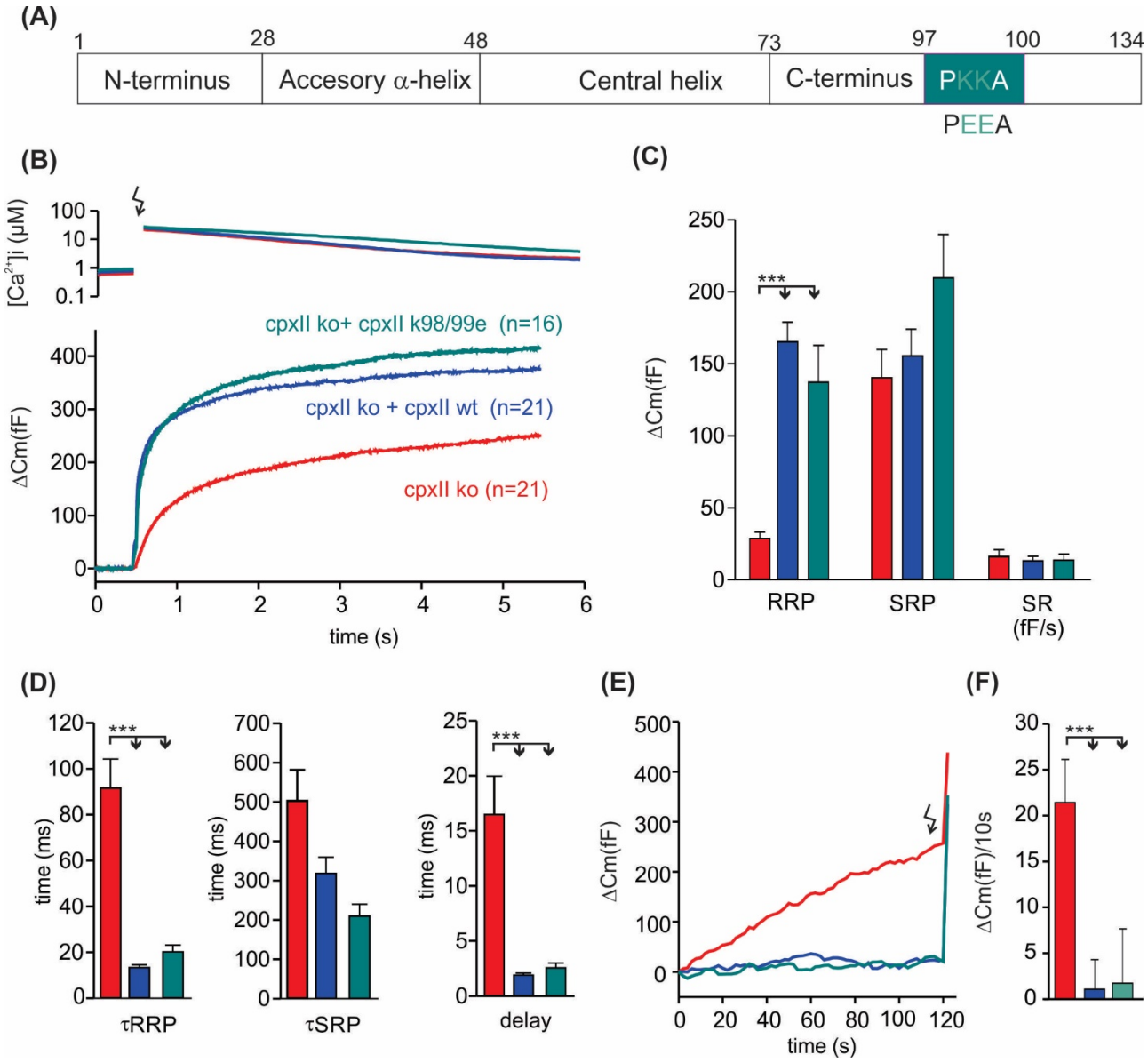

Figure 33. Replacing two conserve amino acids (K98, K99) of Cpx II CTD by glutamic acid completely restores exocytosis. **(A)** Drawing representing the different complexin domains as well as the mutation tested. **(B)** Calcium levels after UV-flash (top) capacitance traces after UV-flash (bottom) **(C)** Average analyses of the capacitance traces **(D)** Average analyses of the release kinetics (τRRP and τSRP) and the delay **(E, F)** Capacitance trace and average of the asynchronous secretion. Statistical analyses were done using one-way ANOVA followed by Tukey-Kramer post test. p<0.05, **, p<0.01, ***, p<0.001. Error bars indicate mean ± SEM,

3.6.8 Structural modifications of the Cpx II CTD do not affect the function of the protein

Protein structure predictions using I-Tasser (Iterative Threading Assembly Refinement) (Zhang, 2008) have shown that exchange of 3 prolines in the Cpx II C-terminus (P89, P97 and P102) by

alanine residues may lead to structural changes in the sequence **(Figure 34)**. Indeed, proline residues are known as alpha helix breakers, because of their lack of hydrogen in their side chain. These amino acids are not able to participate in the hydrogen bonds with other residues and therefore they introduce a destabilizing kink on the helix (Williams and Deber, 1991). Hence, the prolines may provide conformational flexibility that is needed for the back-folding of the Cpx II C-terminal domain in order to bind to membrane-proximal parts of the SNARE complex. To test whether the helix break made by the 3 prolines **(Figure 34, top panel)** is necessary for the back-folding of Cpx II CTD, these amino acids were exchanged by alanines. Alanines, are able to make hydrogen bonds with other residues, therefore they will stabilize the helix **(Figure 34, lower panel)**. The maintenance of the helix due to the introduction of three alanines (Cpx II 3-P/A), may disrupt the flexibility of the region and thereby prevent the back-folding of Cpx II CTD.

To test this hypothesis, capacitance measurements using photolytic uncaging of intracellular calcium were done with the mutant protein, Cpx II 3-P/A **(Figure 35 A)**. The data indicates that the mutant did not impair secretion. Indeed, no changes in the synchronous nor in the asynchronous secretion were detected when compared to the wt protein **(Figure 35 B, E)**. Furthermore, the release kinetics (τRRP and τSRP) and the delay were also unaffected by this mutation **(Figure 35 D)**. On top of that, immunofluorescences analyses performed to compared the expression levels of the proteins use, showed similar expression of Cpx II 3-P/A with Cpx II wt protein **(Figure 40 A-B)**.

It can be concluded that the exchange of 3 prolines to alanines in this region of the protein does not affect the function of Cpx II. This suggests, that the flexibility of this region conferred by the presence of 3 prolines may not be responsible for the folding back of the CTD of Cpx II.

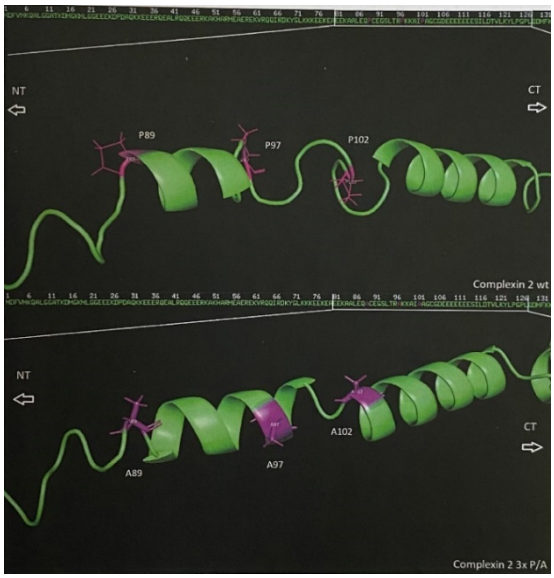

Figure 34. Exchanging three prolines for alanines in the Cpx II CTD leads to structural changes. Cartoon showing the 3D structure of the C-terminus highlighting in purple the 3 prolines: P89, P97, and P102 (top). Note that proline residues, as helix breakers, often bracket the helical regions within the CTD, cartoon showing the 3D structure of the c-terminal with the mutation of the 3 prolines to alanines (bottom). The prolines make a break in the helix (top) while their exchange to alanine makes a continuous helix (bottom). Structure prediction using l-Tasser and structure representation with PYMOL. (*Figure done by Eren Aktas*).

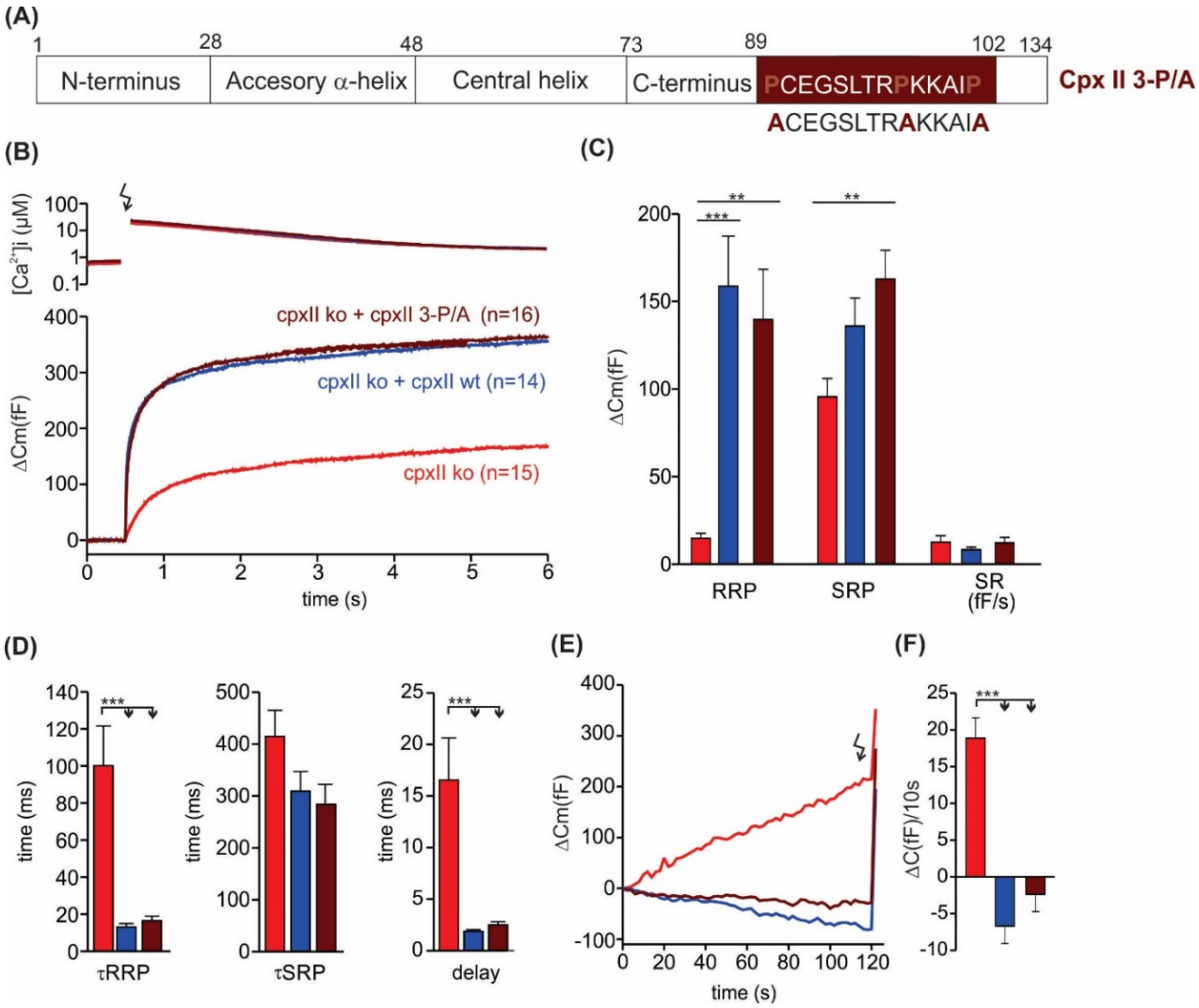

Figure 35. The mutation of 3 Prolines (P89, P97 and P102) to Alanines does not affect the Complexin II function. **(A)** Drawing representing the tested mutation. **(B)** Calcium levels after UV-flash (top) capacitance traces after UV-flash (bottom). **(C)** Average analyses of capacitance traces show similar levels of secretion of the proline mutant (RRP, SRP

and SR) to the Cpx II wt protein. **(D)** The release kinetics (τRRP and τSRP) as well as the delay remain unchanged for the mutant compared to the Cpx II wt protein **(E, F)** Capacitance traces and average of the rate of asynchronous secretion, the ko cells have significantly higher release in this phase compared to the other two groups. Statistical analyses were done using one-way ANOVA followed by Tukey-Kramer post test. $p<0.05$, **, $p<0.01$, ***, $p<0.001$. Error bars indicate mean ± SEM.

3.7 The role of the accessory α-helix of Complexin II

The function of the accessory α-helix (AH) is very controversial. Indeed, over the years, the mechanisms behind the clamping function of the AH has been debated (Mohrmann et al., 2015). Different studies have shown that depending on the model use and the experimental approach, different outcomes concerning the mechanism of inhibition of the AH were described (Cho et al., 2014; Giraudo et al., 2009). In this study we want to further explore the clamping function of the AH by using state of the art electrophysiology measurements monitoring intracellular calcium concentration.

3.7.1 The accessory α-helix of Complexin II regulates the extent of synchronous secretion

To study the role of the accessory α-helix of Complexin II we used a truncated mutant (Cpx II 41-134), this mutant lacks the N-terminal and a large part of the AH **(Figure 36 A)**. However, the mutant protein conserves a small part of the AH, comprising amino acids 41 to 48. The reason why some amino acids of the AH are still present in our truncated protein is because previous studies have shown that the truncated Cpx II protein comprising amino acids 47 to 134 decreases Cpx II binding to the SNARE proteins (Xue et al., 2007). While the one including amino acids 41 to 134 showed the same binding of Cpx II to the SNARE complex as the wt protein (Xue et al., 2007).

Our functional data showed a strong decrease of the synchronous secretion for the mutant protein 41-134 compared to the wt **(Figure 36 B)**. Indeed, the RRP as well as the SRP were significantly decreased **(Figure 36 C)**. Release kinetics were also affected, a slower τRRP and a longer delay were observed with the truncated protein **(Figure 36 D)**. The changes in these features (the slow τRRP and the longer delay) are due to the absence of the N-terminal domain. Indeed, as it has been shown in previous studies the time course of the synchronous secretion is control by the N-terminal domain of Cpx II (Dhara et al., 2014). Finally, regarding the pre-release phase, the 41-134 mutant failed to restore clamping like the wt (50%) **(Figure 36 E-F)**. This phenotype indicates that the AH is necessary, at least in part, for clamping the asynchronous secretion. Collectively, our results highlight a partial inhibitory phenotype of the AH of Cpx II.

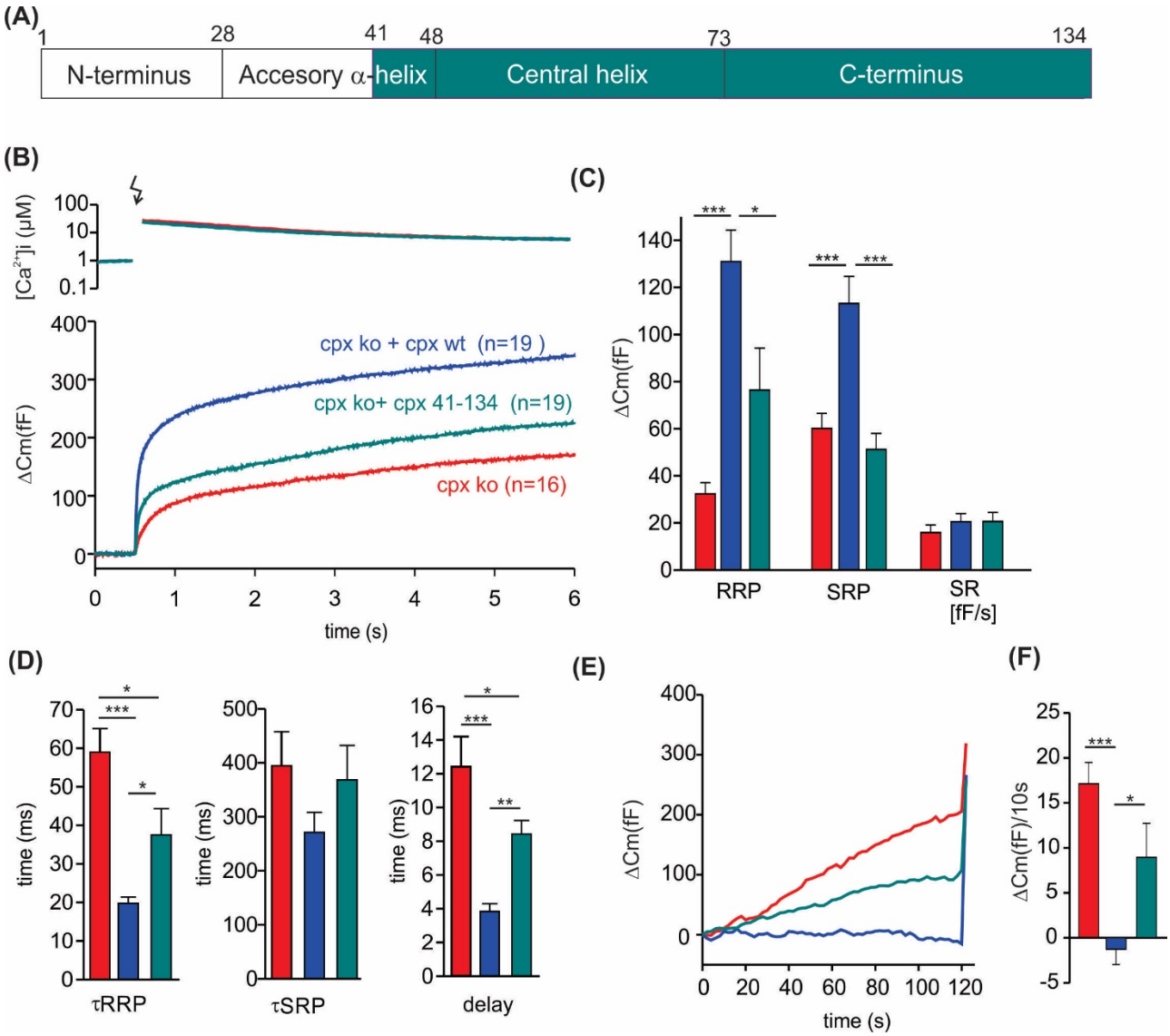

Figure 36. Expression of Cpx II 41-134 strongly diminishes the synchronous secretion and exhibits an unclamping phenotype. (A) Drawing representing the truncation used in the experiments. **(B)** Calcium levels after UV-flash (top) capacitance traces after UV-flash (bottom), the truncated protein shows a strong decrease in the synchronous secretion. **(C)** Average analyses of the capacitance traces shows a decrease in the RRP as well as in the SRP in the truncated mutant compared to the wt protein. **(D)** The τRRP and the delay are significantly slower in Cpx II 41-134 compared to Cpx II wt, whereas the τSRP remains very similar in the three different tested groups **(E, F)** The capacitance and the average trace of the asynchronous secretion shows that the mutant protein, Cpx II 41-134 fails to fully restore the clamping. Statistical analyses were done using one-way ANOVA followed by Tukey-Kramer post test. $p<0.05$, **, $p<0.01$, ***, $p<0.001$. Error bars indicate mean ± SEM.

3.7.2 The Cpx II 41-134 truncated mutant can out-compete the endogenous Cpx II protein

The loss-of-function phenotype of the truncated Cpx II 41-134 mutant may simply be due to misfolding of the protein. In following this up, we expressed the mutant in wt cells in order to test whether it can productively bind to the SNARE complex and compete with the endogenous Cpx II protein. In the latter case, a dominant-negative phenotype is expected. The results showed a similar phenotype to that observed in ko cells expressing the mutant protein **(Figure 36 A-F)**. The synchronous secretion was strongly diminished in the mutant compared to Cpx II wt overexpression. Indeed, a reduction in the RRP and SRP was observed **(Figure 37 B, C)**. The kinetic of the release were also impaired with a slower τRRP and a longer delay **(Figure 37 D)**. Finally, the asynchronous secretion was also significantly increased compared to wt **(Figure 37 E, F)**. These results indicate that the 41-134 truncated protein acts as a dominant-negative mutant protein, meaning that it competes with the endogenous Cpx II protein.

Overall, both sets of data suggest that the AH plays a role in fusion inhibition. However, the mechanisms underlying this function are still unclear.

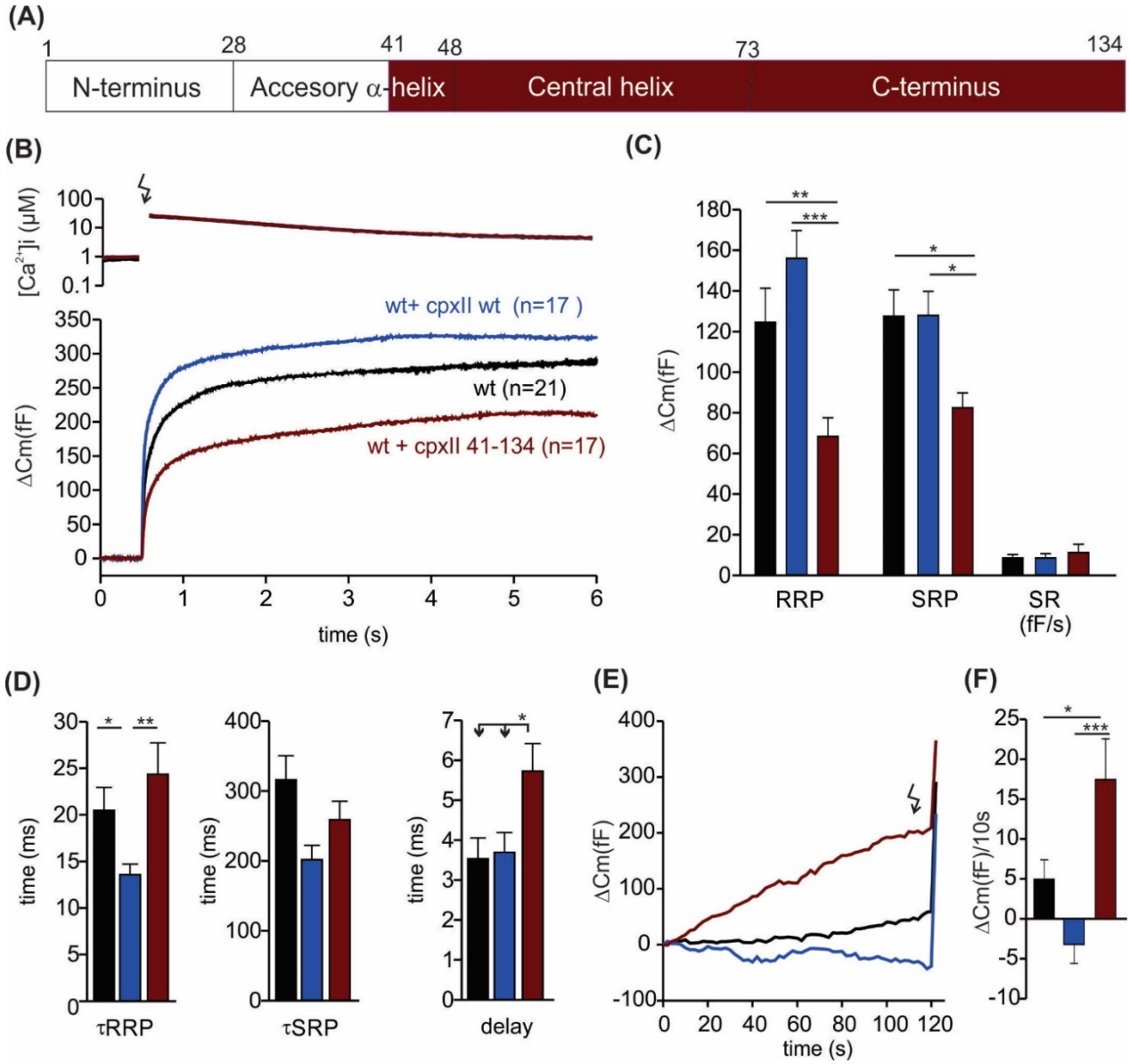

Figure 37. Expression of Cpx II 41-134 in a wt background strongly diminishes synchronous secretion and unclamps secretion. (A) Drawing representing the truncation used in the experiment. **(B)** Calcium levels after UV-flash (top) capacitance traces after UV-flash (bottom), the strong decrease in the synchronous secretion shows that Cpx II 41-134 acts as dominant negative **(C)** Average analyses of the capacitance traces shows a decrease in the RRP as well as in the SRP in the truncated mutant compared to the wt protein. **(D)** The τRRP and the delay are significantly slower in the Cpx II 41-134, whereas the τSRP remains very similar in the three different tested groups **(E, F)** The capacitance and the average trace of the asynchronous secretion shows that Cpx II 41-134 unclamps secretion. Statistical analyses were done using one-way ANOVA followed by Tukey-Kramer post test. $p<0.05$, **, $p<0.01$, ***, $p<0.001$. Error bars indicate mean ± SEM.

3.7.3 VAMP2-mimetic mutations in Cpx II AH do not alter secretion

Previous studies have proposed a variety of different models for the inhibitory AH function, including direct binding to SNAREs (Bykhovskaia et al., 2013; Cho et al., 2014; Giraudo et al., 2009; Kummel et al., 2011; Yang et al., 2010) electrostatic interactions with membranes (Trimbuch et al., 2014), and direct effects on the central CPX helix and its SNARE binding through secondary structure interactions (Chen et al., 2002). In particular, the hypothesis that AH competes with VAMP2 for binding to SNARE complexes has received much attention (Giraudo et al., 2009). Indeed, this idea is based on sequence similarities between the AH of Complexin (aligned in antiparallel orientation) and the Syb II hydrophobic layers (layer position +3, +4 and +7). This idea has been tested *in vivo* and *in vitro* by the generation of Complexin mutants which enhanced the sequence similarities (superclamp mutant) and mutants with modified sequences to decrease the proteins interactions (poorclamp mutant) (Giraudo et al., 2009). While the *in vitro* studies have demonstrated the expected result, *in vivo* studies could not reproduce the phenotype (Giraudo et al., 2009; Yang et al., 2010). Therefore, in our study we wanted to further explore these mutants by measuring changes in capacitance in a physiological environment and using photolytic uncaging of intracellular calcium.

First of all, we studied if changes on capacitance occurred with the superclamp (Giraudo et al., 2009). The amino acids that were exchanged in these mutation to mimic the hydrophobic layer of VAMP2 were: D27L, E34F and R37A **(Figure 38 A)**. The superclamp mutant shows a complete restoration of the EB **(Figure 38 B, C)** and a clamping phenotype like the wt protein **(Figure 38 E, F)**. In addition, no changes were seen in the release kinetics or the delay **(Figure 38 A)**.

Collectively, these results suggest that there may be no competition between VAMP2 and the AH for binding to the SNARE complex. Indeed, if a competition was present, we should see that he mutant proteins clamps better than the wt. Furthermore, since a gain-of-function phenotype is less likely than a loss-of-function, we next tested the poorclamp mutant.

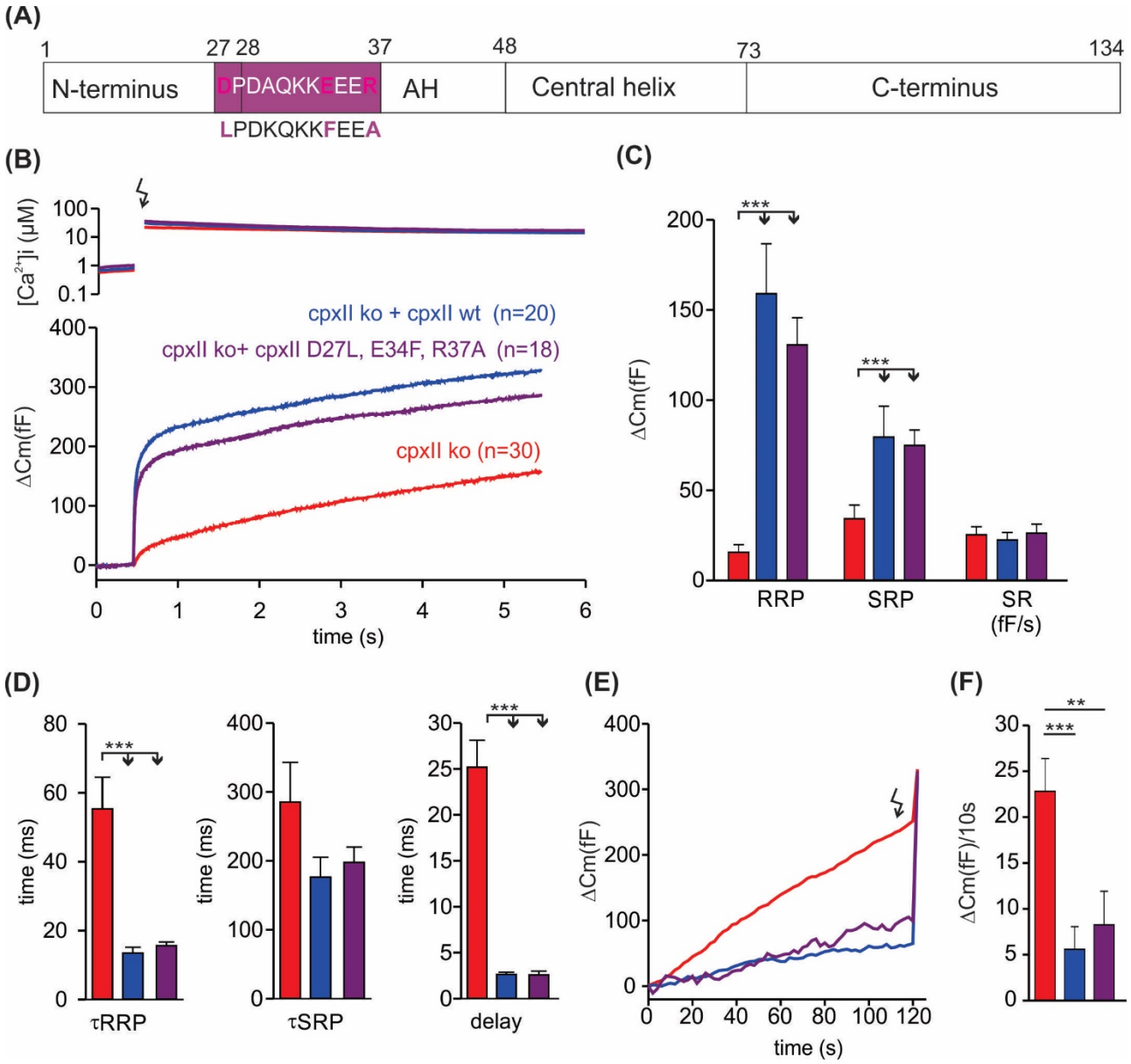

Figure 38. VAMP2 mimetic mutation in the accessory α-helix of Cpx II (D27L, E34F, R37A) does not alter secretion. (A) Drawing representing the mutated amino acids. **(B)** Calcium levels after UV-flash (top), capacitance traces after UV-flash (bottom), the mutant protein shows no differences in the synchronous secretion compared to the wt. **(C)** Average analyses of the capacitance traces shows no differences in the mutant protein compared to the wt in any of the three parameters measured (RRP, SRP and SR). **(D)** The kinetics of the release (τRRP and τSRP) as well as the delay are unchanged in the mutant protein compared to the wt. **(E, F).** The capacitance and the average trace of the asynchronous secretion shows that the mutant protein has a clamping phenotype as the wt protein. Statistical analyses were done using one-way ANOVA followed by Tukey-Kramer post test. $p<0.05$, **, $p<0.01$, ***, $p<0.001$. Error bars indicate mean ± SEM.

3.7.4 VAMP2-divergent mutations in Cpx II AH do not alter secretion

The poorclamp mutant consists on introducing 2 mutations, one on the AH and another on the far N-terminus. These mutations render Cpx II less similar to VAMP2 **(Figure 39 A)**. Our findings indicate that the poorclamp mutant did not show any secretion deficit **(Figure 39 B-F)**. Indeed, the synchronous secretion of the mutant was very similar to the one of the wt protein **(Figure 39 B, C)**. Concerning the asynchronous secretion, similar clamping activity was seen with the poorclamp and the wt **(Figure 39 E, F)**. The release kinetics and the delay were unchanged **(Figure 39 D)**. Altogether, this results confirm the observation made in the previous figure, a competition between VAMP2 and the AH of Cpx II for binding to the SNARE complex seems unlikely. Indeed, if there was a competition between both proteins we should have seen an unclamping phenotype with the poorclamp mutant. Furthermore, for both mutants (the poorclamp and the superclamp) immunofluorescences analysis have been done to rule out the possibility that the phenotype observed is due to different protein expression. The results show that both mutants expressed with similar efficiency as the Cpx II wt protein, therefore the phenotype cannot be due to differences in expression levels **(Figure 40 A, B,)**. Overall, our findings contradict earlier observations suggesting that there is a competition between Cpx II and VAMP2 for binding to the SNARE complex (Giraudo et al., 2009) and leaves the question unanswered about the mechanisms behind the Cpx II AH inhibition phenotype.

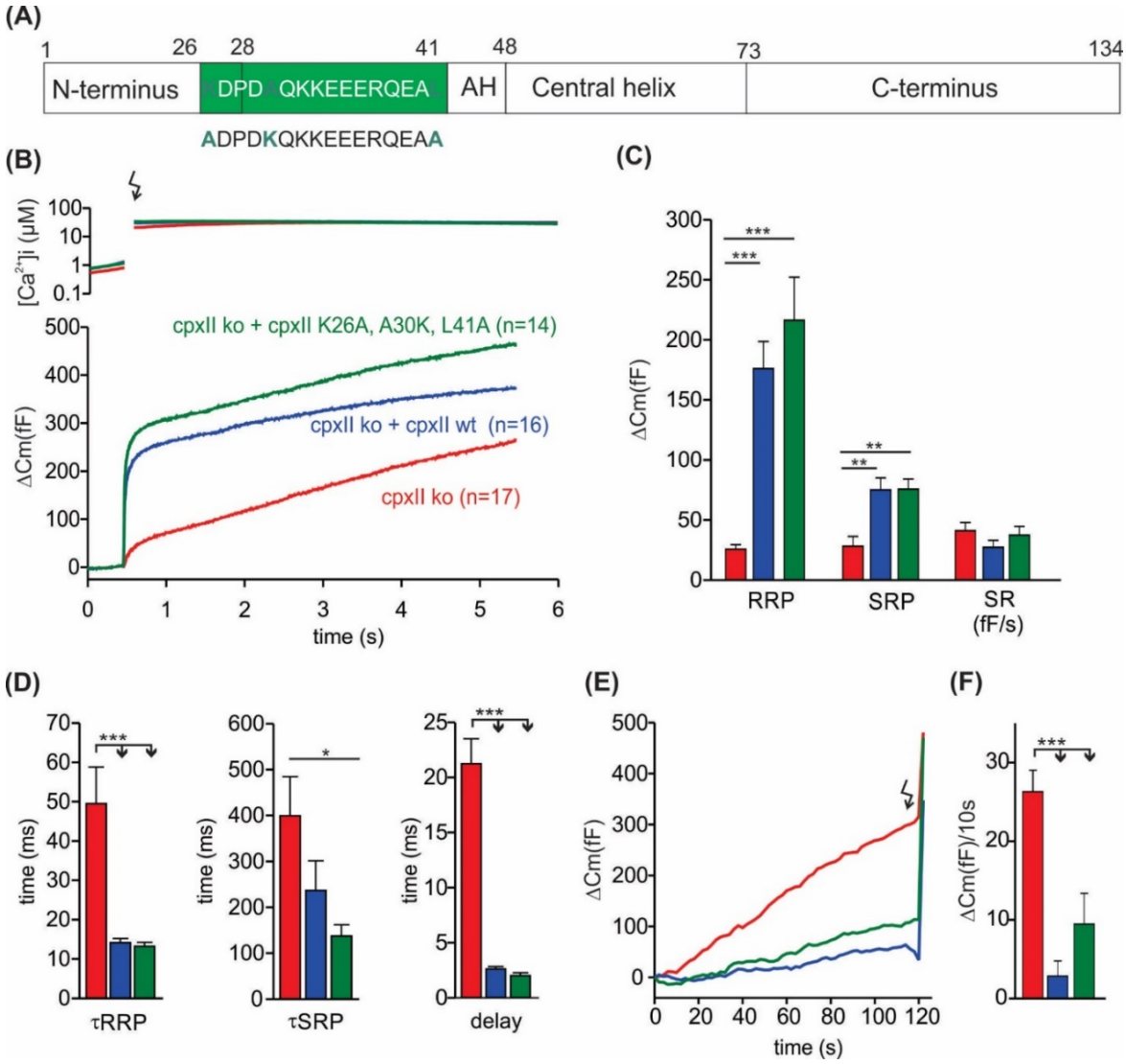

Figure 39. VAMP2 divergent mutations in the accessory α-helix of Cpx II (K26A/A30K, L41A) does not alter secretion. (A) Drawing representing the mutated amino acids. **(B)** Calcium levels after UV-flash (top), capacitance traces after UV-flash (bottom), the mutant protein shows no differences in the synchronous secretion compared to the wt. **(C)** Average analyses of the capacitance traces shows no differences in the mutant protein compared to the wt in any of the three parameters measured (RRP, SRP and SR). **(D)** The kinetics of the release (τRRP and τSRP) as well as the delay are unchanged in the mutant protein compared to the wt. **(E, F).** The capacitance and the average trace of the asynchronous secretion shows that the mutant protein has a clamping phenotype as the wt protein. Statistical analyses were done using one-way ANOVA followed by Tukey-Kramer post test. $p<0.05$, **, $p<0.01$, ***, $p<0.001$. Error bars indicate mean ± SEM.

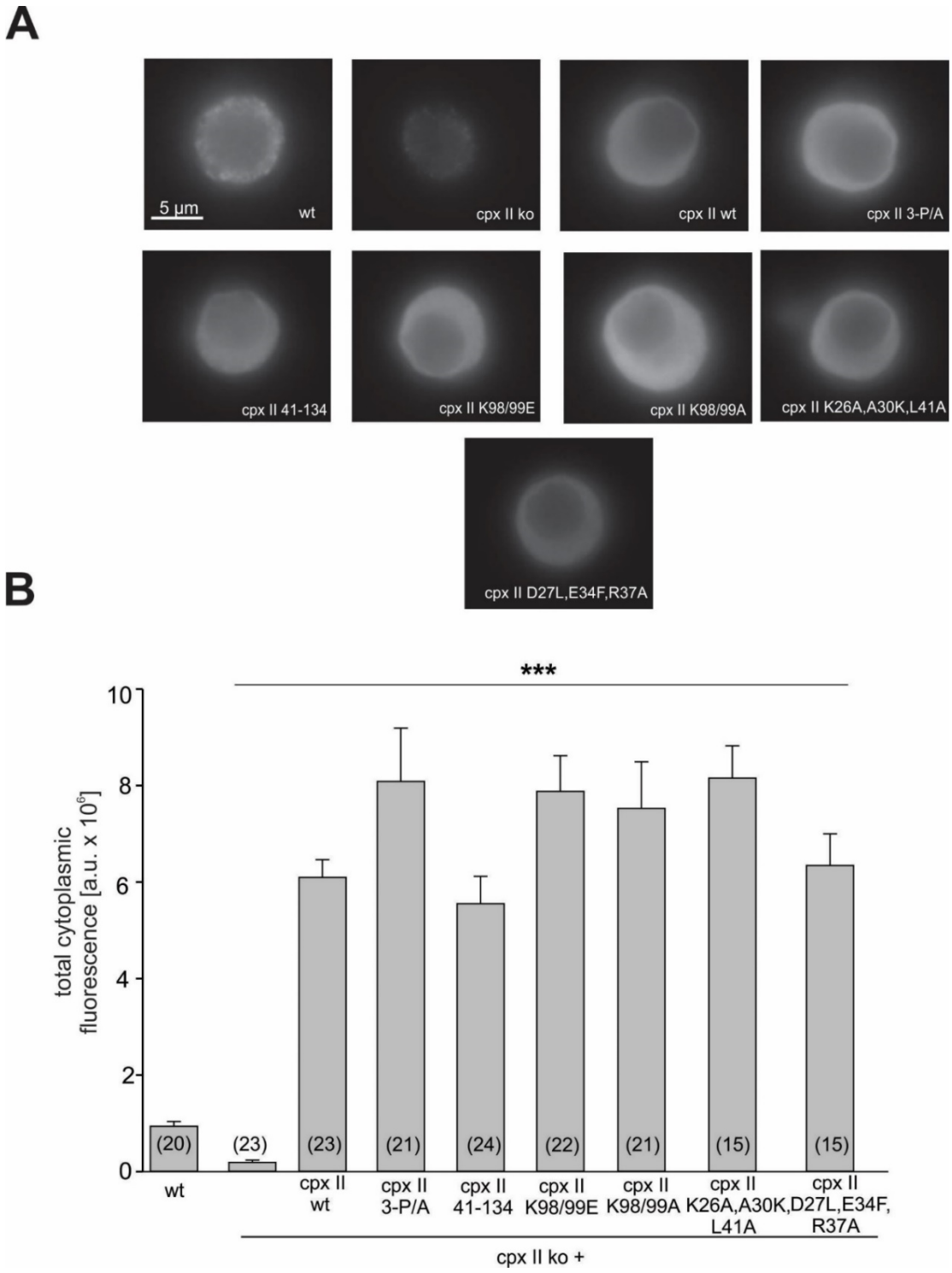

Figure 40. Cpx II mutants express with similar efficiency as Cpx II wt protein. (A) Exemplary images of Cpx II wt, Cpx II ko and Cpx II mutant proteins. Cells were immunostained with a primary antibody against Cpx II (rabbit anti-Cpx II) and a secondary antibody (Alexa Fluor 555-conjugated goat anti-rabbit antibody; dilution 1:1000, Invitrogen). The signals of Cpx II expressing the wt protein or the mutants were stronger than the Cpx II ko or the wt protein, different exposure times were used (e.g. Cpx II wt: 0.030s, Cpx II ko: 1s and wt protein:0.2s) **(B)** Mean total cytoplasmic fluorescence intensity for the different groups mention in A 5.5 hours after transfection with SFV. Data appears as mean ± SEM, ***, $p<0.001$. Statistical analyses were done using one-way analysis of variance followed by Tukey-Kramer post-test.

4. Discussion

For membrane fusion to take place, protein-protein interaction as well as protein- lipid interactions are necessary. In this thesis, we demonstrate that exchanging the TMD of VAMP2 by the one of VAMP1 or VAMP8 (which are responsible of secreting small and large vesicles respectively) does not change the secretion response when compared to VAMP2. We also show that the lipid molecules oleic acid (OA) and lysophosphatidyl choline (LPC) enhance or lower secretion respectively when apply to the intracellular leaflet. Furthermore, we also study the inhibitory mode of action of Complexin, a SNARE regulatory protein which is crucial to impede uncontrolled vesicle fusion. Indeed, we show that the inhibitory role of the C-terminal domain of Cpx is not a consequence of vesicle association but rather due to its SNAP25-SN1 mimetic properties. We also show that in the absence of the accessory α-helix, the truncated Complexin protein is not able to support synchronous secretion and it partially disinhibits premature release. Our results support a model were both, the CTD and the AH are needed to prevent premature vesicle release.

4.1 Naturally occurring v-SNARE TMD variants differentially regulate membrane fusion

For long time, the TMDs of SNARE proteins (Syntaxin and Synaptobrevin) were considered passive anchors of the SNARE complex, without any active role in the fusion process (Zhou et al., 2013). However, subsequent publications have demonstrated that SNARE TMDs play an active role in fusion (Dhara et al., 2016; Fdez et al., 2010). Indeed, it has been suggested that the structural flexibility of the VAMP2-TMD, which is determined by the β-branched amino acids content, is crucial for fusion and pore expansion (Dhara et al., 2016). Based on these findings, we investigated different physiological v-SNARE TMD variants that differ in their content of β-branched amino acids, and are employed for the exocytosis of differentially-sized vesicles (Dhara et al., 2016). For this, two chimeric mutant proteins containing the cytoplasmic domain of VAMP2 and the TMD of either VAMP8 or VAMP1 were generated and membrane capacitance upon photolytic Ca^{2+} uncaging was recorded. The results showed that none of the chimeric mutants tested above affects secretion compared to the wt protein **(Figure 17)**. In addition, viral expression analyses showed that both mutants are expressed at similar levels as the wt protein and are similarly sorted to vesicles **(Figure 18 and 19)** indicating that the phenotype observed is not due to missorting or differences in the protein levels. Overall, it is interesting to note that neither the increased nor the decreased of β-branched amino acids change the secretion response, while their complete absence (poly- L) has been shown to strongly reduce secretion (Dhara et al., 2016). This indicates that only large changes in the number of helix-rigidifying amino acids have an impact on exocytosis initiation and exocytosis

competence. Yet, experiments performed by my colleague Dr. Dhara measuring single vesicle release with carbon fiber amperometry showed that VAMP2-VAMP8 TMD promotes much faster fusion pore expansion than VAMP2-VAMP1 TMD (Dhara et al., 2020). These results demonstrate that the TMD variants of v-SNARE have different effects on the kinetics of the fusion pore. Therefore, these kinetic differences may be physiologically relevant because they may point to an unprecedented mechanism by which SNARE isoforms promote fusion pore expansion of large-sized vesicles through an increased number of β-branched amino acids. By this mechanism, VAMP8 is able to promote release of even bulky cargo molecules from large sized mast cell vesicles (Alvarez de Toledo et al., 1993) without compromising exocytosis. For VAMP1 mediated exocytosis, instead, small sized transmitter molecules like acetylcholine are readily released from synaptic vesicles through the initial fusion pore, enabling rapid recycling without the necessity of full membrane merger. Overall, the content of ß-branched amino acids within the different v-SNARE TMDs seems to be adapted to ensure efficient transmitter release from differentially-sized vesicles.

4.2 Intracellular application of methanol enhances fusion

To overcome the energy barriers for membrane fusion, both, proteins and lipids are expected to cooperate. In particular, dehydration of the opposing membrane as well as membrane bending represent large energy barriers, which have to be surmounted *en route* to membrane fusion. Short chain alcohols, like methanol, are expected to reduce membrane bending rigidity by disordering the packaging of the lipid hydro carbon chains (Gurtovenko and Anwar, 2009). To this end, we applied methanol to see how its insertion affects Ca^{2+} triggered vesicle fusion. Indeed, the results showed that intracellular methanol strongly enhances vesicle fusion. The synchronous secretion is nearly doubled **(Figure 20)** with strong changes in the RRP and to a lesser degree in the SRP. No changes were observed in the sustained phase of secretion. The selective increase of the exocytotic burst may be due to the fact that synchronous secretion requires more energy than asynchronous secretion and therefore benefits from the methanol treatment. This result compares well with previous observations by Kesavan and colleagues, showing that amino acids insertions within the linker domain of Syb II (to dissipate the force transfer between the SNARE motif and the TMD) affect the RRP size more strongly than the sustained phase of secretion (Kesavan et al., 2007). Alternatively, it is possible that the sustained phase of exocytosis is determined by rate-limiting steps like vesicle recruitment and thereby shows an apparent resistance to methanol treatment. Importantly, the results obtained with intracellular methanol application are remarkably similar to those observed in experiments with protein-free liposome (Chanturiya et al., 1999). Here, addition of methanol in the *cis* leaflet increases hemifusion events, whereas addition into the *trans* membrane does not change the total number of

hemifusion events (Chanturiya et al., 1999), an observation that compares well with previous studies in chromaffin cells by M. Borisovska (Borisovska and Bruns, unpublished observation). The fact that methanol affects secretion in a leaflet-specific manner carries several important pieces of information. At first, it shows that only perturbation of the contacting (cis) leaflets affect fusion efficiency. Secondly, the similar leaflet dependency in granule and liposome fusion indicates that both types of fusion proceed through similar lipidic intermediates like the formation of an intermembranous hemifusion stalk (Chanturiya et al., 1999). Last but not least, it provides strong evidence that the observed methanol effects are caused by perturbation of membranes rather than by off-target effects on proteins.

4.3 Lipid molecules differentially affects fusion and may act together with v-SNARE TMDs

The membrane bilayer is composed of lipids that regulate membrane fusion by conferring spontaneous curvature. Among these lipids, we were interested in two species that have different shapes and therefore affect fusion differently. We used OA which has a cone-shaped structure and therefore promotes negative curvature. In addition, we used LPC which has an inverted cone shaped structure and therefore promotes positive curvature. Intracellular application of these lipids shows that OA promotes fusion while LPC inhibits it **(Figure 22)**. Indeed, the RRP is increased with OA and decreased with LPC. No changes in the release kinetics or the exocytosis timing between the two groups were observed. These results suggest that promoting negative curvature in the proximal leaflets of opposing membranes regulates pool formation and exocytosis competence without changing triggering of exocytosis. In contrast, extracellular application of LPC or OA do not alter the overall secretion **(Figure 23)**. The reason why secretion is not affected by this lipid application is because only perturbation of the contacting (cis) leaflets affect fusion efficiency. In addition, these results suggest that the negative curvature conferred by the intracellular application of OA, favors the formation of the intermembrane stalk (which has a net negative curvature) and helps with the lowering of the hydration repulsion forces between the two merging membranes (Chernomordik and Kozlov, 2008; Kawamoto et al., 2015; Smirnova et al., 2019). Nevertheless, these findings contrast previous results by Zhang and Jackson. They showed an increase in membrane capacitance with intracellular LPC and a decrease with OA in response to depolarization of chromaffin cells with high KCl (Zhang and Jackson, 2010). These apparent discrepancies may be due to differences in the experimental approach. In fact, while they used depolarization-evoked response, we used Ca^{2+} infusion experiments and, since both experiments differed in intracellular calcium concentration as well as exocytosis timing, this could explain the differences in the results. In addition, LPC is known to influence the activation of voltage-dependent calcium channels (Ben-Zeev et al., 2010). Thus,

changes in the calcium concentration due to LPC may have mask the actual effect of lipids in membrane fusion. In addition, experiments done by my colleague Dr. Dhara using carbon fiber amperometry extended these findings by showing that intracellular infusion of OA rescued the slow rate of secretion and the reduced capacitance response observed with the TMD poly-L mutant (Dhara et al., 2020). These results allowed to conclude that v-SNARE TMDs and lipids act together to facilitate fusion and pore expansion (Dhara et al., 2020).

4.4 A model for the Cpx II C-terminus inhibition function

Previous experiments have shown that the Cpx II C-terminal domain has a role in inhibiting premature release (Dhara et al., 2014). In more recent work, we extend these findings by showing that deletion of the last 19 amino acids or the last 34 amino acids of Cpx II enhances asynchronous secretion and fails to rescue synchronous secretion to the wt level **(Figure 26)** (Makke et al., 2018). Concerning the mechanism of inhibition of the CTD of Cpx, previous studies done in the C.elegans neuromuscular junction or in murine cortical neurons have shown that the C-terminal region of Complexin is responsible for tethering the protein to synaptic vesicles to allow other regions, such as the AH, to exercise their inhibitory role (Gong et al., 2016; Wragg et al., 2013). Here, we demonstrate that targeting Cpx II $^{1\text{-}100}$ to the vesicular membrane, using a vesicular membrane anchor (CSPα) does not rescue the inhibitory phenotype of the CTD. Indeed, the mutant protein Cpx II $^{1\text{-}100}$ CSPα efficiently sorts to vesicular membranes, as shown by confocal microscopy (Makke et al., 2018), but fails to arrest premature vesicle fusion **(Figure 25)**. In agreement with our hypothesis, studies from Dittman and colleagues have proven that membrane binding is not sufficient for Complexin to exert its inhibitory function. They have shown that mutations in the amphipathic site of worm Complexin do not interfere with membrane binding in an *in vitro* assay, but do interfere with Complexin function, which was not rescue in an *in vivo* assay (Snead et al., 2017; Wragg et al., 2017). Overall, with our experiments, we proved that the function of the CTD of Cpx is not to address the protein to the vesicle membrane. Therefore, next, we wanted to study how the CTD of Cpx II exerts its inhibitory action. Given the high number of hydrophobic residues in the CTD, presented in heptad repeats, this domain may associate with the SNARE proteins and interfere with their zippering. Studies from our laboratory pointed out a high degree of similarity between the Cpx II C-terminal domain and the C-terminal half of the SNAP25-SN1. These similarities suggest a possible competition between the two proteins for binding to the SNARE complex (Makke et al., 2018). To test whether a competition exists, two chimeric mutants were created for which either the last 19 or 34 aa of Cpx II C-terminal domain were replaced with the corresponding regions of SNAP25-SN1. When expressed in Cpx II ko cells the chimeras fully restored magnitude and timing of secretion to the level of the wt protein

(Figure 27 and 28), whereas expression of a Cpx II mutant carrying an unrelated alpha-helix in the last 19 or 34 amino acids of the protein failed to restore exocytosis **(Figure 27 and 28)** presenting similar results to those observed with Cpx II $^{1-100}$ and Cpx II $^{1-115}$ **(Figure 27 and** (Makke et al., 2018). The high degree of similarity between the C-terminal domain of Cpx II and SNAP25-SN1, as well as their functional interchangeability, strongly suggests the presence of a competition between both proteins for binding to the SNARE complex. In this context, it is important to highlight previous studies where chimeric proteins of Cpx II were unable to restore the function of Complexin (Kaeser-Woo et al., 2012; Wragg et al., 2017). For example, a chimeric mutant between Cpx I and Cpx III CTD could not inhibit, in murine cortical neurons, the spontaneous release of synaptic vesicles. This phenotype may be due to differences in the periodicity of hydrophobic residues between both C-terminal sequences (Kaeser-Woo et al., 2012). In the same line, a chimeric mutant protein between worm Cpx I and murine Cpx I failed to restore the Cpx I function in worm (Wragg et al., 2017) an observation which may also be explained by differences in the pattern of periodicity of hydrophobic residues. Overall, the results in this work highlight a novel mechanism of Cpx II clamp action in Ca^{2+} triggered exocytosis where the structural similarities of Cpx II C-terminal domain with SNAP25-SN1 are essential in clamping premature exocytosis. Moreover, these results as well as the intramolecular distance between the far C-terminal domain and the central domain of Cpx II suggest that Cpx II C-terminal region with its amphipathic helix folds back on the SNARE complex to prevent its zippering **(Figure 8 from (Makke et al., 2018).**

4.5 Putative mechanisms for orienting the CTD of Cpx II to the opposite side of the SNARE complex.

Previous studies have shown that Complexin is position in an antiparallel orientation (Chen et al., 2002), therefore for the CTD of Complexin to fold back on the partially assembled SNARE complex, structural flexibility from upstream regions of the C-terminal domain of Cpx are necessary. Previous studies using single molecule FRET have given proof of the folding back of the CTD by showing that the amino acid in position 105 (Cysteine) in the Cpx C-terminal domain interacts with Syntaxin 1a near the ionic (0) layer of the SNARE complex (Bowen et al., 2005). Here, we studied the possible mechanisms that may help with the back-folding of the Cpx II CTD. First, we focused on two lysines residues in position 98 and 99 of Cpx II. These amino acids are conserved in the animal kingdom and may provide electrostatic interactions with the aa E170 in SNAP25-SN2 **(Figure 31)**. In fact, the aa E170 in SNAP25-SN2 has been previously studied, along with another aa, the D166. Mutation of these two amino acids (D166A and E170A) resulted in a deficit of

synchronous secretion (Mohrmann et al., 2013) and an increase in the pre-release phase **(Figure 29)**. It was therefore of interest to investigate whether the two lysines residues are functionally relevant and if a possible interaction between these residues and E170 of SNAP25-SN2 is present. The exchange of the two lysines residues by either alanines (non-charged aa) or glutamic acid (negatively charged aa) showed no secretory deficits **(Figure 32 and 33).** The absence of a phenotypic change could be the consequence of our experimental approach, which relies on overexpression with the viral Semliki Forest system. In addition, it is possible that this mutation affects steps in the exocytotic process like fusion pore expansion which cannot be detected with measurements of membrane capacitance in the `whole-cell´ configuration. Therefore, other techniques such as single vesicle amperometry should be used to further investigate this issue. In parallel, we studied the role of amino acids D166 and E170 of the SNAP25-SN2 protein. Previous studies using liposome fusion assays have shown that mutation of these two amino acids disrupts the clamping function of Complexin (Schupp et al., 2016). To investigate whether these amino acids of SNAP25-SN2 are crucial for hindering premature exocytosis, we reinvestigated in photolytic Ca^{2+} uncaging experiments. Indeed, the results showed an increase in asynchronous secretion of the mutant cells (SNAP-25 D166A/E170A) compared with SNAP25 ko cells, as well as a trend of an increase compared with SNAP25 wt protein **(Figure 29 D, E)**. This phenotype highlights a possible interaction between SNAP25-SN2 (D166 and E170) and Cpx II. This interaction of Cpx II with SNAP25-SN2 could help to orient the CTD of Cpx II towards the opposite side of the SNARE complex. Nevertheless, further experiments are needed to delineate a potential binding between Cpx II and SNAP25-SN2. For example, *in vitro* assays with the mutated SNAP25-SN2 variant and Cpx II should be conducted to examine if the binding of Cpx II to the SNARE complex is altered with this mutation. If this *in vitro* assay confirms the phenotype observed in our experiment, further studies will be required to unravel which amino acids of Cpx II are involved in this interaction.

In addition, we studied a region in the CTD of Cpx II that contains 3 prolines residues (P89, P97 and P102). The reason why we were interested in these residues was because proline residues are known as alpha helix breakers, hence, the prolines may provide the conformational flexibility needed for the back-folding of the Cpx II C-terminal domain in order to bind to membrane-proximal parts of the SNARE complex **(Figure 34, top panel)**. Conversely, when these amino acids are replaced by alanines, the increased helicity of the protein region **(Figure 34, lower panel)** may reduce the likelihood of back-folding. Nevertheless, experiments performed in the mutant protein (P89A, P97A and P102A) showed no functional consequences compared to the wt protein **(Figure 35 A)**. It is

possible that the amino acid substitutions do not suffice to promote the envisioned structural changes. Yet, other scenarios cannot be rigorously excluded either.

4.6 Complexin II inhibitory action by the accessory α-helix

Several studies suggested that the AH exerts an inhibitory role by preventing premature vesicle secretion (Malsam et al., 2020; Xue et al., 2007). A variety of different models explaining the inhibitory function of the AH have been proposed, including direct binding to SNAREs (Bykhovskaia et al., 2013; Cho et al., 2014; Giraudo et al., 2009; Kummel et al., 2011; Yang et al., 2010) electrostatic interactions with membranes (Trimbuch et al., 2014), and direct effects on the central Cpx helix and its SNARE binding through secondary structure interactions (Chen et al., 2002). Moreover, up to date the mechanisms behind this inhibition are unclear. Some of these discrepancies and different interpretation may result from the fact that many experiments are confounded by uncontrolled Ca^{2+} concentration. In this work, the role of the AH was investigated on the background of a well-defined calcium stimulus and by monitoring the asynchronous as well as the synchronous secretion. The data reveal that the truncated mutant of Cpx II, the 41-134 mutant, partially disinhibits the asynchronous secretion and drastically reduces the synchronous secretion **(Figure 36).** The partial disinhibition of the asynchronous secretion indicates that other domains may assist the AH for clamping. Indeed, as it has been shown before, a truncated mutant lacking the last 15 amino acids of Complexin CTD is unable to inhibit asynchronous secretion, showing a similar phenotype to the one seen in Cpx II ko cells **(Figure 27)**. The phenotype of the 41-134 mutant is furthermore characterized by slower exocytosis timing (slow τRRP and longer delay). This result agrees well with previous observations, showing that loss of the Complexin's N-terminal domain (amino acids 1-28) slows down exocytosis timing (Dhara et al., 2014). Additionally, our experiments indicate that the mutant acts in a dominant negative manner, which is the expected consequence if the mutant is not misfolded, but able to out-compete the endogenous protein **(Figure 37)**. Overall, these experiments show that the AH exerts an inhibitory role in the fusion of premature release. Yet, the mechanisms behind the inhibitory function of the AH remained unclear. As mentioned before, several hypotheses have been postulated (Chen et al., 2002; Giraudo et al., 2009; Kummel et al., 2011; Trimbuch et al., 2014). Among all the hypotheses, the most promising at the present time is the one which postulates that there is a competition between VAMP2 and Cpx II AH for binding to the SNARE complex. This hypothesis has been validated by *in vitro* studies (Giraudo et al., 2009) but only mild effects were observed by *in vivo* studies (Giraudo et al., 2009; Yang et al., 2010). Therefore, it seems worthwhile to reinvestigate this mechanism. For that purpose, we tested the 'superclamp' mutant (which has more sequence similarities to VAMP2; D27L, E34F and R37A) and

the ‘poorclamp’ mutant (which has less sequence similarities to VAMP2; K26A, A30K, L41A). The results show that none of these mutants exhibit changes in secretion when compared with the wild type protein **(Figure 38 and 39)**. Our data contradicts previous studies by Giraudo and colleagues in which they found that the ‘superclamp’ mutant exhibits enhanced clamping action to that observed in wt cells. Furthermore, our results do not agree with the phenotype reported for the poorclamp mutant (Giraudo et al., 2009). The disparate results may be due to differences in the experimental approach. Indeed, Giraudo et al., have used a Hela cell line co-expressing the v- and t-SNAREs in a ‘flipped’ orientation on the plasma membrane in order to test their function in a cell-cell fusion assay. In contrast, we have tested these mutants in a more physiological context of granule exocytosis in chromaffin cells. Alternatively, one might speculate that potential alterations in the ability to hinder premature exocytosis are masked in our experimental approach by the degree of overexpression, a notion that has been shown in previous experiments studying the function of Cpx II CTD mutants (Makke et al., 2018). Taken together, our experiments leave open the question of how the AH of Cpx II prevents spontaneous fusion. Recently, Malsam and colleagues have presented with a site-specific photocrosslinking strategy (using photoactivable BPA benzoyl-phenylalanine) evidence that the Cpx AH binds to the C-termini of both, VAMP2 and SNAP25 and thereby suppresses SNARE zippering (Malsam et al., 2020). Furthermore, they showed that respective quadruple mutations (incl. charge reversal) in Cpx II to interfere with either SNAP-25 (D27R, A30R, Q31E, E34R) or with VAMP2 (K33E, R37E, A40K, Q44E) binding impaired the clamping *in vitro* and increased the mEPSC frequency of hippocampal glutamatergic neurons (Malsam et al., 2020). Given these findings, it will be interesting to test the functional impact of such quadruple mutations in our model system where secretion can be monitored on the background of a well-defined Ca^{2+}-stimulus.

4.7 Complexin II inhibitory action by the accessory α-helix and the C-terminal domain

The present work shows that the AH and the C-terminal region of Cpx II have similar functions in preventing premature vesicle release. Indeed, experiments with a mutant protein lacking the last amino acids of the C-terminal domain showed an unclamping phenotype, despite the presence of the AH in these cells **(Figure 26)**. In the same line, experiments lacking the first 40 amino acids of Cpx II (which includes the N-terminal and the AH) similarly exhibited an unclamping phenotype (50%) despite the presence of the C-terminal domain **(Figure 36)**. Thus, the presence of either region is not sufficient for the inhibition of premature release. Overall, it seems reasonable to conclude that both regions, the AH and the C-terminal domain, are required to clamp asynchronous secretion and therefore enable the build-up of a pool of prime vesicles. Based on these results we hypothesize that both regions cooperate in hindering premature exocytosis. In this context it stands to reason that

previous studies have suggested the C-terminal domain is needed to sort Cpx II to vesicular membranes to facilitate the inhibitory action of other Cpx II domains (i.e. AH) in a proximity-accelerated fashion (Gong et al., 2016; Snead et al., 2014; Wragg et al., 2013). We have shown, instead, that the C-terminal region has an active role in arresting premature secretion independent of its binding to membranes **(Figure 25)**. Furthermore, we provide strong evidence that the CTD of Cpx II competes with SNAP25-SN1 for SNARE binding in order to exert its inhibitory action **(Figure 27 and 28)**. Concerning the AH, it remains to be shown whether the observed inhibitory function is due to the competition with VAMP2 **(Figure 38 and 39)** as previous studies have suggested (Giraudo et al., 2009). Since truncation of the AH shows only partial unclamping of the asynchronous secretion, an attractive explanation could be that the AH rather assists the CTD in preventing premature secretion. Nevertheless, further studies will be needed to unravel the precise mechanisms underlying the 'molecular clamp' in Ca^{2+}-triggered exocytosis.

5. Bibliography

Aeffner, S., Reusch, T., Weinhausen, B., and Salditt, T. (2012). Energetics of stalk intermediates in membrane fusion are controlled by lipid composition. Proceedings of the National Academy of Sciences of the United States of America *109*, E1609-1618.

Alabi, A.A., and Tsien, R.W. (2013). Perspectives on kiss-and-run: role in exocytosis, endocytosis, and neurotransmission. Annual review of physiology *75*, 393-422.

Almers, W., and Tse, F.W. (1990). Transmitter release from synapses: does a preassembled fusion pore initiate exocytosis? Neuron *4*, 813-818.

Alvarez de Toledo, G., Fernandez-Chacon, R., and Fernandez, J.M. (1993). Release of secretory products during transient vesicle fusion. Nature *363*, 554-558.

Amatore, C., Arbault, S., Bouret, Y., Guille, M., Lemaitre, F., and Verchier, Y. (2006). Regulation of exocytosis in chromaffin cells by trans-insertion of lysophosphatidylcholine and arachidonic acid into the outer leaflet of the cell membrane. Chembiochem : a European journal of chemical biology *7*, 1998-2003.

Arac, D., Chen, X., Khant, H.A., Ubach, J., Ludtke, S.J., Kikkawa, M., Johnson, A.E., Chiu, W., Sudhof, T.C., and Rizo, J. (2006). Close membrane-membrane proximity induced by Ca(2+)-dependent multivalent binding of synaptotagmin-1 to phospholipids. Nature structural & molecular biology *13*, 209-217.

Archer, D.A., Graham, M.E., and Burgoyne, R.D. (2002). Complexin regulates the closure of the fusion pore during regulated vesicle exocytosis. The Journal of biological chemistry *277*, 18249-18252.

Bark, I.C., Hahn, K.M., Ryabinin, A.E., and Wilson, M.C. (1995). Differential expression of SNAP-25 protein isoforms during divergent vesicle fusion events of neural development. Proceedings of the National Academy of Sciences of the United States of America *92*, 1510-1514.

Bark, I.C., and Wilson, M.C. (1994). Human cDNA clones encoding two different isoforms of the nerve terminal protein SNAP-25. Gene *139*, 291-292.

Baumert, M., Maycox, P.R., Navone, F., De Camilli, P., and Jahn, R. (1989). Synaptobrevin: an integral membrane protein of 18,000 daltons present in small synaptic vesicles of rat brain. EMBO J *8*, 379-384.

Ben-Zeev, G., Telias, M., and Nussinovitch, I. (2010). Lysophospholipids modulate voltage-gated calcium channel currents in pituitary cells; effects of lipid stress. Cell Calcium *47*, 514-524.

Bennett, M.K., Calakos, N., and Scheller, R.H. (1992). Syntaxin: a synaptic protein implicated in docking of synaptic vesicles at presynaptic active zones. Science *257*, 255-259.

Bennett, M.K., Garcia-Arraras, J.E., Elferink, L.A., Peterson, K., Fleming, A.M., Hazuka, C.D., and Scheller, R.H. (1993). The syntaxin family of vesicular transport receptors. Cell *74*, 863-873.

Berridge, M.J. (2006). Calcium microdomains: organization and function. Cell Calcium *40*, 405-412.

Betz, A., Okamoto, M., Benseler, F., and Brose, N. (1997). Direct interaction of the rat unc-13 homologue Munc13-1 with the N terminus of syntaxin. The Journal of biological chemistry *272*, 2520-2526.

Bittner, M.A., and Holz, R.W. (1992). Kinetic analysis of secretion from permeabilized adrenal chromaffin cells reveals distinct components. The Journal of biological chemistry *267*, 16219-16225.

Blasi, J., Chapman, E.R., Link, E., Binz, T., Yamasaki, S., De Camilli, P., Sudhof, T.C., Niemann, H., and Jahn, R. (1993). Botulinum neurotoxin A selectively cleaves the synaptic protein SNAP-25. Nature *365*, 160-163.

Block, M.R., Glick, B.S., Wilcox, C.A., Wieland, F.T., and Rothman, J.E. (1988). Purification of an N-ethylmaleimide-sensitive protein catalyzing vesicular transport. Proceedings of the National Academy of Sciences of the United States of America *85*, 7852-7856.

Bolte, S., and Cordelieres, F.P. (2006). A guided tour into subcellular colocalization analysis in light microscopy. J Microsc *224*, 213-232.

Borisovska, M., Schwarz, Y.N., Dhara, M., Yarzagaray, A., Hugo, S., Narzi, D., Siu, S.W., Kesavan, J., Mohrmann, R., Bockmann, R.A*., et al.* (2012). Membrane-proximal tryptophans of synaptobrevin II stabilize priming of secretory vesicles. The Journal of neuroscience : the official journal of the Society for Neuroscience *32*, 15983-15997.

Borisovska, M., Zhao, Y., Tsytsyura, Y., Glyvuk, N., Takamori, S., Matti, U., Rettig, J., Sudhof, T., and Bruns, D. (2005). v-SNAREs control exocytosis of vesicles from priming to fusion. EMBO J *24*, 2114-2126.

Bowen, M., and Brunger, A.T. (2006). Conformation of the synaptobrevin transmembrane domain. Proceedings of the National Academy of Sciences of the United States of America *103*, 8378-8383.

Bowen, M.E., Weninger, K., Ernst, J., Chu, S., and Brunger, A.T. (2005). Single-molecule studies of synaptotagmin and complexin binding to the SNARE complex. Biophysical journal *89*, 690-702.

Breckenridge, L.J., and Almers, W. (1987). Currents through the fusion pore that forms during exocytosis of a secretory vesicle. Nature *328*, 814-817.

Brose, N. (2008). For better or for worse: complexins regulate SNARE function and vesicle fusion. Traffic *9*, 1403-1413.

Brown, M.F. (2012). Curvature forces in membrane lipid-protein interactions. Biochemistry *51*, 9782-9795.

Bruns, D. (2004). Detection of transmitter release with carbon fiber electrodes. Methods *33*, 312-321.

Burgess, T.L., and Kelly, R.B. (1987). Constitutive and regulated secretion of proteins. Annu Rev Cell Biol *3*, 243-293.

Bykhovskaia, M., Jagota, A., Gonzalez, A., Vasin, A., and Littleton, J.T. (2013). Interaction of the complexin accessory helix with the C-terminus of the SNARE complex: molecular-dynamics model of the fusion clamp. Biophysical journal *105*, 679-690.

Cai, H., Reim, K., Varoqueaux, F., Tapechum, S., Hill, K., Sorensen, J.B., Brose, N., and Chow, R.H. (2008). Complexin II plays a positive role in Ca2+-triggered exocytosis by facilitating vesicle priming. Proceedings of the National Academy of Sciences of the United States of America *105*, 19538-19543.

Chamberlain, L.H., Burgoyne, R.D., and Gould, G.W. (2001). SNARE proteins are highly enriched in lipid rafts in PC12 cells: implications for the spatial control of exocytosis. Proceedings of the National Academy of Sciences of the United States of America *98*, 5619-5624.

Chandler, D.E., and Heuser, J.E. (1980). Arrest of membrane fusion events in mast cells by quick-freezing. J Cell Biol *86*, 666-674.

Chanturiya, A., Leikina, E., Zimmerberg, J., and Chernomordik, L.V. (1999). Short-chain alcohols promote an early stage of membrane hemifusion. Biophysical journal *77*, 2035-2045.

Chen, X., Tomchick, D.R., Kovrigin, E., Arac, D., Machius, M., Sudhof, T.C., and Rizo, J. (2002). Three-dimensional structure of the complexin/SNARE complex. Neuron *33*, 397-409.

Chen, Y.A., Scales, S.J., Patel, S.M., Doung, Y.C., and Scheller, R.H. (1999). SNARE complex formation is triggered by Ca2+ and drives membrane fusion. Cell *97*, 165-174.

Chen, Y.A., and Scheller, R.H. (2001). SNARE-mediated membrane fusion. Nat Rev Mol Cell Biol *2*, 98-106.

Chernomordik, L.V., and Kozlov, M.M. (2003). Protein-lipid interplay in fusion and fission of biological membranes. Annu Rev Biochem *72*, 175-207.

Chernomordik, L.V., and Kozlov, M.M. (2008). Mechanics of membrane fusion. Nature structural & molecular biology *15*, 675-683.

Cho, R.W., Kummel, D., Li, F., Baguley, S.W., Coleman, J., Rothman, J.E., and Littleton, J.T. (2014). Genetic analysis of the Complexin trans-clamping model for cross-linking SNARE complexes in vivo. Proceedings of the National Academy of Sciences of the United States of America *111*, 10317-10322.

Churchward, M.A., Rogasevskaia, T., Hofgen, J., Bau, J., and Coorssen, J.R. (2005). Cholesterol facilitates the native mechanism of Ca2+-triggered membrane fusion. Journal of cell science *118*, 4833-4848.

Deak, F., Shin, O.H., Kavalali, E.T., and Sudhof, T.C. (2006). Structural determinants of synaptobrevin 2 function in synaptic vesicle fusion. The Journal of neuroscience : the official journal of the Society for Neuroscience *26*, 6668-6676.

Dean, C., Dunning, F.M., Liu, H.S., Bomba-Warczak, E., Martens, H., Bharat, V., Ahmed, S., and Chapman, E.R. (2012). Axonal and dendritic synaptotagmin isoforms revealed by a pHluorin-syt functional screen. Molecular Biology of the Cell *23*, 1715-1727.

Dhara, M., Mantero Martinez, M., Makke, M., Schwarz, Y., Mohrmann, R., and Bruns, D. (2020). Synergistic actions of v-SNARE transmembrane domains and membrane-curvature modifying lipids in neurotransmitter release. eLife *9*.

Dhara, M., Yarzagaray, A., Makke, M., Schindeldecker, B., Schwarz, Y., Shaaban, A., Sharma, S., Bockmann, R.A., Lindau, M., Mohrmann, R*., et al.* (2016). v-SNARE transmembrane domains function as catalysts for vesicle fusion. eLife *5*.

Dhara, M., Yarzagaray, A., Schwarz, Y., Dutta, S., Grabner, C., Moghadam, P.K., Bost, A., Schirra, C., Rettig, J., Reim, K*., et al.* (2014). Complexin synchronizes primed vesicle exocytosis and regulates fusion pore dynamics. J Cell Biol *204*, 1123-1140.

Earp, L.J., Delos, S.E., Park, H.E., and White, J.M. (2005). The many mechanisms of viral membrane fusion proteins. Curr Top Microbiol Immunol *285*, 25-66.

Edwardson, J.M., and Daniels-Holgate, P.U. (1992). Reconstitution in vitro of a membrane-fusion event involved in constitutive exocytosis. A role for cytosolic proteins and a GTP-binding protein, but not for Ca2+. Biochem J *285 (Pt 2)*, 383-385.

Elferink, L.A., Trimble, W.S., and Scheller, R.H. (1989). Two vesicle-associated membrane protein genes are differentially expressed in the rat central nervous system. The Journal of biological chemistry *264*, 11061-11064.

Ellis-Davies, G.C., and Kaplan, J.H. (1994). Nitrophenyl-EGTA, a photolabile chelator that selectively binds Ca2+ with high affinity and releases it rapidly upon photolysis. Proceedings of the National Academy of Sciences of the United States of America *91*, 187-191.

Fang, Q., and Lindau, M. (2014). How could SNARE proteins open a fusion pore? Physiology *29*, 278-285.

Fasshauer, D., Otto, H., Eliason, W.K., Jahn, R., and Brunger, A.T. (1997). Structural changes are associated with soluble N-ethylmaleimide-sensitive fusion protein attachment protein receptor complex formation. The Journal of biological chemistry *272*, 28036-28041.

Fava, E., Dehghany, J., Ouwendijk, J., Muller, A., Niederlein, A., Verkade, P., Meyer-Hermann, M., and Solimena, M. (2012). Novel standards in the measurement of rat insulin granules combining electron microscopy, high-content image analysis and in silico modelling. Diabetologia *55*, 1013-1023.

Fdez, E., Martinez-Salvador, M., Beard, M., Woodman, P., and Hilfiker, S. (2010). Transmembrane-domain determinants for SNARE-mediated membrane fusion. Journal of cell science *123*, 2473-2480.

Fernandez-Chacon, R., Konigstorfer, A., Gerber, S.H., Garcia, J., Matos, M.F., Stevens, C.F., Brose, N., Rizo, J., Rosenmund, C., and Sudhof, T.C. (2001). Synaptotagmin I functions as a calcium regulator of release probability. Nature *410*, 41-49.

Garcia, A.G., Garcia-De-Diego, A.M., Gandia, L., Borges, R., and Garcia-Sancho, J. (2006). Calcium signaling and exocytosis in adrenal chromaffin cells. Physiol Rev *86*, 1093-1131.

Gasman, S., and Vitale, N. (2017). Lipid remodelling in neuroendocrine secretion. Biol Cell *109*, 381-390.

Geppert, M., Goda, Y., Hammer, R.E., Li, C., Rosahl, T.W., Stevens, C.F., and Sudhof, T.C. (1994). Synaptotagmin I: a major Ca2+ sensor for transmitter release at a central synapse. Cell *79*, 717-727.

Gerst, J.E. (1999). SNAREs and SNARE regulators in membrane fusion and exocytosis. Cell Mol Life Sci *55*, 707-734.

Gillis, K.D., and Chow, R.H. (1997). Kinetics of exocytosis in adrenal chromaffin cells. Semin Cell Dev Biol *8*, 133-140.

Giraudo, C.G., Garcia-Diaz, A., Eng, W.S., Chen, Y., Hendrickson, W.A., Melia, T.J., and Rothman, J.E. (2009). Alternative zippering as an on-off switch for SNARE-mediated fusion. Science *323*, 512-516.

Gong, J., Lai, Y., Li, X., Wang, M., Leitz, J., Hu, Y., Zhang, Y., Choi, U.B., Cipriano, D., Pfuetzner, R.A*., et al.* (2016). C-terminal domain of mammalian complexin-1 localizes to highly curved membranes. Proceedings of the National Academy of Sciences of the United States of America *113*, E7590-E7599.

Grote, E., Hao, J.C., Bennett, M.K., and Kelly, R.B. (1995). A targeting signal in VAMP regulating transport to synaptic vesicles. Cell *81*, 581-589.

Grynkiewicz, G., Poenie, M., and Tsien, R.Y. (1985). A new generation of Ca2+ indicators with greatly improved fluorescence properties. The Journal of biological chemistry *260*, 3440-3450.

Gurtovenko, A.A., and Anwar, J. (2009). Interaction of ethanol with biological membranes: the formation of non-bilayer structures within the membrane interior and their significance. The journal of physical chemistry B *113*, 1983-1992.

Gustavsson, N., Wu, B., and Han, W. (2012). Calcium sensing in exocytosis. Adv Exp Med Biol *740*, 731-757.

Han, X., Wang, C.T., Bai, J., Chapman, E.R., and Jackson, M.B. (2004). Transmembrane segments of syntaxin line the fusion pore of Ca2+-triggered exocytosis. Science *304*, 289-292.

Hayashi, T., McMahon, H., Yamasaki, S., Binz, T., Hata, Y., Sudhof, T.C., and Niemann, H. (1994). Synaptic vesicle membrane fusion complex: action of clostridial neurotoxins on assembly. EMBO J *13*, 5051-5061.

He, L., Wu, X.S., Mohan, R., and Wu, L.G. (2006). Two modes of fusion pore opening revealed by cell-attached recordings at a synapse. Nature *444*, 102-105.

Heinemann, C., Chow, R.H., Neher, E., and Zucker, R.S. (1994). Kinetics of the secretory response in bovine chromaffin cells following flash photolysis of caged Ca2+. Biophysical journal *67*, 2546-2557.

Hille, B. (1992) Ion channels of Excitable Membranes. 2nd Edition, Sinauer Associates, Inc., Massachusetts.

Hohenstein, A.C., and Roche, P.A. (2001). SNAP-29 is a promiscuous syntaxin-binding SNARE. Biochemical and biophysical research communications *285*, 167-171.

Humeau, Y., Doussau, F., Grant, N.J., and Poulain, B. (2000). How botulinum and tetanus neurotoxins block neurotransmitter release. Biochimie *82*, 427-446.

Hunt, J.M., Bommert, K., Charlton, M.P., Kistner, A., Habermann, E., Augustine, G.J., and Betz, H. (1994). A post-docking role for synaptobrevin in synaptic vesicle fusion. Neuron *12*, 1269-1279.

Hussain, S., Ringsevjen, H., Schupp, M., Hvalby, O., Sorensen, J.B., Jensen, V., and Davanger, S. (2019). A possible postsynaptic role for SNAP-25 in hippocampal synapses. Brain structure & function *224*, 521-532.

Imig, C., Min, S.W., Krinner, S., Arancillo, M., Rosenmund, C., Sudhof, T.C., Rhee, J., Brose, N., and Cooper, B.H. (2014). The morphological and molecular nature of synaptic vesicle priming at presynaptic active zones. Neuron *84*, 416-431.

Kaeser-Woo, Y.J., Yang, X., and Sudhof, T.C. (2012). C-terminal complexin sequence is selectively required for clamping and priming but not for Ca2+ triggering of synaptic exocytosis. The Journal of neuroscience : the official journal of the Society for Neuroscience *32*, 2877-2885.

Kandel, E.R., Schwartz, J.H., and Jessell, T.M. (2000). Principles of neural science, 4th edn (New York: McGraw-Hill, Health Professions Division).

Kawamoto, S., Klein, M.L., and Shinoda, W. (2015). Coarse-grained molecular dynamics study of membrane fusion: Curvature effects on free energy barriers along the stalk mechanism. J Chem Phys *143*, 243112.

Kee, Y., Lin, R.C., Hsu, S.C., and Scheller, R.H. (1995). Distinct domains of syntaxin are required for synaptic vesicle fusion complex formation and dissociation. Neuron *14*, 991-998.

Kelly, R.B. (1985). Pathways of protein secretion in eukaryotes. Science *230*, 25-32.

Kemble, G.W., Danieli, T., and White, J.M. (1994). Lipid-anchored influenza hemagglutinin promotes hemifusion, not complete fusion. Cell *76*, 383-391.

Kesavan, J., Borisovska, M., and Bruns, D. (2007). v-SNARE actions during Ca(2+)-triggered exocytosis. Cell *131*, 351-363.

Klenchin, V.A., and Martin, T.F. (2000). Priming in exocytosis: attaining fusion-competence after vesicle docking. Biochimie *82*, 399-407.

Konishi, M., Hollingworth, S., Harkins, A.B., and Baylor, S.M. (1991). Myoplasmic calcium transients in intact frog skeletal muscle fibers monitored with the fluorescent indicator furaptra. J Gen Physiol *97*, 271-301.

Kummel, D., Krishnakumar, S.S., Radoff, D.T., Li, F., Giraudo, C.G., Pincet, F., Rothman, J.E., and Reinisch, K.M. (2011). Complexin cross-links prefusion SNAREs into a zigzag array. Nature structural & molecular biology *18*, 927-933.

Langosch, D., Crane, J.M., Brosig, B., Hellwig, A., Tamm, L.K., and Reed, J. (2001). Peptide mimics of SNARE transmembrane segments drive membrane fusion depending on their conformational plasticity. J Mol Biol *311*, 709-721.

Langosch, D., Hofmann, M., and Ungermann, C. (2007). The role of transmembrane domains in membrane fusion. Cell Mol Life Sci *64*, 850-864.

Lin, R.C., and Scheller, R.H. (2000). Mechanisms of synaptic vesicle exocytosis. Annu Rev Cell Dev Biol *16*, 19-49.

Lindau, M., and Gomperts, B.D. (1991). Techniques and concepts in exocytosis: focus on mast cells. Biochim Biophys Acta *1071*, 429-471.

Lindau, M., and Neher, E. (1988). Patch-clamp techniques for time-resolved capacitance measurements in single cells. Pflugers Arch *411*, 137-146.

Link, E., Edelmann, L., Chou, J.H., Binz, T., Yamasaki, S., Eisel, U., Baumert, M., Sudhof, T.C., Niemann, H., and Jahn, R. (1992). Tetanus toxin action: inhibition of neurotransmitter release linked to synaptobrevin proteolysis. Biochemical and biophysical research communications *189*, 1017-1023.

Makke, M., Mantero Martinez, M., Gaya, S., Schwarz, Y., Frisch, W., Silva-Bermudez, L., Jung, M., Mohrmann, R., Dhara, M., and Bruns, D. (2018). A mechanism for exocytotic arrest by the Complexin C-terminus. eLife *7*.

Malsam, J., Barfuss, S., Trimbuch, T., Zarebidaki, F., Sonnen, A.F., Wild, K., Scheutzow, A., Rohland, L., Mayer, M.P., Sinning, I*., et al.* (2020). Complexin Suppresses Spontaneous Exocytosis by Capturing the Membrane-Proximal Regions of VAMP2 and SNAP25. Cell Rep *32*, 107926.

Manders, E.M.M., Verbeek, F.J., and Aten, J.A. (1993). Measurement of Colocalization of Objects in Dual-Color Confocal Images. Journal of Microscopy-Oxford *169*, 375-382.

Masedunskas, A., Porat-Shliom, N., and Weigert, R. (2012). Regulated exocytosis: novel insights from intravital microscopy. Traffic *13*, 627-634.

McMahon, H.T., Missler, M., Li, C., and Sudhof, T.C. (1995). Complexins: cytosolic proteins that regulate SNAP receptor function. Cell *83*, 111-119.

McMahon, H.T., Ushkaryov, Y.A., Edelmann, L., Link, E., Binz, T., Niemann, H., Jahn, R., and Sudhof, T.C. (1993). Cellubrevin is a ubiquitous tetanus-toxin substrate homologous to a putative synaptic vesicle fusion protein. Nature *364*, 346-349.

McNew, J.A., Parlati, F., Fukuda, R., Johnston, R.J., Paz, K., Paumet, F., Sollner, T.H., and Rothman, J.E. (2000a). Compartmental specificity of cellular membrane fusion encoded in SNARE proteins. Nature *407*, 153-159.

McNew, J.A., Weber, T., Parlati, F., Johnston, R.J., Melia, T.J., Sollner, T.H., and Rothman, J.E. (2000b). Close is not enough: SNARE-dependent membrane fusion requires an active mechanism that transduces force to membrane anchors. J Cell Biol *150*, 105-117.

Melia, T.J., You, D., Tareste, D.C., and Rothman, J.E. (2006). Lipidic antagonists to SNARE-mediated fusion. The Journal of biological chemistry *281*, 29597-29605.

Melikyan, G.B. (2010). Driving a wedge between viral lipids blocks infection. Proceedings of the National Academy of Sciences of the United States of America *107*, 17069-17070.

Melikyan, G.B., Markosyan, R.M., Roth, M.G., and Cohen, F.S. (2000). A point mutation in the transmembrane domain of the hemagglutinin of influenza virus stabilizes a hemifusion intermediate that can transit to fusion. Mol Biol Cell *11*, 3765-3775.

Ming, M., Schirra, C., Becherer, U., Stevens, D.R., and Rettig, J. (2015). Behavior and Properties of Mature Lytic Granules at the Immunological Synapse of Human Cytotoxic T Lymphocytes. PLoS One *10*, e0135994.

Mohrmann, R., de Wit, H., Connell, E., Pinheiro, P.S., Leese, C., Bruns, D., Davletov, B., Verhage, M., and Sorensen, J.B. (2013). Synaptotagmin interaction with SNAP-25 governs vesicle docking, priming, and fusion triggering. The Journal of neuroscience : the official journal of the Society for Neuroscience *33*, 14417-14430.

Mohrmann, R., Dhara, M., and Bruns, D. (2015). Complexins: small but capable. Cell Mol Life Sci *72*, 4221-4235.

Monck, J.R., and Fernandez, J.M. (1996). The fusion pore and mechanisms of biological membrane fusion. Curr Opin Cell Biol *8*, 524-533.

Morgan, A., and Burgoyne, R.D. (1997). Common mechanisms for regulated exocytosis in the chromaffin cell and the synapse. Semin Cell Dev Biol *8*, 141-149.

Mostafavi, H., Thiyagarajan, S., Stratton, B.S., Karatekin, E., Warner, J.M., Rothman, J.E., and O'Shaughnessy, B. (2017). Entropic forces drive self-organization and membrane fusion by SNARE proteins. Proceedings of the National Academy of Sciences of the United States of America *114*, 5455-5460.

Nadelhaft, I. (1973). Measurement of the size distribution of zymogen granules from rat pancreas. Biophysical journal *13*, 1014-1029.

Neher, E., and Zucker, R.S. (1993). Multiple calcium-dependent processes related to secretion in bovine chromaffin cells. Neuron *10*, 21-30.

O'Sullivan, A.J., Cheek, T.R., Moreton, R.B., Berridge, M.J., and Burgoyne, R.D. (1989). Localization and heterogeneity of agonist-induced changes in cytosolic calcium concentration in single bovine adrenal chromaffin cells from video imaging of fura-2. EMBO J *8*, 401-411.

Okada, Y. (2012). Patch clamp techniques : from beginning to advanced protocols (Tokyo ; New York: Springer).

Oyler, G.A., Higgins, G.A., Hart, R.A., Battenberg, E., Billingsley, M., Bloom, F.E., and Wilson, M.C. (1989). The identification of a novel synaptosomal-associated protein, SNAP-25, differentially expressed by neuronal subpopulations. J Cell Biol *109*, 3039-3052.

Pabst, S., Margittai, M., Vainius, D., Langen, R., Jahn, R., and Fasshauer, D. (2002). Rapid and selective binding to the synaptic SNARE complex suggests a modulatory role of complexins in neuroexocytosis. The Journal of biological chemistry *277*, 7838-7848.

Park, Y., and Ryu, J.K. (2018). Models of synaptotagmin-1 to trigger Ca(2+) -dependent vesicle fusion. FEBS letters *592*, 3480-3492.

Parlati, F., McNew, J.A., Fukuda, R., Miller, R., Sollner, T.H., and Rothman, J.E. (2000). Topological restriction of SNARE-dependent membrane fusion. Nature *407*, 194-198.

Paxman, J., Hunt, B., Hallan, D., Zarbock, S.R., and Woodbury, D.J. (2017). Drunken Membranes: Short-Chain Alcohols Alter Fusion of Liposomes to Planar Lipid Bilayers. Biophysical journal *112*, 121-132.

Perin, M.S., Johnston, P.A., Ozcelik, T., Jahn, R., Francke, U., and Sudhof, T.C. (1991). Structural and Functional Conservation of Synaptotagmin (P65) in Drosophila and Humans. Journal of Biological Chemistry *266*, 615-622.

Pieren, M., Desfougères, Y., Michaillat, L., Schmidt, A., and Mayer, A. (2015). Vacuolar SNARE protein transmembrane domains serve as nonspecific membrane anchors with unequal roles in lipid mixing. The Journal of biological chemistry *290*, 12821-12832.

Poirier, M.A., Xiao, W., Macosko, J.C., Chan, C., Shin, Y.K., and Bennett, M.K. (1998). The synaptic SNARE complex is a parallel four-stranded helical bundle. Nat Struct Biol *5*, 765-769.

Rea, S., Martin, L.B., McIntosh, S., Macaulay, S.L., Ramsdale, T., Baldini, G., and James, D.E. (1998). Syndet, an adipocyte target SNARE involved in the insulin-induced translocation of GLUT4 to the cell surface. The Journal of biological chemistry *273*, 18784-18792.

Regazzi, R., Sadoul, K., Meda, P., Kelly, R.B., Halban, P.A., and Wollheim, C.B. (1996). Mutational analysis of VAMP domains implicated in Ca2+-induced insulin exocytosis. EMBO J *15*, 6951-6959.

Regazzi, R., Wollheim, C.B., Lang, J., Theler, J.M., Rossetto, O., Montecucco, C., Sadoul, K., Weller, U., Palmer, M., and Thorens, B. (1995). VAMP-2 and cellubrevin are expressed in pancreatic beta-cells and are essential for Ca(2+)-but not for GTP gamma S-induced insulin secretion. EMBO J *14*, 2723-2730.

Rego, E.H., and Shao, L. (2015). Practical structured illumination microscopy. Methods in molecular biology *1251*, 175-192.

Reim, K., Mansour, M., Varoqueaux, F., McMahon, H.T., Sudhof, T.C., Brose, N., and Rosenmund, C. (2001). Complexins regulate a late step in Ca2+-dependent neurotransmitter release. Cell *104*, 71-81.

Reim, K., Wegmeyer, H., Brandstatter, J.H., Xue, M., Rosenmund, C., Dresbach, T., Hofmann, K., and Brose, N. (2005). Structurally and functionally unique complexins at retinal ribbon synapses. J Cell Biol *169*, 669-680.

Rizo, J., and Sudhof, T.C. (2002). Snares and Munc18 in synaptic vesicle fusion. Nat Rev Neurosci *3*, 641-653.

Rizo, J., and Xu, J.J. (2015). The Synaptic Vesicle Release Machinery. Annual Review of Biophysics, Vol 44 *44*, 339-367.

Roggero, C.M., De Blas, G.A., Dai, H., Tomes, C.N., Rizo, J., and Mayorga, L.S. (2007). Complexin/synaptotagmin interplay controls acrosomal exocytosis. The Journal of biological chemistry *282*, 26335-26343.

Ryu, J.K., Min, D., Rah, S.H., Kim, S.J., Park, Y., Kim, H., Hyeon, C., Kim, H.M., Jahn, R., and Yoon, T.Y. (2015). Spring-loaded unraveling of a single SNARE complex by NSF in one round of ATP turnover. Science *347*, 1485-1489.

Sakmann, B., and Neher, E. (1984). Patch clamp techniques for studying ionic channels in excitable membranes. Annual review of physiology *46*, 455-472.

Sala, F., Nistri, A., and Criado, M. (2008). Nicotinic acetylcholine receptors of adrenal chromaffin cells. Acta physiologica *192*, 203-212.

Salaun, C., James, D.J., Greaves, J., and Chamberlain, L.H. (2004). Plasma membrane targeting of exocytic SNARE proteins. Biochim Biophys Acta *1693*, 81-89.

Sander, L.E., Frank, S.P., Bolat, S., Blank, U., Galli, T., Bigalke, H., Bischoff, S.C., and Lorentz, A. (2008). Vesicle associated membrane protein (VAMP)-7 and VAMP-8, but not VAMP-2 or VAMP-3, are required for activation-induced degranulation of mature human mast cells. Eur J Immunol *38*, 855-863.

Schaub, J.R., Lu, X., Doneske, B., Shin, Y.K., and McNew, J.A. (2006). Hemifusion arrest by complexin is relieved by Ca2+-synaptotagmin I. Nature structural & molecular biology *13*, 748-750.

Schoch, S., Deak, F., Konigstorfer, A., Mozhayeva, M., Sara, Y., Sudhof, T.C., and Kavalali, E.T. (2001). SNARE function analyzed in synaptobrevin/VAMP knockout mice. Science *294*, 1117-1122.

Schupp, M., Malsam, J., Ruiter, M., Scheutzow, A., Wierda, K.D., Sollner, T.H., and Sorensen, J.B. (2016). Interactions Between SNAP-25 and Synaptotagmin-1 Are Involved in Vesicle Priming, Clamping Spontaneous and Stimulating Evoked Neurotransmission. The Journal of neuroscience : the official journal of the Society for Neuroscience *36*, 11865-11880.

Shaaban, A., Dhara, M., Frisch, W., Harb, A., Shaib, A.H., Becherer, U., Bruns, D., and Mohrmann, R. (2019). The SNAP-25 linker supports fusion intermediates by local lipid interactions. eLife *8*.

Smirnova, Y.G., Risselada, H.J., and Muller, M. (2019). Thermodynamically reversible paths of the first fusion intermediate reveal an important role for membrane anchors of fusion proteins. Proceedings of the National Academy of Sciences of the United States of America *116*, 2571-2576.

Snead, D., Lai, A.L., Wragg, R.T., Parisotto, D.A., Ramlall, T.F., Dittman, J.S., Freed, J.H., and Eliezer, D. (2017). Unique Structural Features of Membrane-Bound C-Terminal Domain Motifs Modulate Complexin Inhibitory Function. Frontiers in molecular neuroscience *10*, 154.

Snead, D., Wragg, R.T., Dittman, J.S., and Eliezer, D. (2014). Membrane curvature sensing by the C-terminal domain of complexin. Nat Commun *5*, 4955.

Sollner, T., Bennett, M.K., Whiteheart, S.W., Scheller, R.H., and Rothman, J.E. (1993). A protein assembly-disassembly pathway in vitro that may correspond to sequential steps of synaptic vesicle docking, activation, and fusion. Cell *75*, 409-418.

Stevens, D.R., Schirra, C., Becherer, U., and Rettig, J. (2011). Vesicle pools: lessons from adrenal chromaffin cells. Front Synaptic Neurosci *3*, 2.

Sudhof, T.C. (1995). The synaptic vesicle cycle: a cascade of protein-protein interactions. Nature *375*, 645-653.

Sudhof, T.C. (2012). Calcium control of neurotransmitter release. Cold Spring Harbor perspectives in biology *4*, a011353.

Sudhof, T.C., and Rothman, J.E. (2009). Membrane fusion: grappling with SNARE and SM proteins. Science *323*, 474-477.

Sutton, R.B., Fasshauer, D., Jahn, R., and Brunger, A.T. (1998). Crystal structure of a SNARE complex involved in synaptic exocytosis at 2.4 A resolution. Nature *395*, 347-353.

Tadokoro, S., Nakanishi, M., and Hirashima, N. (2005). Complexin II facilitates exocytotic release in mast cells by enhancing Ca2+ sensitivity of the fusion process. Journal of cell science *118*, 2239-2246.

Takamori, S., Holt, M., Stenius, K., Lemke, E.A., Gronborg, M., Riedel, D., Urlaub, H., Schenck, S., Brugger, B., Ringler, P*., et al.* (2006). Molecular anatomy of a trafficking organelle. Cell *127*, 831-846.

Tang, J., Maximov, A., Shin, O.H., Dai, H., Rizo, J., and Sudhof, T.C. (2006). A complexin/synaptotagmin 1 switch controls fast synaptic vesicle exocytosis. Cell *126*, 1175-1187.

Tokumaru, H., Shimizu-Okabe, C., and Abe, T. (2008). Direct interaction of SNARE complex binding protein synaphin/complexin with calcium sensor synaptotagmin 1. Brain Cell Biol *36*, 173-189.

Toonen, R.F., Kochubey, O., de Wit, H., Gulyas-Kovacs, A., Konijnenburg, B., Sorensen, J.B., Klingauf, J., and Verhage, M. (2006). Dissecting docking and tethering of secretory vesicles at the target membrane. EMBO J *25*, 3725-3737.

Trimble, W.S., Cowan, D.M., and Scheller, R.H. (1988). VAMP-1: a synaptic vesicle-associated integral membrane protein. Proceedings of the National Academy of Sciences of the United States of America *85*, 4538-4542.

Trimbuch, T., Xu, J., Flaherty, D., Tomchick, D.R., Rizo, J., and Rosenmund, C. (2014). Re-examining how complexin inhibits neurotransmitter release. eLife *3*, e02391.

Veit, M., Sollner, T.H., and Rothman, J.E. (1996). Multiple palmitoylation of synaptotagmin and the t-SNARE SNAP-25. FEBS letters *385*, 119-123.

Verhage, M., and Sorensen, J.B. (2008). Vesicle docking in regulated exocytosis. Traffic *9*, 1414-1424.

Viotti, C. (2016). ER to Golgi-Dependent Protein Secretion: The Conventional Pathway. Methods in molecular biology *1459*, 3-29.

Voets, T. (2000). Dissection of three Ca2+-dependent steps leading to secretion in chromaffin cells from mouse adrenal slices. Neuron *28*, 537-545.

Weber, T., Zemelman, B.V., McNew, J.A., Westermann, B., Gmachl, M., Parlati, F., Sollner, T.H., and Rothman, J.E. (1998). SNAREpins: minimal machinery for membrane fusion. Cell *92*, 759-772.

Weimer, R.M., and Richmond, J.E. (2005). Synaptic vesicle docking: a putative role for the Munc18/Sec1 protein family. Curr Top Dev Biol *65*, 83-113.

Williams, K.A., and Deber, C.M. (1991). Proline residues in transmembrane helices: structural or dynamic role? Biochemistry *30*, 8919-8923.

Wolfes, A.C., and Dean, C. (2020). The diversity of synaptotagmin isoforms. Curr Opin Neurobiol *63*, 198-209.

Wragg, R.T., Parisotto, D.A., Li, Z., Terakawa, M.S., Snead, D., Basu, I., Weinstein, H., Eliezer, D., and Dittman, J.S. (2017). Evolutionary Divergence of the C-terminal Domain of Complexin Accounts for Functional Disparities between Vertebrate and Invertebrate Complexins. Frontiers in molecular neuroscience *10*, 146.

Wragg, R.T., Snead, D., Dong, Y., Ramlall, T.F., Menon, I., Bai, J., Eliezer, D., and Dittman, J.S. (2013). Synaptic vesicles position complexin to block spontaneous fusion. Neuron *77*, 323-334.

Wu, L.G., Hamid, E., Shin, W., and Chiang, H.C. (2014). Exocytosis and endocytosis: modes, functions, and coupling mechanisms. Annual review of physiology *76*, 301-331.

Wu, M.M., Llobet, A., and Lagnado, L. (2009a). Loose coupling between calcium channels and sites of exocytosis in chromaffin cells. J Physiol *587*, 5377-5391.

Wu, X.S., McNeil, B.D., Xu, J., Fan, J., Xue, L., Melicoff, E., Adachi, R., Bai, L., and Wu, L.G. (2009b). Ca(2+) and calmodulin initiate all forms of endocytosis during depolarization at a nerve terminal. Nature neuroscience *12*, 1003-1010.

Xu, Y., Zhang, F., Su, Z., McNew, J.A., and Shin, Y.K. (2005). Hemifusion in SNARE-mediated membrane fusion. Nature structural & molecular biology *12*, 417-422.

Xue, M., Craig, T.K., Xu, J., Chao, H.T., Rizo, J., and Rosenmund, C. (2010). Binding of the complexin N terminus to the SNARE complex potentiates synaptic-vesicle fusogenicity. Nature structural & molecular biology *17*, 568-575.

Xue, M., Reim, K., Chen, X., Chao, H.T., Deng, H., Rizo, J., Brose, N., and Rosenmund, C. (2007). Distinct domains of complexin I differentially regulate neurotransmitter release. Nature structural & molecular biology *14*, 949-958.

Xue, M., Stradomska, A., Chen, H., Brose, N., Zhang, W., Rosenmund, C., and Reim, K. (2008). Complexins facilitate neurotransmitter release at excitatory and inhibitory synapses in mammalian central nervous system. Proceedings of the National Academy of Sciences of the United States of America *105*, 7875-7880.

Yang, L., and Huang, H.W. (2002). Observation of a membrane fusion intermediate structure. Science *297*, 1877-1879.

Yang, X., Cao, P., and Sudhof, T.C. (2013). Deconstructing complexin function in activating and clamping Ca2+-triggered exocytosis by comparing knockout and knockdown phenotypes. Proceedings of the National Academy of Sciences of the United States of America *110*, 20777-20782.

Yang, X., Kaeser-Woo, Y.J., Pang, Z.P., Xu, W., and Sudhof, T.C. (2010). Complexin clamps asynchronous release by blocking a secondary Ca(2+) sensor via its accessory alpha helix. Neuron *68*, 907-920.

Yoon, T.Y., and Munson, M. (2018). SNARE complex assembly and disassembly. Curr Biol *28*, R397-R401.

Zhang, Y. (2008). I-TASSER server for protein 3D structure prediction. BMC Bioinformatics *9*, 40.

Zhang, Z., and Jackson, M.B. (2010). Membrane bending energy and fusion pore kinetics in Ca(2+)-triggered exocytosis. Biophysical journal *98*, 2524-2534.

Zhao, M., Wu, S., Zhou, Q., Vivona, S., Cipriano, D.J., Cheng, Y., and Brunger, A.T. (2015). Mechanistic insights into the recycling machine of the SNARE complex. Nature *518*, 61-67.

Zhou, P., Bacaj, T., Yang, X., Pang, Z.P., and Sudhof, T.C. (2013). Lipid-anchored SNAREs lacking transmembrane regions fully support membrane fusion during neurotransmitter release. Neuron *80*, 470-483.

Zhou, Q., Zhou, P., Wang, A.L., Wu, D., Zhao, M., Sudhof, T.C., and Brunger, A.T. (2017). The primed SNARE-complexin-synaptotagmin complex for neuronal exocytosis. Nature *548*, 420-425.

Zimmerberg, J., Vogel, S.S., and Chernomordik, L.V. (1993). Mechanisms of membrane fusion. Annu Rev Biophys Biomol Struct *22*, 433-466.

6. Acknowledgements

First of all, I would like to express my gratitude to Prof. Dr. Dieter Bruns for the opportunity to do my doctoral thesis in his laboratory and for all the scientific knowledge I have learned from him. Thanks to him, I learned to solve scientific and technical problems, as well as to be critical with my data and to interpret them properly. I would also like to give special thanks to our lab manager, Marina Roter, for making things so much easier for me, as from my arrival in Germany until the end of my thesis she not only helped me with the organization of the lab (mice, lab essentials, etc.) but also with all the administrative paperwork. I also like to thank all the technicians who have been in this lab and I would like to express my special thanks to Vanessa Schmitt and Walentina Frisch for their help with genotyping, virus production and especially for offering their advice and help when I have needed it. I would also like to thank all my laboratory colleagues for their support, especially Mazen Makke, Madhurima Dhara, Katharina Oleinikov, Yvonne Schwarz and Alejandro Pastor. Special thanks to Mazen Makke, who has always helped me when I had a technical problem or advised me on how to improve my experiments, and to Katharina Oleinikov and Yvonne Schwarz, who have always been a support inside the lab, but also outside the lab, we had very good times while running. I also want to thank all the people from the synapse club, because those meetings allowed me to grow as a scientist and to lose the fear of presenting. I would also like to thank all the people at CIPMM that I had the opportunity to meet and a special thanks to my dear friend Ana Moreno who has always been there for me and Brittany Balint for all the support, help and friendship.

Thanks to my dear friends from Spain and France who have always supported me even from far away, a special thanks to Ariadna Cordones and two of my friends from France, Yoan Arribat and Salim Benlefki who have always helped and supported me from far away.

I would like to end with a big thank you to my partner Florian Copin who has supported and understood me until the end of my thesis writing. And of course to my family, I thank my father Rafael Mantero who always believed in me no matter what, and my mother Mercedes Martinez who always tried to encourage me to be the best. They both gave me the best education they could give me and I can never thank them enough. And last but not least, my little brother Manel Mantero who is always there for me.